

Multi-photon entanglement and interferometry

Jian-Wei Pan,^{1,2,*} Zeng-Bing Chen,^{1,†} Marek Żukowski,^{3,‡} Harald Weinfurter,^{4,5,§} and Anton Zeilinger^{6,7,¶}

¹Hefei National Laboratory for Physical Sciences at Microscale and Department of Modern Physics, University of Science and Technology of China, Hefei, Anhui 230026, China

²Physikalisches Institut, Universität Heidelberg, Philosophenweg 12, D-69120 Heidelberg, Germany

³Instytut Fizyki Teoretycznej i Astrofizyki, Uniwersytet Gdański, PL-80-952 Gdańsk, Poland

⁴Department für Physik, Ludwig-Maximilians-Universität, D-80799 München, Germany

⁵Max-Planck-Institut für Quantenoptik, D-85748 Garching, Germany

⁶Institut für Experimentalphysik, Universität Wien, Boltzmannngasse 5, A-1090 Wien, Austria

⁷Institut für Quantenoptik und Quanteninformation (IQOQI), Österreichische Akademie der Wissenschaften, Boltzmannngasse 3, A-1090 Wien, Austria

(Dated: October 29, 2018)

Multi-photon interference reveals strictly non-classical phenomena. Thus in quantum information, a significant fraction of key experimental progresses achieved so far comes from multi-photon state manipulation. The applications of multi-photon interferometry range from quantum information processing to fundamental tests of quantum mechanics. We review the progresses, both theoretical and experimental, of this rapidly advancing research. The emphasis is given to the creation of photonic entanglement of various forms, tests of the completeness of quantum mechanics (in particular, violations of local realism), quantum information protocols (e.g., quantum teleportation, entanglement purification and quantum repeater) for quantum communication, and quantum computation with linear optics.

Contents

I. Introduction	2	2. GHZ interferometry	13
A. Quantum optics	2	D. Bell's theorem	14
B. The essence of quantum world: entanglement	3	1. Bell's inequality	14
C. Sources of photonic entanglement	3	2. Bell theorem without inequalities	15
D. Applications in quantum information	4	E. Refutation of certain nonlocal realistic theories	16
E. Our aims	4	F. Non-contextual hidden variable theories	18
F. Related reviews	5	V. Photonic entanglement: creation and measurement	18
II. Interference: classical vs. quantum	5	A. Spontaneous parametric down-conversion process	18
A. Classical interference	5	1. The two-photon states produced by SPDC	19
1. Interference expressed by intensity variations	5	2. Early SPDC interference experiments	21
2. Interference in intensity correlations	5	3. Various types of entanglement	22
B. Quantum interference	6	B. Hyper-entangled photons	23
1. Single-particle quantum interference	6	1. Polarization-path entanglement	24
2. Two-particle quantum interference	6	2. Polarization-time entanglement	24
C. Other interference phenomena	7	3. Entanglement in more degrees of freedom	24
III. Photonic qubits and linear optics	7	C. Photonic entanglement in higher dimensions	25
A. Photon-number states	7	D. Twin-beam multi-photon entanglement	25
B. Photonic qubits	7	E. Multi-photon polarization entanglement	26
C. Simple linear-optical elements	8	1. Entanglement construction	26
D. Quantum interference due to indistinguishability of particles: the Hong-Ou-Mandel dip	10	2. First proposal	28
IV. Entanglement and completeness of quantum mechanics	10	3. Experimental realizations	28
A. Formal theory of entanglement	11	F. Photonic polarization entanglement analyzers	29
B. Basic quantum circuit for preparing and measuring entanglement	12	1. Bell-state analyzer	29
C. Multi-particle interferometry	13	2. GHZ-state analyzer	30
1. EPR interferometry	13	VI. Falsification of realistic world view	30
V. Interference and quantum communication	13	A. Testing Bell's inequalities with photons	31
1. Two-photon interference	13	B. GHZ paradox in the laboratory	31
2. Three-photon interference	14	1. Three-photon test	32
3. Four-photon interference	14	2. Four-photon test	32
4. Multi-photon interference	14	C. Two-observer GHZ-like correlations	33
5. Quantum communication	14	D. Experimental test of a nonlocal realism	33
1. Quantum teleportation	14	E. Quantum vs. noncontextual hidden variables	34
2. Quantum entanglement	14	VII. Quantum communication	34
3. Quantum cryptography	14	A. Quantum dense coding	34
4. Quantum key distribution	14	B. Quantum teleportation	35
5. Quantum repeater	14	1. The protocol	35
6. Quantum communication with linear optics	14	2. Experimental teleportation of photonic states	37
7. Quantum communication with nonlinear optics	14	3. Teleportation onto freely propagating qubits	37

*Electronic address: pan@ustc.edu.cn

†Electronic address: zbchen@ustc.edu.cn

‡Electronic address: marek.zukowski@univie.ac.at

§Electronic address: harald.weinfurter@physik.uni-muenchen.de

¶Electronic address: anton.zeilinger@univie.ac.at

4. Teleportation of a qubit encoded in one of EPR particles	38
5. Various approaches to teleportation	39
6. More involved teleportation schemes	39
C. Entanglement swapping	40
D. Beating noisy entanglement	41
1. Entanglement concentration	42
2. Entanglement purification	42
3. Linear-optical entanglement purification	43
E. Quantum repeater: towards long-distance quantum communication	46
1. Original theoretical proposal	46
2. Implementation with atomic ensembles and linear optics	47
3. Quantum state transfer between matter and photons: quantum memory	48
4. Quantum interference of independent photons	50
F. Free-space entanglement distribution	51
VIII. Quantum computing	52
A. Criteria for optical quantum computing	52
B. Linear-optical two-qubit logic gates	53
C. One-way quantum computing with photons	54
1. Cluster states and one-way quantum computing: general ideas	54
2. Linear-optical one-way quantum computing	56
3. Experimental one-way quantum computing	59
IX. Concluding Remarks	60
Acknowledgments	60
References	60

I. INTRODUCTION

In his 1704 treatise *Opticks* Newton claimed that light is composed of particles, but also introduced waves to explain the diffraction phenomena. Later on in classical Maxwellian electrodynamics the wave approach seemed to be sufficient. Yet, 201 year after Newton, during his *annus mirabilis* Albert Einstein re-introduced *lichtquanten* (light particles) and explained the photoelectric effect (Einstein, 1905).¹ The final theory, in which photons are elementary excitations of the quantized electromagnetic field interacting with charges, was given by Dirac (1927), and its internal consistency was proved by Dyson, Feynman, Schwinger and Tomonaga around twenty years later. Photons, as all quantum particles, reveal both wave-like and particle-like properties—a phenomenon known as wave-particle duality. The wave nature is revealed by interference, while the particle nature in detection events. The interference involving single photons, except from the discrete detection events (which could possibly be thought as due to discrete ionization events), does not reveal any non-classical phenomena. The real quantum effects begin with two or

more photon interference: a plethora of classically impossible phenomena occurs—most of them completely incomprehensible with any classical concepts. As always in the history of human scientific endeavor, harnessing of new phenomena leads to applications. The aim of this review is to describe the magic beauty of multiphoton manipulation, and its applications in amazing quantum protocols of communication, and even computation.

A. Quantum optics

An intensive research of the quantum properties of light started around half a century ago. Its advances allow one to gain a coherent control of quantum optical systems, enabling true quantum engineering. As a result, quantum optical methods made possible to actually perform *gedanken* experiments on the foundations of quantum theory. This control of quantum phenomena allows one to search for novel information processing paradigms, which now promise new technologies based on quantum information science.

Soon after Einstein’s introduction of light quanta, Taylor (1909) tried to find some new effects in a two-slit Young-type experiment using extremely faint light, so faint that on average only one photon at a time was inside the apparatus. No deviation from the classical interference was observed. Now, with fully developed theory of quantized light we know that experiments of this type cannot differentiate between the classical explanation (based on the interference of electric field waves) and the quantum explanation (based on the interference of probability amplitudes for photons passing through either of the two slits). The inherently “quantum nature of the electromagnetic field”, as we know now, is revealed directly only in multiphoton experiments, which, century ago, were impossible.

Still, quantum interference of *truly* individual photons is certainly a fascinating phenomenon. The first experiment aimed at that was performed by Grangier, Roger, and Aspect (1986). They used photon pairs emitted in atomic cascades, one of the photons was used as a trigger, and the other was fed into a Mach-Zehnder interferometer. The usual (wave-like) interference pattern was observed. Nevertheless, when the detectors were observing both output ports of the entry beamsplitter of the interferometer, besides background no coincidence was observed, i.e., a photon was detected only in one of the outputs – a typical particle-like behavior.

Modern quantum optics was effectively born in 1956 after the famous Hanbury-Brown and Twiss (1956) experiment on intensity interferometry. It was the first serious attempt to study the correlations between intensities recorded at two separated detectors. It motivated more sophisticated photon-counting and correlation experiments. The quantum theory of optical coherence of Glauber (1963) gave theoretical clues to search for unambiguously quantum optical phenomena. Carmichael

¹ The current term *photon* was introduced by Lewis (1926).

and Walls (1976) predicted photon antibunching in a resonance-fluorescence, which was observed experimentally by Kimble, Dagenais and Mandel (1977, 1978). The early experiments used atomic beams as sources. Thus, atomic number (and thus the emission statistics) fluctuations were unavoidable. Later, Diedrich and Walther (1987) realized such experiments using single atoms in traps and observed photon antibunching as well as sub-Poissonian statistics in the system. Squeezed states were experimentally generated by using four-wave mixing in atomic sodium (Slusher *et al.*, 1985) and in optical fibers (Shelby *et al.*, 1986), or by using an optical parametric oscillator (Wu *et al.*, 1986). We shall not discuss the above mentioned aspects of quantum optics, as an interested reader can find excellent presentations in, e.g., Walls and Milburn (1994), Mandel and Wolf (1995), Scully and Zubairy (1997), and Lounis and Orrit (2005).

The study on photon statistics and photon counting techniques enables a direct examination of some of the fundamental distinctions between the quantum and classical concepts of light. Parallel developments in neutron, atomic, and molecular interferometry, as well as modern methods of cooling and trapping ions, etc., allowed one to probe ever deeper the properties of *individual* quantum systems and to realize many of the *gedanken* (thought) experiments of fundamental interest in quantum physics. Central to these fundamental questions is the phenomenon of quantum entanglement.

B. The essence of quantum world: entanglement

Einstein, Podolsky and Rosen (EPR, 1935) suggested that quantum mechanics might be incomplete. The trio, EPR, tried to argue that the outcome of a measurement on a physical system is determined prior to and independent of the measurement (realism) and that the outcome cannot depend on any actions in space-like separated regions (Einstein’s locality). This EPR criterion of “local realism” looks quite reasonable to us, particularly as all our classical world and experience fully adhere to it. Moreover, they suggested that perfect quantum correlations, which occur for two particles in a maximally entangled state², can be used to define a missing element in quantum theory, namely, “elements of reality”.

The EPR paradox seemed to be interesting [see especially, (Feynman *et al.*, 1963)], but untestable for almost 30 years. Suddenly, Bell (1964) derived his inequalities which revealed that the two-particle correlations for the two spin- $\frac{1}{2}$ singlet disagree with any local realistic model. The pioneering “Bell experiment”, with polar-

ization entangled photons, was due to Freedman and Clauser (1972). It was refined in the famous experiments by Aspect *et al.* (1981, 1982a, 1982b) and followed by many others.³ The early experiments used polarization entangled photon pairs from atomic cascades (Clauser and Shimony, 1978). In late 1980’s this technique was overshadowed by parametric down conversion, and will not be discussed here.⁴

A quarter of century after Bell’s paper it turned out that the conflict of local realism with quantum mechanics⁵ is even more striking for certain three or more particle entangled states. The Greenberger-Horne-Zeilinger (GHZ) theorem (Greenberger, Horne, and Zeilinger, 1989; Greenberger *et al.*, 1990; Mermin, 1990a) showed that the concept of EPR’s elements of reality is self-contradictory.⁶ That is, there are situations for which local realism and quantum mechanics make completely opposite predictions, even for definite measurement results.⁷ The GHZ papers showed that three or more particle interferometry is a rich untested area, full of exciting paradoxical phenomena. However, at that time no effective sources of three or four photon entanglements were present. Thus, a new chapter in experimental multiphoton quantum optics had to wait for new ideas and experimental techniques.⁸

C. Sources of photonic entanglement

The standard source of entangled photon pairs is nowadays the nonlinear optical process of spontaneous parametric down-conversion (SPDC; see Burnham and Weinberg, 1970), the inverse of frequency up-conversion. In SPDC photons from a pump laser beam, within a nonlinear crystal, can spontaneously be converted into pairs that are momentum and frequency entangled, and in the so-called type-II process can be also polarization entangled (Kwiat *et al.*, 1995). Today, SPDC sources of entangled photon pairs with increasing quality and brightness can be routinely realized. New techniques, like entanglement due to two-photon emission from quantum dots

² The term entanglement was introduced by Schrödinger (1935). He regarded entanglement as *the* essential feature of quantum mechanics. Bohm’s version of the EPR thought experiment (Bohm, 1951) used the singlet state of two spin- $\frac{1}{2}$ particles, which is nowadays an icon and a yardstick of entanglement.

³ See Aspect (1999) and Tittel and Wiehs (2001) for a recent survey.

⁴ For a review of early experiments see (Clauser and Shimony, 1978).

⁵ Often, somehow misleadingly, such a conflict was described as “quantum nonlocality”.

⁶ Two-party versions of the GHZ contradiction were recently shown to exist (Cabello, 2001a, 2001b; Chen *et al.*, 2003).

⁷ We have “all-versus-nothing” proof (Mermin, 1990a) of Bell’s theorem.

⁸ The GHZ-type paradox was finally experimentally demonstrated with three-photon entanglement (Pan *et al.*, 2000). Next were experiments with four-photon GHZ paradox (Zhao *et al.*, 2003a) and two-photon hyper-entanglement GHZ-type paradox (Yang *et al.*, 2005, and in a slightly oversimplified version by Cinelli *et al.*, 2005).

(Stevenson *et al.*, 2006; Young *et al.*, 2006; Akopian *et al.*, 2006), also emerge.

However, since the GHZ paper, and even more after the birth of quantum information, three or more photon entanglement was in demand. It turned out that using the primary two-photon entanglement, by a procedure which is called entanglement swapping (Zukowski *et al.*, 1993), one can entangle without any direct interaction particles which were independent of each other, or what is more important for us, *construct* entanglement of higher order. Since photons basically do not interact with each other this method has a special importance in creating multi-photon entanglements. Practical versions of this technique (Zukowski *et al.*, 1995; Rarity, 1995; Zeilinger *et al.*, 1997) are behind all three or more entangled photon interference experiments.

D. Applications in quantum information

Quantum information processing was born once it was realized that the non-classical aspects of quantum mechanics give us a new set of phenomena, thus new practical applications are possible, especially in information transfer and processing.⁹ In quantum cryptography [Wiesner, 1983; Bennett and Brassard, 1984; Ekert, 1991; for a review see (Gisin *et al.*, 2002)] the complementarity of different measurements on a quantum system is used to establish a secret key shared by two partners, thus enabling for the first time a provably secure communication. In quantum teleportation (Bennett *et al.*, 1993) it is possible to faithfully transfer an unknown qubit state from one system to another by employing entangled states as a quantum channel and transfer of only two bits of classical information.¹⁰

Photons being the fastest information carriers have only very weak coupling to the environment, and are thus best suited for quantum communication tasks. Currently, quantum key distribution was realized for distances 144 km (Ursin *et al.*, 2007; Schmitt-Manderbach *et al.*, 2007) over a free space, and over more than 100 km in fiber (Rosenberg *et al.*, 2007; Peng *et al.*, 2007). Via optical fibers one could distribute photonic entangled states over more than 50 km (Marcikic *et al.*, 2004). Distribution of entanglement in the atmosphere over Vienna reached 7.8 km (Resch *et al.*, 2005) and even 13 km over Hefei (Peng

et al., 2005).¹¹

For quantum computation, implementations with localized systems like atoms, ions or solid-state devices seem to be preferable. Yet, surprisingly, even for quantum computation algorithms, photons offer interesting possibilities, despite the difficulty in storing them. After the discovery that some gates could be realized through teleportation (Gottesman and Chuang, 1999), an important breakthrough was the suggestion by Knill, Laflamme, and Milburn (2001) that even with linear optical elements, in principle, universal quantum computation could be realized. Following these suggestions, various quantum computation primitives have been demonstrated with photons alone (see section VIII.B). A new and probably more practical approach is the concept of a “one-way quantum computer” (Raussendorf and Briegel, 2001; Nielsen, 2004; for its linear optical implementation, see section VIII.C.2). The idea is to start with the so-called “cluster states”¹² (Briegel and Raussendorf, 2001). The computation algorithm is then performed by applying a sequence of one-qubit measurements. The cluster states, involving several entangled photons, have recently been realized (Zhang *et al.*, 2006a; Walther *et al.*, 2005b; Kiesel *et al.*, 2005; Schmid *et al.*, 2007; Lu *et al.*, 2007), and applied to demonstrate elementary quantum gates and algorithms (Walther *et al.*, 2005b).

World-wide laboratories are developing many different physical implementations both of quantum communication devices and of quantum gates. It will be interesting to see which technologies win.

E. Our aims

In this review, we want to highlight the exciting progresses, both theoretical and experimental, in multiphoton interferometry, with applications ranging from photonic quantum information processing to fundamental test of quantum mechanics. An emphasis will be given to the creation of photonic entanglements of various forms, and several important quantum information protocols with photons. Besides manipulation of photons with linear-optical elements, photons can also be manipulated by interaction with matter.

We shall try to make our review almost self-contained, by providing the basic tools for understanding these topics which are to be discussed in detail. Thus, e.g., we start with the general theory of photons and linear op-

⁹ To put it shortly, classical information can be encoded in bits (two fully distinguishable states), whereas quantum one is encoded in qubits (quantum superpositions of two fully distinguishable states). While classical information can be repeatedly and precisely copied, an unknown quantum state cannot be perfectly cloned—a statement known as the no-cloning theorem (Dieks, 1982; Wootters and Zurek, 1982). This is one of the most crucial differences between classical information and quantum one.

¹⁰ Note that to describe mathematically a quantum state one needs infinitely many bits.

¹¹ Both distances surpass the effective thickness of the atmosphere. The experiments imply that quantum communication via satellites could cover global distances.

¹² Cluster states [or, more generally, graph states (Hein *et al.*, 2004, 2006)] also play a significant role in other protocols of quantum information, like quantum error correction (Shor, 1995; Steane, 1996; Calderbank and Shor, 1996; Bennett *et al.*, 1996; Gottesman, 1997).

tics, next followed by basic tools and recipes for creating multiphoton entanglement. With these tools we then discuss fundamental tests of the completeness of quantum mechanics. This moves us to applications in quantum information.

F. Related reviews

There exist already many reviews or textbooks that cover topics strongly linked the current review, but not covered here. Here, we give a *partial* list. For an introduction to quantum information and quantum computation, textbooks by Nielson and Chuang (2000), by Bouwmeester *et al.* (2001) and by Preskill (1998) are widely used; for a short survey, see Bennett and DiVincenzo (2000). The linear optical quantum computing can be found in a recent review (Kok *et al.*, 2007), which is a nice supplement to the optical quantum computing part of this review. Quantum cryptography has been reviewed by Gisin *et al.* (2002) and thus will be mentioned here only for some basic concepts or specific purposes. Braunstein and van Loock (2005) review various aspects of quantum information with “continuous variables” (quantum variables like position and momentum). Zeilinger *et al.* (2005) gave a very concise survey on some photonic effects. For a detailed discussion on quantum entanglement, we refer to Alber *et al.* (2001) and Horodecki *et al.* (2007). Reviews on recent status of Bell’s theorem can be found in Laloë (2001), Werner and Wolf (2001), and Genovese (2005). The earlier stages of the research in photonic entanglement can be studied in Clauser and Shimony (1978) and Mandel and Wolf (1995).

II. INTERFERENCE: CLASSICAL VS. QUANTUM

Classical interference is a macroscopic expression of the quantum one. The interference phenomena in the quantum realm are richer and more pronounced. We discuss here the basic differences between the classical interference understood as interference of waves in space, and quantum one which is interference of various, operationally indistinguishable processes.

A. Classical interference

In classical physics interference results from the superposition of waves. It may express itself in the form of intensity variations or intensity correlations.

1. Interference expressed by intensity variations

Consider two quasi-monochromatic plane waves linearly polarized in the same direction, described by

$$E_j(\mathbf{r}, t) = E_j e^{i[\mathbf{k}_j \cdot \mathbf{r} - \omega t - \phi_j(t)]} + c.c. \quad (1)$$

where E_j is the real amplitude of one of the fields, \mathbf{k}_j the wave vector, ω the frequency of both waves, $j = 1, 2$ the index numbering the fields, and finally *c.c.* denotes the complex conjugate of the previous expression. The intensity of the superposed fields at a certain point in space is given by

$$I(\mathbf{r}, t) = E_1^2 + E_2^2 + 2E_1E_2 \cos[\Delta_{12}\mathbf{k} \cdot \mathbf{r} - \Delta_{12}\phi(t)], \quad (2)$$

where Δ_{12} is the difference of the respective parameters for the two fields, e.g., $\Delta_{12}\phi(t) = \phi_1(t) - \phi_2(t)$. For $\Delta_{12}\phi(t)$ constant in time, or of values varying but always much less than π , this formula (after averaging over time) describes a Young-type interference pattern. In the opposite case, of widely fluctuating $\Delta_{12}\phi(t)$ no interference can be observed, because the pattern washes out. In the case of $E_1 = E_2$ one has maximal possible interference. This can be expressed in terms of the interferometric contrast, or visibility, $V = (I_{max} - I_{min}) / (I_{max} + I_{min})$, which in the aforementioned case is 1.

2. Interference in intensity correlations

Hanbury-Brown-Twiss experiment introduced to optics the intensity correlation measurements. Such correlations at two points in space and two moments of time, for two classical fields are described by the intensity correlation function

$$G^{(2)}(\mathbf{r}_1, t_1; \mathbf{r}_2, t_2) = \langle I(\mathbf{r}_1, t_1)I(\mathbf{r}_2, t_2) \rangle_{av} . \quad (3)$$

The average is taken over an ensemble, and for stationary fields this is equivalent to the temporal average. Even when no intensity variations are observable (i.e., for averaged intensity constant in space), the intensity correlations can reveal interference effects. Assume that the phases of the two fields fluctuate independently of one another. Then for $t_1 = t_2$, the $G^{(2)}$ function still exhibits a spatial modulation or maximal visibility of 50% exhibited by the formula:

$$G^{(2)}(\mathbf{r}_1, t; \mathbf{r}_2, t) = (I_1 + I_2)^2 + 2I_1I_2 \cos[(\Delta_{12}\mathbf{k})(\mathbf{r}_1 - \mathbf{r}_2)] , \quad (4)$$

where $I_i = E_i^2$, $i = 1, 2$. This formula can be easily reached by noting that the temporal average of

$$\cos[\alpha + \Delta_{12}\phi(t)] \cos[\alpha' + \Delta_{12}\phi(t)], \quad (5)$$

where $\Delta\phi(t) = \phi_1(t) - \phi_2(t)$, is given by

$$\begin{aligned} & \cos \alpha \cos \alpha' \langle \cos^2 \Delta_{12}\phi(t) \rangle_{av} + \\ & \sin \alpha \sin \alpha' \langle \sin^2 \Delta_{12}\phi(t) \rangle_{av} - \\ & \frac{1}{2} \sin(\alpha + \alpha') \langle \sin 2\Delta_{12}\phi(t) \rangle_{av}, \end{aligned} \quad (6)$$

and due to the random nature of $\Delta_{12}\phi(t)$ only the first two terms survive because both $\langle \cos^2 \Delta_{12}\phi(t) \rangle_{av}$ and $\langle \sin^2 \Delta_{12}\phi(t) \rangle_{av}$ give $\frac{1}{2}$, whereas $\langle \sin 2\Delta_{12}\phi(t) \rangle_{av} = 0$.

In addition to the phase fluctuations one can take into account also amplitude fluctuations. Nevertheless, the basic features of the earlier formula must be retained, as the amplitude fluctuations tend to lower even further the visibility of the intensity correlations patterns. Thus, the visibility of intensity correlations is never full, maximally 50%. As we shall see there is no bound on visibility in the quantum case. For a broader treatment of these matters see Paul (1986).

B. Quantum interference

Quantum interference rests on the concept of superposition of probability amplitudes.

1. Single-particle quantum interference

The single-particle interference looks almost identical to the classical one. We replace the fields (waves) by amplitudes, $A(\mathbf{x}, t)$, which differ only by the fact that they are suitably normalized. Suppose that the amplitude to detect a photon at \mathbf{x} , is given by

$$A_{\mathbf{b}_1}(\mathbf{x}, t) = e^{i[\mathbf{k}_1 \cdot (\mathbf{x} - \mathbf{b}_1) + \Phi_{\mathbf{x}, \mathbf{b}_1}(t)]}, \quad (7)$$

if it originates from point \mathbf{b}_1 , and by

$$A_{\mathbf{b}_2}(\mathbf{x}, t) = e^{i[\mathbf{k}'_1 \cdot (\mathbf{x} - \mathbf{b}_2) + \Phi_{\mathbf{x}, \mathbf{b}_2}(t)]}, \quad (8)$$

it originates from \mathbf{b}_2 . The quantum mechanical probability density that a particle is detected at \mathbf{x} is given by

$$\begin{aligned} P(\mathbf{x}_1, t) &\sim |A_{\mathbf{b}_1}(\mathbf{x}, t) + A_{\mathbf{b}_2}(\mathbf{x}, t)|^2 \\ &\sim 1 + \cos[\Delta\mathbf{k}_1 \cdot \mathbf{x} + \Phi_0 + \Phi_{\mathbf{x}, \mathbf{b}_1}(t) - \Phi_{\mathbf{x}, \mathbf{b}_2}(t)], \end{aligned} \quad (9)$$

where $\Delta\mathbf{k}_1 = \mathbf{k}'_1 - \mathbf{k}_1$, and Φ_0 is an irrelevant constant phase. Thus if the phase difference, $\Phi_{\mathbf{x}, \mathbf{b}_1}(t) - \Phi_{\mathbf{x}, \mathbf{b}_2}(t)$, is stable, one can have the Young-type interference patterns of up to 100% visibility. Such a stable phase difference can be secured in, e.g., double-slit experiment. Classical intensity is simply the probability density times the initial intensity I_0 of the stream of particles.

As we see this description differs a lot from the classical *particle* picture, in which one would expect that a process originating with state A and with possible intermediate stages B_1, \dots, B_N , leading to an event C , would be described by

$$P(C|A) = \sum_{j=1}^N P(C|B_j)P(B_j|A) \quad (10)$$

In the quantum case $P(C|A) = |\langle C|A \rangle|^2$, but one has

$$\langle C|A \rangle = \sum_{j=1}^N \langle C|B_j \rangle \langle B_j|A \rangle \quad (11)$$

In our case $\langle A|B_j \rangle = \frac{1}{\sqrt{2}}$ are the amplitudes to reach the slits, $\langle C|B_j \rangle = A_{\mathbf{b}_j}$, and $N = 2$.

The difference between (10) and (11) is in the assumption [inherent in (10)] that the particle had to be in *one* of the intermediate situations (states) B_i . In the quantum case any attempt to verify which of the situations actually took place by measurement¹³ puts one back to the classical formula (10). The formula (11) leads to interference phenomena, and may be thought as a manifestation of a wave nature of particles, whereas, if we make measurements at B_i , we learn by which way (*welcher weg*) the particles travel, and the particle nature pops up. We have a wave-particle duality, which seems to describe all that.

2. Two-particle quantum interference

All this becomes much more puzzling once we consider a two-particle experiment. Already, Einstein, Podolsky and Rosen (1935) pointed out some strange features of such a case. Schrödinger noticed that these features are associated with what he called “entangled states”, which will be discussed in detail later. At the moment consider these as superpositions of fully distinguishable products of single-particle states, by which we mean that there is a specific pair of local measurements for which the two subsystems are perfectly correlated (a result of measurement on one immediately reveals the unique value of the other observable for the second subsystem, which is correlated with the result).

Consider such a correlation: assume that if particle 1 is at b_1 , then particle 2 is also at b_1 , and, whenever 1 is at b_2 then particle 2 is at b_2 . Later on the particles are detected at two different point, \mathbf{x}_1 and \mathbf{x}_2 . Then, according to the rules given above

$$\begin{aligned} P(\mathbf{x}_1, \mathbf{x}_2, t) &\sim |A_{b_1}(\mathbf{x}_1, t)A_{b_1}(\mathbf{x}_2, t) + A_{b_2}(\mathbf{x}_1, t)A_{b_2}(\mathbf{x}_2, t)|^2 \\ &\sim 1 + \cos(\Delta\mathbf{k}_1 \cdot \mathbf{x}_1 + \Delta\mathbf{k}_2 \cdot \mathbf{x}_2 + \Delta\Phi_{b_1, b_2}), \end{aligned} \quad (12)$$

with

$$\Delta\Phi_{b_1, b_2} = \Delta\Phi_{\mathbf{x}_1, b}(t) + \Delta\Phi_{\mathbf{x}_2, b}(t) + \Phi'_o,$$

where the amplitudes for the second particle are given by formulas (7) and (8), with \mathbf{x}_2 replacing \mathbf{x}_1 and \mathbf{k}_2 replacing \mathbf{k}_1 , and $\Delta\Phi_{\mathbf{x}_i, b}(t) = \Phi_{\mathbf{x}_i, b_1}(t) - \Phi_{\mathbf{x}_i, b_2}(t)$, with $i = 1, 2$. Thus if the phase relation between the two amplitudes is stable one can have absolutely noiseless interference with

¹³ Or by securing the possibility of a postponed measurement (which could be made by correlating our particle, while it is at the intermediate stage B_i , with another system, which could be measured later).

100% visibility, while there is no single particle interference:

$$P(\mathbf{x}_1, t) = \int d\mathbf{x}_2 P(\mathbf{x}_1, \mathbf{x}_2, t) = \text{const.}$$

As we shall see, the unbounded visibility is not the only feature by which such interference differs from classical one. For more details see, e.g., Bialynicki-Birula and Bialynicka-Birula (1975).

C. Other interference phenomena

There is a plethora of other strictly quantum interference phenomena, associated with photons which are in specific quantum states. These phenomena are of an entirely non-classical character. In the next chapters we shall present many such interference effects (particularly, see section IV.C). However, as the non-classicality is linked with entanglement, we have to present first some basic properties of this phenomenon, and later on we shall present experimental techniques to get entanglements in various forms.

III. PHOTONIC QUBITS AND LINEAR OPTICS

The possibility of applying coherent control of quantum optical systems to perform quantum information-processing tasks is based on the fact that quantum information can be encoded in quantum states of certain degrees of freedom (e.g., polarizations or spatial modes) of individual photons, and these individual photons can be manipulated by simple optical elements (e.g., various linear-optical elements and interferometers), or by letting them interact with matter (trapped ions, atoms and so on) at a photon-matter interface. Here we shall show to what extent a photon can represent a qubit, and the simplest elements that are used to manipulate it. To this end, let us first begin with a formal definition of photons and their states, i.e., the Fock states.

A. Photon-number states

The formal theory of quantization of electromagnetic field was formulated by Dirac (1927). Here we only give its basic mathematical devices for completeness; for detailed treatment, we refer to standard textbooks on quantum optics, e.g., Walls and Milburn (1994), Mandel and Wolf (1995), Scully and Zubairy (1997).

A single-photon pure state can be characterized by a specific wave packet profile $g_{\lambda\mathbf{k}}$, i.e., by the quantum amplitudes for a given momentum \mathbf{k} and polarization λ . According to the Born rule $|g_{\lambda\mathbf{k}}|^2$ gives the probability density of measuring the single photon with the momentum $\hbar\mathbf{k}$ and polarization λ . Thus, one has

$\sum_{\lambda=1,2} \int d\mathbf{k} |g_{\lambda\mathbf{k}}|^2 = 1$. The wave packet profiles are vectors in a Hilbert space with a scalar product given by

$$\langle g|h \rangle = \sum_{\lambda=1,2} \int d\mathbf{k} g_{\lambda\mathbf{k}}^* h_{\lambda\mathbf{k}}. \quad (13)$$

One can introduce an arbitrary orthonormal basis $g^l(\lambda\mathbf{k})$, where l are natural numbers and $\langle g^n|g^m \rangle = \delta_{nm}$. Two different orthonormal bases, to be denoted respectively as primed, and unprimed, are related by a unitary operation: $g'^m = \sum_{l=1}^{\infty} U_{ml} g^l$. The complex numbers U_{lm} satisfy $\sum_{n=1}^{\infty} U_{ml} U_{kl}^* = \sum_{l=1}^{\infty} U_{lm}^* U_{lk} = \delta_{mk}$. One can choose a specific basis of the wave packet profiles of the single photon, say g_l , and with each element of such a basis one associates a quantum oscillator-like construction to introduce number states, namely, the Fock states. One introduces the vacuum state $|\Omega\rangle$, the state with no photons at all. Next for a chosen basis wave packet profiles g_l one associates a pair of operators satisfying the usual relations for creation and annihilation operators, namely, $[\hat{a}_l, \hat{a}_l^\dagger] = 1$ and requires that $\hat{a}_l|\Omega\rangle = 0$. Using the standard oscillator algebra one constructs the state $\frac{\hat{a}_l^{\dagger n_l}}{\sqrt{n_l!}}|\Omega\rangle$, which is the state of the electromagnetic field in which one has n_l identical photons of the same wave packet profile g^l , and no other photons elsewhere. This is denoted by $|0, \dots, 0, n_l, 0, 0, \dots\rangle$. Finally, one assumes that $[\hat{a}_n, \hat{a}_m] = 0$ and $[\hat{a}_n, \hat{a}_m^\dagger] = \delta_{nm}$, that is, creation and annihilation operators of photons with orthogonal wave packet profiles always commute. A general (normalized) basis state of the Fock space is therefore of the following form:

$$|n_1, n_2, n_3, \dots\rangle = \prod_{l=1}^{\infty} \frac{\hat{a}_l^{\dagger n_l}}{\sqrt{n_l!}} |\Omega\rangle. \quad (14)$$

All vectors of the Fock space are linear combinations of the above basis states, which have a finite norm. It is easy to see that if one defines the creation operators with respect to an alternative basis of wave packet profiles (here the primed ones) one has:

$$\hat{a}'_m{}^\dagger = \sum_{n=1}^{\infty} U_{mn} \hat{a}_n^\dagger. \quad (15)$$

The vacuum state is invariant with respect to such transformation, i.e., one still has $\hat{a}'_m|\Omega\rangle = 0$.

B. Photonic qubits

A quantum bit, or *qubit*, is the most elementary carrier of quantum information. It is a generalization of the classical bit, which is used to encode classical information. A classical bit has two distinguishable states “0” and “1”. The same holds for a qubit. But since it is a carrier of quantum information with its two distinguishable (orthogonal) states $|0\rangle$ and $|1\rangle$ (which form the

so-called computational basis), it can also be prepared, in contradistinction to its classical counterpart, in any superposition of these two states:

$$|\Psi_{qubit}\rangle = \alpha_0|0\rangle + \alpha_1|1\rangle. \quad (16)$$

Thus, a qubit can do everything that is expected from a bit, but additionally has powers which bits do not have.

Any two-level quantum system can represent a qubit.¹⁴ Thus, an archetypal qubit is spin-1/2. But experiments with spin-1/2 systems are difficult. Fortunately, photons possess a ready and easily controllable qubit degree of freedom: polarization. As we shall see, there are also other methods to make photons carry qubits.

Polarization qubits.—The most commonly used photonic qubits are realized using polarization. In this case arbitrary qubit states can be $\alpha_0|H\rangle + \alpha_1|V\rangle$, where H and V stand for horizontal and vertical polarizations, respectively. The advantage of using polarization qubits stems from the fact that they can easily be created and manipulated with high precision (at 99% level) by simple linear-optical elements such as polarizing beam splitters (PBS), polarizers and waveplates.

Spatial qubits.—A single photon can also appear in two different spatial modes or paths, a and b : the general state reads $\alpha_0|a\rangle + \alpha_1|b\rangle$. This may occur, e.g., if a single photon exits a beamsplitter (BS), with two output modes a and b . Any state of spatial qubits can be prepared by using suitable phase shifters and beamsplitters. A disadvantage of using spatial qubits is that the coherence between $|a\rangle$ and $|b\rangle$ is sensitive to the relative phase for the paths a and b between BS, and this is difficult to control in long-distance cases.

Time-bin qubits.—For a more robust long-distance transmission of quantum information, one can use *time-bin* qubits. The computational basis consists of two states which are of the same spectral shape, but time shifted by much more than the coherence time: $|early\rangle$ and $|late\rangle$. Any state of time-bin qubits¹⁵ can be realized as following. Suppose that a single-photon pulse is sent through an unbalanced Mach-Zehnder interferometer. Its wavepacket is split by the first BS, with transmission coefficient $T = |\alpha_0|^2$ and reflection coefficient $R = |\alpha_1|^2$ into two pulses. The transmitted one propagates along

the short arm, and the reflected one along the long arm. If the pulse duration is shorter than the arm length difference, the output from of the output ports of the second, 50:50, exit BS is two wavepackets well separated in time. If no photon is registered in say output port I, in the other output one has a single photon in a coherent superposition of two time-bin states $\alpha_0|early\rangle + \alpha_1|late\rangle$. The phase relation can be controlled with a phase shifter in one of the arms of the interferometer. For more details, see the comprehensive review by Gisin *et al.* (2002).

While in this review we are mainly concerned with the above three implementations of photonic qubits, one should keep in mind that other implementations are possible. In a recent experiment, Madsen *et al.* (2006) realized a photonic frequency qubit represented by two resolved frequencies. Meanwhile, quantum d -level (high-dimensional) systems (“qudit”) can also be realized using, e.g., orbital angular momentum states of photons (Mair *et al.*, 2001), or using simultaneously two or more degrees of freedom listed above. For instance, for the latter case a polarized single photon in a coherent superposition of two spatial modes is a ideal realization of quantum system in a four-dimensional Hilbert space (Chen *et al.*, 2003).

Bell states of polarization qubits.—Two qubits can form entangled states. Particularly interesting are the so-called Bell states, which form a basis in the four-dimensional two-qubit state space, which has the property that all its members are maximally entangled. The Bell states of photonic polarization qubits can be, for example:

$$\begin{aligned} |\psi^\pm\rangle_{12} &= \frac{1}{\sqrt{2}} (|H\rangle_1 |V\rangle_2 \pm |V\rangle_1 |H\rangle_2) , \\ |\phi^\pm\rangle_{12} &= \frac{1}{\sqrt{2}} (|H\rangle_1 |H\rangle_2 \pm |V\rangle_1 |V\rangle_2) . \end{aligned} \quad (17)$$

C. Simple linear-optical elements

In the photonic domain, quantum states of photons can be easily manipulated by simple passive linear-optical devices [see Leonhardt (2003) for a survey] with a high precision, at about 99% level. These linear-optical elements include beamsplitter (BS), polarizing beamsplitter (PBS), half- and quarter-wave plates and phase shifters. Classically, such devices conserve energy: Total input energy equals the total output energy, and there is no energy transfer between different frequencies. A passive linear optical device is described by a unitary transformation of annihilation operators for the same frequency:

$$\hat{a}_m^{out} = \sum_n U_{mn} \hat{a}_n^{in}, \quad (18)$$

where U is a unitary matrix, and the indices denote a basis of orthogonal modes with the same frequency.

The BS is one of the most important optical elements. It has two spatial input modes a and b and two output modes c and d (Fig. 1). The theory of the lossless BS was developed by Zeilinger (1981), and Fearn and Loudon

¹⁴ Qubits can only be implemented approximately, though the approximation could be rather good. For a single photon, its states can be characterized by its frequency spectrum, time of arrival, transverse momentum, and so on. All of these variables have to be controlled precisely to ensure that the photon represents within a good approximation a qubit with only two distinct quantum states.

¹⁵ It was usually thought that arbitrary single-qubit operations are very difficult to implement for time-bin qubits (Kok *et al.*, 2007). However, using the “time-path transmitter” introduced by Chen *et al.* (2006d), one could map a time-bin qubit state into a path qubit state which can be subject to arbitrary single-qubit operations. A reverse time-path transmitter will map the rotated path state back to the time-bin state.

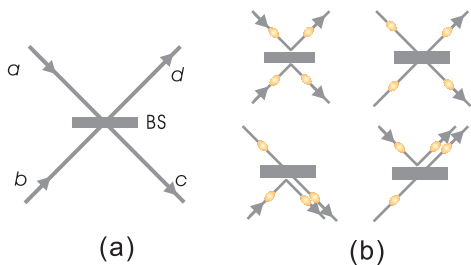


FIG. 1 The function of a BS. (a) The BS coherently transforms two input spatial modes (a, b) into two output spatial modes (c, d). (b) Two particles incident onto the BS, one from each side. Four possibilities exist how the two particles can leave the BS.

(1987). For lossy BS, see Barnett *et al.* (1989). In a simplified theory of a BS, one assumes identical action for every relevant frequency. Quantum mechanically, the action of the BS on the incident modes of a given frequency can be written as

$$\begin{pmatrix} \hat{c} \\ \hat{d} \end{pmatrix} = U \begin{pmatrix} \hat{a} \\ \hat{b} \end{pmatrix}. \quad (19)$$

where U is a unitary 2×2 matrix. Thus one can always construct a BS which is capable of performing a specific $U(2)$ transformation of the annihilation operators for the modes.

The most commonly used BS is the symmetric 50:50 BS characterized by the following transformation

$$\begin{aligned} a &\longrightarrow \frac{1}{\sqrt{2}}c + \frac{i}{\sqrt{2}}d, \\ b &\longrightarrow \frac{i}{\sqrt{2}}c + \frac{1}{\sqrt{2}}d. \end{aligned} \quad (20)$$

Here an outgoing particle can be found with equal probability (50%) in either of the output modes c and d , no matter through which single input beam it came. The factor i in Eq. (20) is a consequence of unitarity. It describes a phase jump upon reflection (Zeilinger, 1981). A standard BS is polarization independent.

Using two 50:50 BS and phase shifters one can build a universal BS, which is called Mach-Zehnder interferometer. This device performs the following unitary transformation:

$$U_{MZ} = U_\psi U_{BS} U_\theta U_{BS} U_\phi, \quad U_\xi = \begin{pmatrix} 1 & 0 \\ 0 & e^{i\xi} \end{pmatrix}. \quad (21)$$

It is elementary to show that it is capable of performing any two-dimensional $U(2)$ unitary transformation. A $U(2)$ matrix can always be decomposed in the following way

$$\begin{aligned} \mathcal{U}(2) &= e^{i\gamma/2} \begin{pmatrix} e^{i\alpha/2} & 0 \\ 0 & e^{-i\alpha/2} \end{pmatrix} \begin{pmatrix} \cos \frac{\theta}{2} & \sin \frac{\theta}{2} \\ -\sin \frac{\theta}{2} & \cos \frac{\theta}{2} \end{pmatrix} \\ &\times \begin{pmatrix} e^{i\beta/2} & 0 \\ 0 & e^{-i\beta/2} \end{pmatrix}. \end{aligned} \quad (22)$$

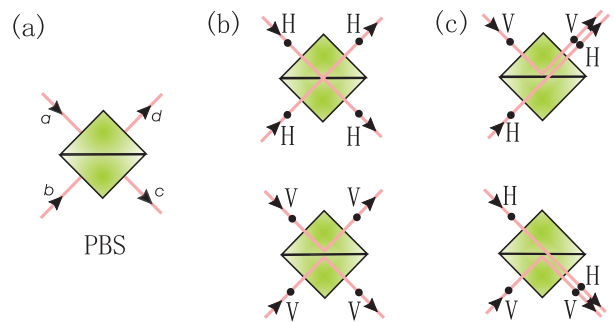


FIG. 2 The function of a PBS. (a) The PBS transmits horizontal, and reflects vertical, polarization. (b) If the two photons incident onto the PBS have identical polarization, then they will always go out along different directions, so there will be one photon in each of the two output modes. (c) On the other hand, if the two incident photons have opposite polarization, then they will always go out along the same direction, so there will be two photons in one of the two outputs and none in the other. In essence, a PBS can thus be used as a polarization comparer (Pan and Zeilinger, 1998; Pan *et al.*, 2001b).

The two input modes gain a relative phase β , and further on are optically mixed with the reflection and transmission coefficients $R = \sin^2 \frac{\theta}{2}$ and $T = \cos^2 \frac{\theta}{2}$, respectively, finally the output modes acquire the relative phase α and the overall phase $\gamma/2$. All that can be done using a Mach-Zehnder interferometer.

Another important component is the polarizing beam-splitter (see Fig. 2). The standard PBS transmits the horizontal and reflects the vertical polarization. The transformations between the incoming modes (a and b) and the outgoing modes (c and d) is as follows

$$\hat{a}_H \rightarrow \hat{c}_H \text{ and } \hat{a}_V \rightarrow \hat{d}_V; \quad \hat{b}_H \rightarrow \hat{d}_H \text{ and } \hat{b}_V \rightarrow \hat{c}_V \quad (23)$$

by replacing the BS in Fig. 1 with the PBS.

For polarization qubits, any single-qubit operation can be accomplished by using a sequence of suitably oriented quarter- and half-wave plates. Simply, a half-wave plate retarding the 45° polarization acts on the H and V modes exactly as a certain 50:50 BS, etc. Now, the input modes are two orthogonal polarizations instead of two orthogonal spatial input modes of a Mach-Zehnder interferometer. The rotation matrix is identical with (22). Thus one can implement any single-qubit operation on polarization qubits.

Lastly, in certain interferometric setups, one often needs to add phase shift along a path. Physically, this is realized by using a slab of transparent material with an index of refraction that is different from the one for free space. The phase shift is determined by the thickness of the material and the index of refraction, or alternatively, by changing the path length differences between interferometric arms.

With these simple optical elements, large optical networks can be constructed, mapping an input state onto

an output state via a *linear* transformation determined by the networks. As a possible generalization of the usual interferometers with two ports, an N -port interferometer was proposed by Reck *et al.* (1994), which can realize any $U(N)$ transformation for N optical spatial modes by using an arrangement of BS, phase shifters and mirrors. Weihs *et al.* (1996) realized an all-fiber three-path Mach-Zehnder interferometer, which is based on the idea of symmetric unbiased multiport beamsplitters (Zeilinger *et al.*, 1993). However, this device is not capable to produce an arbitrary $U(N)$ transformation.

However, for certain applications (e.g., realizing two-photon quantum gates) nonlinearity, i.e., photon-photon interaction, is explicitly required. This kind of nonlinearity can be accomplished either by medium-induced photon-photon interactions (such as the nonlinearity in a Kerr medium, known as the Kerr nonlinearity) or by measurement-induced effective optical nonlinearity. The currently available Kerr nonlinearity is too tiny to be useful for the specified purpose. The effective nonlinearity induced by standard projective measurements (detection events) is now recognized as a feasible way of implementing, e.g., probabilistic two-qubit gates with photons (Knill, Laflamme, and Milburn, 2001; Kok *et al.*, 2007).

D. Quantum interference due to indistinguishability of particles: the Hong-Ou-Mandel dip

Quantum interference may occur also entirely due to indistinguishability of particles. We shall present this for photons, i.e., bosons. One can obtain all effects due to the indistinguishability by suitable symmetrization of the amplitudes for elementary processes, in which we do not know which particle ended up in a given final state (for bosons amplitudes do not change sign when particles are interchanged). However it is much more convenient to use the formalism of bosonic creation and annihilation operators (see subsection III.A), as its algebra directly takes into account the symmetrization. Here we shall present the most elementary optical effect due to the indistinguishability of photons, the Hong-Ou-Mandel interference behind a beamsplitter.

As we have seen previously, upon reflection off a symmetric 50:50 beamsplitter (with input modes a_1 and a_2 and output modes b_1 and b_2) a photon picks a phase shift i . Thus, if we have two spectrally identical photons each hitting at the same moment an opposite input port of the beamsplitter, the initial state $\hat{a}_1^\dagger \hat{a}_2^\dagger |\Omega\rangle$, where 1, 2 denote the input ports, is transformed into

$$\frac{1}{\sqrt{2}}(\hat{a}_1^\dagger + i\hat{a}_2^\dagger) \frac{1}{\sqrt{2}}(\hat{a}_2^\dagger + i\hat{a}_1^\dagger) |\Omega\rangle = i \frac{1}{2}(\hat{a}_1^{\dagger 2} + \hat{a}_2^{\dagger 2}) |\Omega\rangle.$$

Since $i^2 = -1$, this results in the cancellation of the two terms, which describe the cases in which each photon exits by a different exit port (the exit port reachable via transmission from the given input port shares the index with it). This cancellation occurs due to the

assumed perfect indistinguishability of the two photons ($\hat{a}_1 \hat{a}_2 = \hat{a}_2 \hat{a}_1$). The final state reads $i \frac{1}{2}[(\hat{a}_1^\dagger)^2 + (\hat{a}_2^\dagger)^2] |\Omega\rangle$, namely, the two photons will exit the BS at the same output port—the so-called photon’s bunching effect due to the bosonic character of photons, and there are no coincidences between the output ports.

The fourth-order interference of two photons described above constitutes the basis of the Hong-Ou-Mandel dip in coincidence recording between two single-photon detectors in modes b_1 and b_2 as function of the flight time difference of the incident photons; no coincidence can be observed for zero flight time difference for the usual symmetric spatial state of the two photons.¹⁶

If the photons are not indistinguishable (in this case we shall describe them by annihilation operators \hat{a} and \hat{b}) the initial state $\hat{a}_1^\dagger \hat{b}_2^\dagger |\Omega\rangle$ is transformed into

$$\frac{1}{\sqrt{2}}(\hat{a}_1^\dagger + i\hat{a}_2^\dagger) \frac{1}{\sqrt{2}}(\hat{b}_2^\dagger + i\hat{b}_1^\dagger) |\Omega\rangle.$$

Since $a \neq b$ there is no cancellation of the terms. The following terms contribute to the cases in which each photon exits by a different exit port: $\frac{1}{2}(\hat{a}_1^\dagger \hat{b}_2^\dagger - \hat{a}_2^\dagger \hat{b}_1^\dagger) |\Omega\rangle$. The probability of such an event is given by the square of the norm of this component of the state. In general $\hat{b} = \alpha^* \hat{a} + \beta^* \hat{c}$, with $|\alpha|^2 + |\beta|^2 = 1$, and \hat{c} being an annihilation operator of a photon that is totally distinguishable from the photon \hat{a} . Simply, α is the overlap amplitude of the two wave packet profiles. Thus, we get

$$\begin{aligned} & \frac{1}{2}(\hat{a}_1^\dagger(\alpha\hat{a}_2^\dagger + \beta\hat{c}_2^\dagger) - \hat{a}_2^\dagger(\alpha\hat{a}_1^\dagger + \beta\hat{c}_1^\dagger)) |\Omega\rangle \\ &= \frac{1}{2}(\hat{a}_1^\dagger \beta \hat{c}_2^\dagger - \hat{a}_2^\dagger \beta \hat{c}_1^\dagger) |\Omega\rangle \end{aligned}$$

The norm of this vector is $\frac{1}{4}2|\beta|^2$. Thus, if $|\beta| = 1$ implying that the photons \hat{a} and \hat{b} are absolutely distinguishable, this probability reads $1/2$; if $\beta = 0$ implying that the photons are indistinguishable, it vanishes. Therefore, the Hong-Ou-Mandel effect depends entirely on the distinguishability of photons.

IV. ENTANGLEMENT AND COMPLETENESS OF QUANTUM MECHANICS

Entanglement, according to Erwin Schrödinger (1935)—the inventor of this term—contains “*the essence of quantum mechanics*”. Consider a spin-0 particle which decays into two spin-1/2 particles (Bohm, 1951). The quantum state is such that along any chosen direction, say the

¹⁶ The two incident photons can also be in an antisymmetric spatial state (which occurs if the two-photon polarization state is also antisymmetric). In this case, the two amplitudes interfere constructively. This results in the two photons always exiting in separate beams for zero flight time difference (antibunching), namely, a coincidence peak (instead of dip) appears here.

z -axis, the spin of particle 1 can either be up or down, which in turn, by momentum conservation, implies that for particle 2 it is down or up. The spin state is the rotationally invariant singlet

$$|\psi\rangle_{12} = \frac{1}{\sqrt{2}}(|+\rangle_1|-\rangle_2 - |-\rangle_1|+\rangle_2), \quad (24)$$

where, e.g., $|+\rangle_1$ describes the state of particle 1 with its spin up along the z -direction. The minus sign is necessary to get the rotational invariance. The state describes a coherent superposition of the two product states: there is no information in *the whole Universe* on which of the two possibilities will be detected at the measurement stage. None of those two possibilities is the actual case. Actualization can happen only via a measurement. This superposition, like any other, e.g. in the famous double slit experiment, survives as long as no measurement actualizing one of those possibilities is performed, and the particles do not interact with any environment. None of the possibilities actually takes place, but both of them affect the predictions for all measurements. Another property of the state (24) is that it does not make *any* prediction about an individual spin measurement on one of the two particles, the results are random. The spin state of one of the particles is described by a reduced density operator, which is a totally random state $\frac{1}{2}I$, where I is the unit operator. All information contained in the state in Eq. (24) defines only joint properties (Schrödinger, 1935): *the two spins, if measured with respect to the same direction, will be found opposite*. As a matter of fact this property fully defines the singlet state.

Imagine that the two particles are far apart, one in the laboratory of Alice and the other one in Bob's. As soon as Alice measures the value of a spin projection along some axis, new information is gained, and for her the state of Bob's particle is well defined. This is independent of the spatial separation between them. Thus a state like (24) is a perfect device to study, and reveal, the EPR paradox,¹⁷ and its consequences. Basically, all earlier studies of entanglement concentrated on that aspect of such states [for a review see (Clauser and Shimony, 1978)]. Later, we saw an emergence of research on en-

tanglement of three or more particles, practically with the advent of quantum information.

A. Formal theory of entanglement

The most important tool for the analysis of pure states of two subsystems is the so-called Schmidt decomposition. For any pure state, $|\Psi\rangle$, of a *pair* of subsystems, one described by a Hilbert space of dimension N , the other by a space of dimension M , say $N \leq M$, one can find preferred bases, one for the first system, the other one for the second, such that the state is a sum of bi-orthogonal terms, i.e.,

$$|\Psi\rangle = \sum_{i=1}^N r_i |a_i\rangle_1 |b_i\rangle_2 \quad (25)$$

with ${}_n\langle x_i | x_j \rangle_n = \delta_{ij}$, for $x = a, b$ and $n = 1, 2$. The coefficients r_i are real. The appropriate single subsystem bases, here $|a_i\rangle_1$ and $|b_j\rangle_2$, depend upon the state. A proof of Schmidt decomposition can be found in the book by Peres (2002). A Generalization of Schmidt decomposition to more than two subsystems is not straightforward [see (Carteret, Higuchi, and Sudbery, 2000)]. It is easy to show that the two reduced density matrices of (25) are endowed with the same spectrum. This does not hold for three or more particle subsystems.

Thus, every pure state of two spins can be put into the following form:

$$\cos(\alpha/2) |+\rangle_1 |+\rangle_2 + \sin(\alpha/2) |-\rangle_1 |-\rangle_2,$$

where the states $|\pm\rangle_n$, $n = 1, 2$, are the eigenstates of the $\mathbf{z}^{(n)} \cdot \sigma^{(n)}$ operator. The unit vectors $\mathbf{z}^{(n)}$ are individually defined for each of the particles. They define the basis for the Schmidt decomposition for each of the subsystems.

More complicated is the theory of entanglement of mixed states. A state (pure or mixed) described by a density matrix ρ_{AB} of a composite quantum system consisting of two generic sub-systems A and B is separable if and only if ρ_{AB} is a convex combination of local density matrices, ρ_A^λ and ρ_B^λ , of the two sub-systems, namely, $\rho_{AB} = \sum_\lambda p_\lambda \rho_A^\lambda \otimes \rho_B^\lambda$, where $p_\lambda \geq 0$ and $\sum_\lambda p_\lambda = 1$. Otherwise, ρ_{AB} is entangled (Werner, 1989). For composite systems of more than two sub-systems this definition can be generalized in a straightforward way.

Basic structural criteria, which decide whether the given density operator represents an entangled state, were first given by Peres (1996) and Horodecki *et al.* (1996). The full set of separable mixed states is a convex set in a multidimensional real space of hermitian operators. Thus, any entangled state is separated from the set of separable states by a hyperplane. The equation of such a hyperplane is defined by an element of the space, namely, a hermitian operator \tilde{W} , which is called "entanglement witness" (Horodecki *et al.*, 1996; Terhal, 2000; Lewenstein *et al.*, 2000; Bruß *et al.*, 2002). Since the

¹⁷ One can apply the EPR reality criterion to the singlet state (24): "If, without in any way disturbing a system, we can predict with certainty (i.e., with probability equal to unity) the value of a physical quantity, then there exists an element of physical reality corresponding to this physical quantity". This would imply that to any possible spin measurement on any one of our particles we can assign such an element of physical reality on the basis of a corresponding measurement on the other particle. Whether or not we can assign an element of reality to a specific spin component of one of the systems must be independent of which measurement we actually perform on the other system and even independent of whether we care to perform any measurement at all on that system. In this way EPR argued for incompleteness of quantum mechanics, as it is a theory without their elements of reality

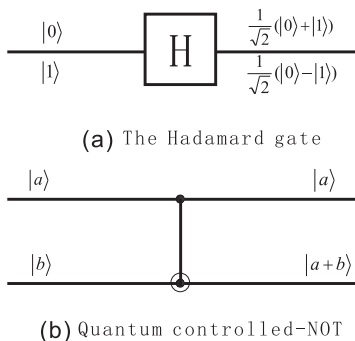


FIG. 3 Graphical representations of Hadamard and the quantum CNOT gates. Here, $a + b$ denotes addition modulo 2.

scalar product in the operator space is given by $\text{Tr}(\hat{A}^\dagger \hat{B})$, the equation of the hyperplane is given by $\text{Tr}(\hat{W}\rho) = 0$. For all separable states one has $\text{Tr}(\hat{W}\rho) \geq 0$, whereas for the entangled states in question one has $\text{Tr}(\hat{W}\rho_{ent}) < 0$. Thus, via measurement of a suitably chosen witness operator one can detect entanglement.

For more details on entanglement theory, see, e.g., Alber *et al.* (2001), Mintert *et al.* (2005), and Horodecki *et al.* (2007).

B. Basic quantum circuit for preparing and measuring entanglement

As entanglement plays a central role in fundamental aspects of quantum mechanics as well as in practical applications in quantum information science, it is one of the most important tasks to create, manipulate and detect entanglement. According to the basic principle of universal quantum computation (section VIII; see also Nielsen and Chuang, 2000; Bouwmeester *et al.*, 2001; Preskill, 1999), with universal quantum logic gates, one can construct a suitable quantum circuit to produce and identify any of the maximally entangled states for any number of particles (Bruß *et al.*, 1997). In fact, using a simple Hadamard gate [Fig. 3(a)] and the CNOT gate [Fig. 3(b)], one can prepare and identify any of N -particle entangled states. The action of a CNOT gate is to flip the second of two qubits if and only if the first is $|1\rangle$, namely,

$$|0\rangle|a\rangle \rightarrow |0\rangle|a\rangle, \quad |1\rangle|a\rangle \rightarrow |1\rangle|\bar{a}\rangle, \quad (26)$$

where a can take the values 0 and 1 and \bar{a} denotes NOT- a .

Consider now the network shown in Fig. 4(a). Under the action of the gates on the left-hand side of the network, the two qubits can be prepared in any Bell state by choosing appropriate input states. It is also easy to verify that the reversed quantum network [right-hand side of Fig. 4(a)] can be used to implement the so-called *Bell-state measurement* on the two qubits by disentangling the Bell states. In this way, the Bell-state measurement is reduced to two single-particle measurements. The method

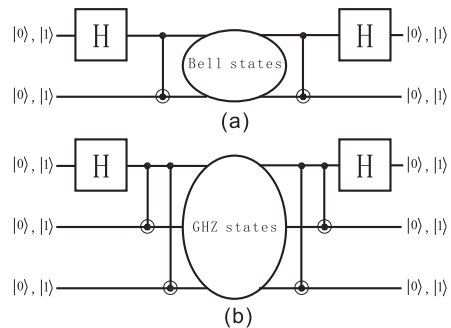


FIG. 4 (a) The Bell-state measurement: the gates on the left hand side allow us to generate the four Bell states from the four possible different inputs. Reversing the order of the gates (right-hand side of the diagram) corresponds to a Bell-state measurement. (b) The GHZ measurement: the same as in (a) for the eight GHZ states.

can be directly extended to a three-qubit case. Figure 4(b) shows how to prepare eight maximally entangled three-particle states, known as the GHZ states (Greenberger *et al.*, 1989, 1990). Reversing the procedure reduces the GHZ-state measurement to the three single-particle measurements.

Generalizing the above procedure, one can see that, in general, any measurement on any number of qubits can be implemented using only single-qubit operations and the CNOT gates. This follows again from the basic theorem for universal quantum computation (section VIII). Thus if we want to measure observable A pertaining to n qubits, we could construct a compensating unitary transformation U which maps 2^n states of the form $|a_1\rangle|a_2\rangle\dots|a_n\rangle$, where $a_i = 0, 1$, into the eigenstates of A . This allows both to prepare the eigenstates of A , which in general can be highly entangled, and to reduce the measurement described by A to n simple, single-qubit measurements.

In the photon domain, however, the manipulation of photonic quantum states is accomplished by optical circuits which can be thought of as a black box with incoming and outgoing modes of the electromagnetic field. The black box transforms a state of the incoming modes into a different state of the outgoing modes. The modes might be mixed by BS/PBS, pick up relative phase shifts or polarisation rotations, and be subject to possible measurements. For single photonic qubits, preparation and measurement are rather trivial as single-qubit rotations can easily be done with linear optical elements (see section III.C). However, they are highly nontrivial for entangled photons due to the difficulty of two-qubit operations for photons.

Actually, two-qubit logic gates with linear optics are necessarily probabilistic (see section VIII.B). This in turn implies that the above quantum circuits can only be implemented probabilistically if one uses only linear optics. In practice, currently the most used entangled photon pairs are created directly via certain nonlin-

ear optical processes (see section V), but not by quantum circuits. For the linear optical identification of the Bell/GHZ states, the task can be accomplished, again in a probabilistic way (see section V.F).

C. Multi-particle interferometry

Entanglement can manifest itself in strictly quantum interference phenomena that are of an entirely non-classical character. To show this, below we present the basic idea of the so-called multi-particle interferometry, which is one of the most important concepts underlying the arguments testing the completeness of quantum theory.

1. EPR interferometry

Recall that in a single-particle interferometry as in Young's double-slit experiment, the interference pattern appears as far as the particle's two paths are indistinguishable. However, for interferometries with two or more identical particles, dramatically new features arise. Figure 5 is a sketch of a two-photon interferometry (Horne and Zeilinger, 1986; Żukowski and Pykacz, 1988; Horne *et al.*, 1989, 1990; Greenberger *et al.*, 1993), in which a central source emits two photons in an entangled state

$$|\psi\rangle_{12} = \frac{1}{\sqrt{2}}(|a\rangle_1 |a'\rangle_2 + |b\rangle_1 |b'\rangle_2). \quad (27)$$

Here $|a\rangle$ and $|b\rangle$ ($|a'\rangle$ and $|b'\rangle$) are two different spatial modes of photon-1 (photon-2). The entanglement of $|\psi\rangle_{12}$ is actually called momentum entanglement (Rarity and Tapster, 1990), whose creation will be described in section V. Before being combined at a 50:50 BS and then subject to single-photon detections, the two paths of each photon acquire a relative phase shift.

By taking into account the phase shifts α and β and the action of the two BS, the probabilities of the *coincidence detections* of single photons at the detector pairs ($D_{1c/d}, D_{2c/d}$) read (Horne *et al.*, 1989; Greenberger *et al.*, 1993)

$$\begin{aligned} p_{1c,2d}(\alpha, \beta) &= p_{1d,2c}(\alpha, \beta) = \frac{1}{4}[1 + \cos(\alpha - \beta)], \\ p_{1c,2c}(\alpha, \beta) &= p_{1d,2d}(\alpha, \beta) = \frac{1}{4}[1 - \cos(\alpha - \beta)]. \end{aligned} \quad (28)$$

Thus, by simultaneously monitoring the detectors on both sides of the interferometry while varying the phase shifts α and β , the interference fringes will be observed as shown by the sinusoidal terms, being characteristic of quantum interference. By contrast, in any single detector, the counting rate shows no interference. For example, $p_{1c} = p_{1c,2c}(\alpha, \beta) + p_{1c,2d}(\alpha, \beta) = \frac{1}{2}$, independent of α and β .

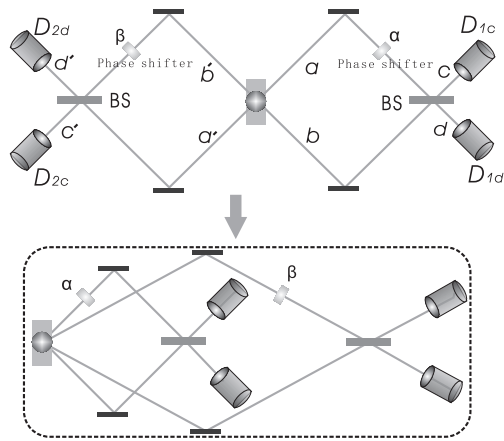


FIG. 5 A two-photon interferometry with variable phase shifts α and β . Before being combined at the 50:50 BS and then subject to single-photon detections, the two paths of each photon acquire a relative phase shift. The lower panel shows the topologically equivalent apparatus of the two-photon interferometry.

The fact that the apparatus in Fig. 5 exhibits two-photon correlations [see Eq. (28)] rather than single-photon interference has some important consequences, both conceptual and practical. Conceptually, entanglement plays a vital role in the two-photon interferometry (Horne *et al.*, 1989): the “nonlocal” correlations exhibited by the coincidence rate (28) stems exactly from the entangled two-photon state $|\psi\rangle_{12}$ and are stronger than what is allowed by local realism. This latter fact underlies the long-term intensive efforts on Bell's theorem and its experimental test. On a practical side, the weird entanglement finds profound applications in quantum information science, to be reviewed below.

2. GHZ interferometry

A slight generalization of the EPR interferometry yields the three-photon interferometry (Greenberger *et al.*, 1990; 1993) shown in Fig. 5. Though such a step from 2 to 3 seems to be small, it nevertheless leads to much profound applications, one of which is the GHZ theorem (GHZ; Greenberger *et al.*, 1990; Mermin, 1990a). The center of the interferometry is a source emitting three photons in a GHZ-entangled state

$$|\text{GHZ}\rangle_{123} = \frac{1}{\sqrt{2}}(|a_1\rangle_1 |b_1\rangle_2 |c_1\rangle_3 + |a_2\rangle_1 |b_2\rangle_2 |c_2\rangle_3). \quad (29)$$

Here each photon has two different spatial modes, which are, e.g., for photon-1 $|a_1\rangle$ and $|a_2\rangle$.

By taking into account the actions of the relative phase shifts and 50:50 BS, one can read out three novel features of three-particle interference (Greenberger *et al.*, 1990). First, the respective three-fold coincidence detection probability for each triple of output modes

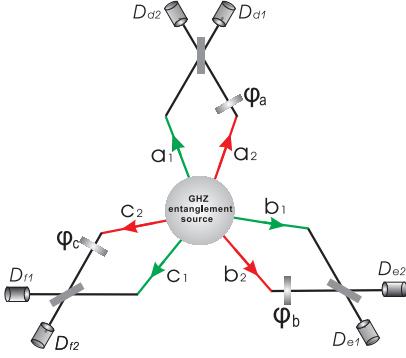


FIG. 6 A three-photon interferometry with variable phase shifts ϕ_a , ϕ_b and ϕ_c .

$[(d_1, e_1, f_1); (d_1, e_1, f_2); \dots]$ can easily be obtained. For instance,

$$p_{d_1 e_1 f_1}(\phi_a, \phi_b, \phi_c) = \frac{1}{8}[1 + \sin(\phi_a + \phi_b + \phi_c)],$$

$$p_{d_2 e_1 f_1}(\phi_a, \phi_b, \phi_c) = \frac{1}{8}[1 - \sin(\phi_a + \phi_b + \phi_c)]. \quad (30)$$

The three-fold coincidence rates given in Eq. (30) as an example display the sinusoidal oscillations (with $\phi_a + \phi_b + \phi_c$), which are characteristic of the three-particle interference. Second, the three-particle interferometer will not exhibit any two-particle fringes. For example, if only two-particle coincidence e_1 - f_1 are detected, while the modes d_1 and d_2 are ignored, the observed two-particle coincidence rate for modes e_1 and f_1 are predicted to be $p_{d_1 e_1 f_1}(\phi_a, \phi_b, \phi_c) + p_{d_2 e_1 f_1}(\phi_a, \phi_b, \phi_c) = \frac{1}{4}$, which is completely independent of the phases. Finally, a similar argument shows that no single-particle fringes can be observed in the three-particle interferometer. Actually, an n -particle interferometer generalized along the above reasoning will only exhibit n -particle fringes, but no $(n-1)$ -, $(n-2)$ -, ..., single-particle fringes are observable (Greenberger *et al.*, 1990).

A few remarks are in order. The above two- and three-photon interferometry is demonstrated using photon's path degree of freedom. However, similar interference can certainly be observed using photon's other degrees of freedom, such as polarization and emission time. Moreover, the above argument should be understood as a special case of the wider concept, i.e., multiparticle interferometry, where entangled massive particles (e.g. electrons and atoms) could also display multiparticle interference. Finally, an N -port interferometer is also feasible, as proposed by Reck *et al.* (1994).

D. Bell's theorem

Bell (1964, 1987) proved that there is a conflict between quantum mechanics and the *local realistic theo-*

*ries*¹⁸. His famous theorem is of profound scientific and philosophical consequences. Since the conflict is limited to entangled states, Bell's discovery showed that the previously ignored class of states is very important in distinguishing between the classical and the quantum.

1. Bell's inequality

Consider pairs of photons simultaneously emitted in opposite directions. They arrive at two very distant measuring devices A and B operated by, respectively, Alice and Bob. Their apparatuses have a knob, which specifies which dichotomic (i.e., two-valued, yes-no) observable they measure.¹⁹ One can assign to the two possible results (eigen-) values ± 1 (for yes/no).²⁰ Alice and Bob are at any time (also in a "delayed choice" mode, after an emission) *free* to choose the knob settings.

Assume that each particle pair carries full information (deterministic or probabilistic) on the values of the results of all possible experiments that can be performed on it²¹ (*realism*). Also, by *locality*, random choices made by them, which can be simultaneous in certain reference frames, cannot influence each other, and the choice made on one side cannot influence the results on the other side, and *vice versa*. Alice chooses to measure either observable \hat{A}_1 or \hat{A}_2 , and Bob either \hat{B}_1 or \hat{B}_2 . Let us denote the hypothetical results that they may get for the j -th pair by A_1^j and A_2^j for Alice's two possible choices, and B_1^j and B_2^j for Bob's. The numerical values of these can be ± 1 . The assumption of local realism allows one to treat A_1^j and A_2^j on equal footing as two numbers, one of them revealed in the experiment, the second one unknown, but still ± 1 . Thus, their sum and difference always exist. Since, either $|A_1^j - A_2^j| = 2$ and $|A_1^j + A_2^j| = 0$, or $|A_1^j - A_2^j| = 0$ and $|A_1^j + A_2^j| = 2$, and similarly for Bob's values the following trivial relation holds

$$\sum_{s_1=\pm 1} \sum_{s_2=\pm 1} S(s_1, s_2)(A_1^j + s_1 A_2^j)(B_1^j + s_2 B_2^j) = \pm 4,$$

where $S(s_1, s_2)$ is an arbitrary "sign" function of s_1 and s_2 , that is $|S(s_1, s_2)| = 1$. Imagine now that N pairs of photons are emitted, pair by pair, and N is sufficiently

¹⁸ Realism, the cornerstone of classical physics, is a view that any physical system (also a subsystem of a compound system) carries full information (deterministic or probabilistic) on results of *all* possible experiments that can be performed upon it. A theory is local if it assumes that information, and influences, cannot travel faster than light.

¹⁹ E.g., for a device consisting of a polarizing beamsplitter and two detectors behind its outputs, this knob specifies the orientation of the polarizer, etc.

²⁰ We assume that we have a perfect situation in which the detectors never fail to register a photon.

²¹ Note, that this openly goes beyond "what is speakable" in quantum mechanics: it violates complementarity.

large, $\sqrt{1/N} \ll 1$. The average value of the products of the local values for a joint test (the Bell correlation function) during which, for all photon pairs, only one pair of observables (say \hat{A}_n and \hat{B}_m) is chosen, is given by

$$E(A_n, B_m) = \frac{1}{N} \sum_{j=1}^{j=N} A_n^j B_m^j, \quad (31)$$

where $n = 1, 2$ and $m = 1, 2$. The relation (31) after averaging implies that for the four *possible* choices the following *Bell inequality* must be satisfied²²

$$\begin{aligned} -4 \leq & \sum_{s_1=\pm 1, s_2=\pm 1} S(s_1, s_2)[E(A_1, B_1) + s_2 E(A_1, B_2) \\ & + s_1 E(A_2, B_1) + s_1 s_2 E(A_2, B_2)] \leq 4, \end{aligned} \quad (33)$$

If one chooses a non-factorizable $S(s_1, s_2)$, say $\frac{1}{2}(1 + s_1 + s_2 - s_1 s_2)$, the famous CHSH (Clauser, Horne, Shimony, and Holt, 1969) inequality is recovered²³

$$\begin{aligned} S_{\text{Bell}} \equiv & |E(A_1, B_1) + E(A_1, B_2) \\ & + E(A_2, B_1) - E(A_2, B_2)| \leq 2, \end{aligned} \quad (34)$$

which is the first experimentally testable Bell inequality²⁴.

In the actual experiment, if the choices of actual observables are random and independent from all other processes in the experiment, only in part of the cases (around 1/4-th) the given pair of observables would be measured. However, as N is large, the correlation function obtained on a randomly pre-selected subensemble²⁵ of pairs cannot differ too much from the one that would have been obtained for the full ensemble. Therefore, for the values of the *actually* chosen measurements the inequality (34)

²² All such inequalities boil down to just a single one

$$\begin{aligned} \sum_{s_1=\pm 1} \sum_{s_2=\pm 1} & |E(A_1, B_1) + s_2 E(A_1, B_2) \\ & + s_1 E(A_2, B_1) + s_1 s_2 E(A_2, B_2)| \leq 4, \end{aligned} \quad (32)$$

see Weinfurter and Żukowski (2001), Werner and Wolf (2001).

²³ The simple algebra to reach this result rests on the fact that $\sum_{s_j=\pm 1} s_j = 0$, while $\sum_{s_j=\pm 1} s_j^2 = 2$.

²⁴ The original Bell (1964) inequality, since it assumes perfect correlations of the singlet state, cannot be tested experimentally, as in such a case correlations are never perfect. A generalization of the original inequality to the imperfect case leads to the CHSH inequality.

²⁵ Note that the subensemble is selected by the choice of observables made by Alice and Bob *before* the actual measurements. If the choices are statistically independent of any other processes in the experiment, which is equivalent to Alice and Bob having free will, expectation values of correlation functions conditioned on a particular choice of local settings do not differ from the unconditional ones, like Eq. (31). For more details see Gill *at al.* (2002).

also must hold. Note that the presented Bell-type argument avoids any explicit introduction of hidden variables, other than the hypothetical local realistic results.

Some quantum processes involving entangled states violate this inequality. The predictions for the spin-1/2 singlet are an example, in which S_{Bell} can acquire the maximal value $2\sqrt{2}$ allowed by quantum mechanics, known as the Cirel'son bound (Cirel'son, 1980; Landau, 1987). In fact, predictions for any pure, non-factorizable (i.e., not necessarily maximally entangled) two-system state lead to violations (Gisin and Peres, 1992). This is also the case for a wide range of mixed states (Horodecki, Horodecki and Horodecki, 1995). In this review we present many laboratory violations of Bell's inequalities, as well as of higher-order inequalities for more than two particles.

2. Bell theorem without inequalities

If there are $N > 2$ maximally entangled quantum systems (qubits), and if measurements on them are performed in N mutually spatially separated regions by N independent observers, the correlations in such an experiment violate bounds imposed by local realism much stronger than in the two-particle case. The new feature is that instead of purely statistical reasoning for deriving Bell's inequality, one can follow the spirit of the EPR paper, attempt to define "elements of reality" basing on specific perfect correlations of the entangled state, and with the same perfect correlations show contradiction of these elements with exactly those quantum predictions which were used to define them (Greenberger, Horne, and Zeilinger, 1989).

Take a GHZ state of $N = 3$ particles:

$$|\psi(3)\rangle = \frac{1}{\sqrt{2}} (|a\rangle|b\rangle|c\rangle + |a'\rangle|b'\rangle|c'\rangle) \quad (35)$$

where $\langle x|x'\rangle = 0$ ($x = a, b, c$, and kets denoted by one letter pertain to one of the particles). The observers, Alice, Bob and Cecil, measure the observables: $\hat{A}(\phi_A)$, $\hat{B}(\phi_B)$, $\hat{C}(\phi_C)$, defined by

$$\hat{X}(\phi_X) = |+, \phi_X\rangle\langle+, \phi_X| - |-, \phi_X\rangle\langle-, \phi_X| \quad (36)$$

and

$$|\pm, \phi_X\rangle = \frac{1}{\sqrt{2}} (\pm i|x'\rangle + \exp(i\phi_X)|x\rangle). \quad (37)$$

where $X = A, B, C$. The quantum expectation value of the product of the three local observables is given by

$$\begin{aligned} E(\phi_A, \phi_B, \phi_C) &= \langle \psi | \hat{A}(\phi_A) \hat{B}(\phi_B) \hat{C}(\phi_C) | \psi \rangle \\ &= \sin(\phi_A + \phi_B + \phi_C). \end{aligned}$$

Therefore, if $\phi_A + \phi_B + \phi_C = \pi/2 + k\pi$ (k : integer), one has perfect correlations. For instance, for $\phi_A = \pi/2$, $\phi_B = 0$ and $\phi_C = 0$, whatever may be the results of local measurements of the observables, for say the particles

belonging to the i -th triple represented by the quantum state $|\psi(3)\rangle$, they have to satisfy

$$A^i(\pi/2)B^i(0)C^i(0) = 1, \quad (38)$$

where $X^i(\phi)$ ($X = A, B$ or C) is the value of a local measurement of the observable $\hat{X}(\phi)$ that *would have been* obtained for the i -th particle triple if the setting of the measuring device is ϕ . Locality assumption forces one to assume that $X^i(\phi)$ depends solely on the local parameter. Equation (38) indicates that we can predict with certainty the result of measuring the observable pertaining to one of the particles (say C) by choosing to measure suitable observables for the other two. Hence the values $X^i(\phi)$ for the angles specified in the equality are EPR elements of reality. However, if the local apparatus settings are different, one *would have had*, e.g.,

$$A^i(0)B^i(0)C^i(\pi/2) = 1, \quad (39)$$

$$A^i(0)B^i(\pi/2)C^i(0) = 1, \quad (40)$$

$$A^i(\pi/2)B^i(\pi/2)C^i(\pi/2) = -1. \quad (41)$$

Since $X^i(\phi) = \pm 1$, if one multiplies Eqs. (38-40) side by side, the result is

$$A^i(\pi/2)B^i(\pi/2)C^i(\pi/2) = +1, \quad (42)$$

which contradicts (41). Thus the EPR elements of reality program breaks down, because it leads to a $1 = -1$ contradiction. Introduction of EPR elements of reality leads to a prediction concerning one of the perfect correlations, (42), which is *opposite* with respect to the quantum prediction. We have a ‘‘Bell theorem without inequalities’’ (Greenberger *et al.*, 1990).

Multiparticle Bell inequalities.—In laboratory one cannot expect perfect correlations. Thus, any test of local realism based on the GHZ correlations has to resort to some Bell-type inequalities. Series of such inequalities were discovered by Mermin (1990b), Ardehali (1991) and Belinskii and Klyshko (1993). To get the full set of such inequalities, for correlation functions involving the product of the result of all parties, it is enough to generalize the relation (31) to the situation in question. E.g., for three partners one has

$$\begin{aligned} & \sum_{s_1, s_2, s_3 = \pm 1} S(s_1, s_2, s_3)(A_1^j + s_1 A_1^j)(B_1^j + s_2 B_2^j) \\ & \times (C_1^j + s_3 C_2^j) = \pm 8, \end{aligned} \quad (43)$$

with the new symbols being an obvious extension of the ones in (31). This leads to the following Bell inequality [Werner and Wolf (2001); Weinfurter and Żukowski (2001)]:

$$\sum_{s_1, s_2, s_3 = \pm 1} \left| \sum_{k, l, m = 1, 2} s_1 s_2 s_3 E(A_k, B_l, C_m) \right| \leq 8,$$

which is the *necessary and sufficient* condition for correlation functions involved in it, $E(A_k, B_l, C_m)$, to have

a local realistic model [for proofs see Werner and Wolf (2001), Żukowski and Brukner (2002)]. The reasoning is trivially generalizable to an arbitrary number of parties.²⁶ The noise resistance²⁷ of violations of such inequalities by N -particle GHZ states $|\text{GHZ}_N\rangle$ is growing exponentially with N . This is an important fact, because one expects noise to increase the more photons are involved in an interferometric experiment (due to the increasing complications, and alignment problems). Thus non-classicality of the GHZ correlations can be significant even for many particles (Mermin, 1990b; Klyshko, 1993; Roy and Singh, 1991; Żukowski 1993; Gisin and Bechmann-Pasquinucci, 1998).

Two-observer variations of the GHZ theorem were discovered recently (Cabello, 2001a, 2001b; Chen *et al.*, 2003). So far, the GHZ-(type) theorem has been tested with three-photon entanglement (Pan *et al.*, 2000), four-photon entanglement (Zhao *et al.*, 2003a) and two-photon hyper-entanglement (Yang *et al.*, 2005, and somewhat indirectly by Cinelli *et al.*, 2005). All experiments confirm the quantum predictions.

There are many other fundamental tests of quantum mechanics. For instance, for two-particle states, Hardy (1993) has found situations, where quantum mechanics predicts a specific result to occur *sometimes*, and local realism predicts the same result never to occur (for an experiment see Boschi *et al.*, 1997). In a remarkable paper by Ekert (1991), Bell’s inequalities and entanglement have a direct application in quantum cryptography.²⁸ Actually, there is a fascinating link (Scarani and Gisin, 2001; Gisin *et al.*, 2002) between security of certain quantum communication protocols and Bell’s theorem. This link extends also to (quantum) communication complexity protocols (Brukner *et al.*, 2004). A recently discovered two-observer variation of the GHZ theorem also plays a key role in a deterministic and efficient quantum cryptography protocol (Chen *et al.*, 2006d).

E. Refutation of certain nonlocal realistic theories

The logical conclusion one can draw from the violation of local realism is that at least one of its assumptions fails. Specifically, either locality or realism or both cannot provide a foundational basis for quantum theory. Each of the resulting possible positions has strong supporters and opponents in the scientific community. However, Bell’s theorem is unbiased with respect to these views: on the basis

²⁶ As a matter of fact this single inequality either implies all earlier derived tight inequalities, e.g., those of Mermin (1990b), or is tighter.

²⁷ As measured by the decreasing threshold visibility V in the mixture $(1-V)\frac{1}{2^N}\hat{I} + V|\text{GHZ}_N\rangle\langle\text{GHZ}_N|$ which is sufficient to violate the inequalities.

²⁸ For a cryptographic protocols involving GHZ states see (Żukowski *et al.*, 1998; Chen *et al.*, 2005).

of this theorem, one cannot, even in principle, favour one over the other. It is therefore important to ask whether incompatibility theorems similar to Bell's can be found in which at least one of these concepts is relaxed. A recent work (Groblacher *et al.*, 2007) addresses a broad class of nonlocal hidden-variable theories that are based on a very plausible type of realism and that provide an explanation for all existing Bell-type experiments. Nevertheless, their conflict with quantum predictions were demonstrated, both in theory and experiment, following the recent approach of Leggett (2003), who introduced the class of nonlocal models and formulated an incompatibility theorem.

It is sufficient for our purposes to focus our description on the polarization degree of freedom of photons. The theories are based on the following assumptions: (1) all measurement outcomes are determined by pre-existing properties of particles independent of the measurement (realism); (2) physical states are statistical mixtures of subensembles with definite polarization, where (3) polarization is defined such that expectation values taken for each subensemble obey Malus' law (the cosine dependence of the intensity of a polarized beam behind an ideal polarizer).

These assumptions provide a natural explanation of quantum mechanically separable states (polarization states indeed obey Malus' law). In addition, they do not explicitly demand locality; namely, measurement outcomes may very well depend on parameters in space-like separated regions. As a consequence, such theories can explain some important features of quantum mechanically entangled (non-separable) states of two particles: first, they do not allow information to be transmitted faster than the speed of light; second, they reproduce perfect correlations for all measurements in the same bases, which is a fundamental feature of the Bell singlet state; and third, they provide a model for all earlier performed experiments in which the CHSH inequality was violated. Nevertheless, we will show that all models based on assumptions (1)-(3) are at variance with other quantum predictions.

A general framework of such models is the following: assumption (1) requires that an individual binary measurement outcome A for a polarization measurement along direction \mathbf{a} (that is, whether a single photon is transmitted or absorbed by a polarizer set at a specific angle) is predetermined by some set of hidden-variables λ , and a three-dimensional vector \mathbf{u} , as well as by some set of other possibly non-local parameters η (for example, measurement settings in space-like separated regions) – that is, $A = A(\lambda, \mathbf{u}, \mathbf{a}, \eta)$. According to assumption (3), particles with the same \mathbf{u} but with different λ build up subensembles of “definite polarization” described by a probability distribution $\rho_{\mathbf{u}}(\lambda)$. The expectation value $\overline{A}(\mathbf{u})$, obtained by averaging over λ , fulfils Malus' law, that is, $\overline{A}(\mathbf{u}) = \int d\lambda \rho_{\mathbf{u}}(\lambda) A(\lambda, \mathbf{u}, \mathbf{a}, \eta) = \mathbf{u} \cdot \mathbf{a}$. Finally, with assumption (2), the measured expectation

value for a general physical state is given by averaging over the distribution $F(\mathbf{u})$ of subensembles, that is, $\langle A \rangle = \int d\mathbf{u} F(\mathbf{u}) \overline{A}(\mathbf{u})$.

The correlation function of measurement results for a source emitting well-polarized photons is defined as the average of the products of the individual measurement outcomes:

$$\overline{AB}(\mathbf{u}, \mathbf{v}) = \int d\lambda \rho_{\mathbf{u}, \mathbf{v}}(\lambda) A(\mathbf{a}, \mathbf{b}, \lambda) B(\mathbf{b}, \mathbf{a}, \lambda) \quad (44)$$

For a general source producing mixtures of polarized photons the observable correlations are averaged over a distribution of the polarizations $F(\mathbf{u}, \mathbf{v})$, and the general correlation function E is given by:

$$E = \langle AB \rangle = \int d\mathbf{u} d\mathbf{v} F(\mathbf{u}, \mathbf{v}) \overline{AB}(\mathbf{u}, \mathbf{v}) \quad (45)$$

It is a very important trait of this model that there exist subensembles of definite polarizations (independent of measurements) and that the predictions for the subensembles agree with Malus' law. It is clear that other classes of non-local theories, possibly even fully compliant with all quantum mechanical predictions, might exist that do not have this property when reproducing entangled states. Such theories may, for example, include additional communication (Bacon and Toner, 2003) or dimensions (Ne'eman, 1986). A specific case deserving comment is Bohm's theory (Bohm, 1951). There the non-local correlations are a consequence of the non-local quantum potential, which exerts suitable torque on the particles leading to experimental results compliant with quantum mechanics. In that theory, neither of the two particles in a maximally entangled state carries any angular momentum at all when emerging from the source (Dewdney *et al.*, 1987).

The theories described here are incompatible with quantum theory. The basic idea of the incompatibility theorem (Leggett, 2003) uses the following identity, which holds for any numbers $A = \pm 1$ and $B = \pm 1$:

$$-1 + |A + B| = AB = 1 - |A - B|. \quad (46)$$

Then the following generalized Leggett-type inequality can be obtained (Groblacher *et al.*, 2007):

$$\begin{aligned} S_{NLHV} &= |E_{11}(\varphi) + E_{23}(0)| + |E_{22}(\varphi) + E_{23}(0)| \\ &\leq 4 - \frac{4}{\pi} \left| \sin \frac{\varphi}{2} \right|, \end{aligned} \quad (47)$$

where $E_{kl}(\varphi)$ is a uniform average of all correlation functions, defined in the plane of \mathbf{a}_k and \mathbf{b}_l , with the same relative angle φ ; the subscript NLHV stands for “nonlocal hidden-variables”.²⁹ For the inequality to be applicable,

²⁹ Inequalities more useful in experiments were recently derived (Paterek *et al.*, 2007; Branciard *et al.*, 2007, 2008).

the vectors \mathbf{a}_1 and \mathbf{b}_1 necessarily have to lie in a plane orthogonal to the one defined by \mathbf{a}_2 and \mathbf{b}_2 . This contrasts with the standard experimental configuration used to test the CHSH inequality, which is maximally violated for settings in one plane.

Quantum theory violates inequality (47). Consider the quantum predictions for the polarization singlet state of two photons, $|\Psi^-\rangle_{AB} = \frac{1}{\sqrt{2}} [|H\rangle_A |V\rangle_B - |V\rangle_A |H\rangle_B]$, where, for example, $|H\rangle_A$ denotes a horizontally polarized photon propagating to Alice. The quantum correlation function for the measurements \mathbf{a}_k and \mathbf{b}_l performed on photons depends only on the relative angles between these vectors, and therefore $E_{kl} = -\mathbf{a}_k \cdot \mathbf{b}_l = -\cos\varphi$. Thus the left hand side of inequality (47), for quantum predictions, reads $|2(\cos\varphi + 1)|$. The maximal violation of inequality (47) is for $\varphi_{max} = 18.8^\circ$. For this difference angle, the bound given by inequality (47) equals 3.792 and the quantum value is 3.893. Thus the case for realistic theories receives yet another hit.

F. Non-contextual hidden variable theories

Another class of theorems, which show the drastic difference between the classical and the quantum, are the no-go theorems for non-contextual hidden variables (NCHV) interpretations of quantum mechanics [Bell, 1966; Kochen and Specker, 1967; Mermin, 1990c; for a survey, see (Mermin, 1993)]. Such realistic theories assume that hidden variables fix the values of measurement results of all possible observables for the given system, and that such values are not dependent on the measurement context. That is, they do not depend on which other observables are commensurable with them. The measurement context is defined by a maximal observable.³⁰ It is interesting that already in the lowest dimensional case, for which a degenerate observable can exist, and only such observables can be measurable in different contexts, that is for dimension 3, non-contextual hidden variable models of quantum mechanics are impossible (Kochen and Specker, 1967).³¹

Bell's theorem is a case of no-go theorem for NCHV for which non-contextuality is given by the locality assumption. As locality forbids the result on Alice's side to depend on the actual observable chosen to be measured by Bob, etc., the non-contextuality is enforced by the relativistic causality. This is very appealing, because relativity is assumed to be a principle setting theory for causal links. Non-contextuality, without the help from relativistic principles, seems to be a much stronger assumption. Nevertheless, both NCHV theories and local realistic ones can be reduced to the assumption of the

existence of a joint probability distribution for noncommensurable observables.³²

V. PHOTONIC ENTANGLEMENT: CREATION AND MEASUREMENT

Ever since the seminal work of EPR there has been a quest for generating entanglement between quantum particles.³³ Entangled photon sources play a central role in the experimental study of quantum mechanical foundations and are vital resource in optical quantum information processing. The early Bell-test experiments used entangled photons from atomic cascades. Such a source has a drawback. The directions of emissions are uncorrelated. Thus, the collection efficiency of the entangled photons is low. Fortunately, it was discovered in mid eighties that the process of spontaneous parametric down-conversion [first observation by Burnham and Weinberg (1970)] allows pairs of entangled photons to be collected with reasonable intensity and with very high purity.

Today, entangled photon sources with increasing quality, brightness and numbers of entangled photons can be routinely realized, which enabled a significant fraction of key progresses in quantum information science. In this section, we shall thus focus on the creation of photonic entanglement of various forms and on photonic entanglement measurements (especially photonic polarization entanglement analyzers such as the Bell-state and GHZ-state analyzers).

A. Spontaneous parametric down-conversion process

In the SPDC process in a non-centrosymmetric crystal, with a high nonlinear electric susceptibility, an incoming higher-energy pump photon sometimes splits into two lower-energy daughter photons such that energy and momentum inside the crystal are almost precisely conserved. Thus, the photon pair is strongly correlated in energy and momentum, or, complementarily, in space and time.

The quantum nature of SPDC was first studied by Klyshko and Zel'dovich (Klyshko, 1967, 1988; Zel'dovich and Klyshko, 1969). In the works of Mollow (1973) and Hong and Mandel (1985) the theory reached its final form. The predicted strong quantum correlations between the photon pairs created in SPDC, were first experimentally observed by Burnham and Weinberg (1970). Quantum interference of (type-I) SPDC photons was first used to violate Bell's inequality, Alley and Shih

³⁰ An observable is maximal if it has a non-degenerate spectrum.

³¹ For dimension 2 a degenerate observable is just a constant.

³² Note that such distributions are impossible in quantum formalism.

³³ We concentrate on photon-photon entanglement. The matter-photon entanglement was realized for, e.g., atom-photon interfaces (Blinov *et al.*, 2004) and for atomic ensemble-photon (Matsukevich *et al.*, 2006a).

(1986), Shih and Alley (1988), and Hong, Ou, and Mandel (1987). The process was shown to be a ready source of (path) entangled pairs by Horne, Shimony and Zeilinger (1989), and polarization entanglement in type-II process was discovered by Kwiat *et al.* (1995).

In the following we will give a brief introduction to the physics of SPDC and the entangled photons in various distinct degrees of freedom [such as polarization, momentum, or time (time bin)]. For a comprehensive survey of SPDC, we also refer to, e.g., (Shih, 2003).

1. The two-photon states produced by SPDC

If one shines strong laser light on a crystal, the pump photons have some probability to split into correlated pairs of lower energy. This is called spontaneous parametric down conversion (SPDC). The new photons, customarily called “signal” and “idler”, satisfy the conservation-like (so called *phase matching*) relations: within the crystal one has $\mathbf{k}_0 \approx \mathbf{k}_i + \mathbf{k}_s$ where subscripts 0, s and i denote, respectively, pump, signal and idler wave vectors, and the respective frequencies satisfy $\omega_o \approx \omega_i + \omega_s$. These relations have a form of conservation laws, but they result out of an interference process within the crystal. The emerging pairs of photons are tightly correlated in time and emission directions.

Crystal-field interaction.—In the interaction Hamiltonian of the electromagnetic field with an atom or a molecule, the dominating part is $\hat{H}_{a-f} \sim \hat{\boldsymbol{\mu}}_e \cdot \mathbf{E}(\mathbf{x}, t)$, i.e., scalar product of the dipole moment, $\boldsymbol{\mu}$, of the atoms or molecules with the local electric field. Since the electric polarization, $\mathbf{p}(\mathbf{x}, t)$, of a medium is given by the mean dipole moment of the atoms or molecules per unit volume, the principal term of the field-crystal interaction Hamiltonian, H_{int} , is proportional to $\int_V \mathbf{p}(\mathbf{x}, t) \cdot \mathbf{E}(\mathbf{x}, t) d^3x$, where V is the volume of the crystal. One can assume that $\mathbf{E}(\mathbf{x}, t)$ interacts with $\mathbf{p}(\mathbf{x}, t)$ only in the point \mathbf{x} , thus the i -th component of polarization is in the most general case given by

$$p_i(\mathbf{x}, t) = \sum_{j=1}^3 \chi_{ij}^{(1)}(\mathbf{x}) E_j(\mathbf{x}, t) + \sum_{j,k=1}^3 \chi_{ijk}^{(2)}(\mathbf{x}) E_j(\mathbf{x}, t) E_k(\mathbf{x}, t) + \dots, \quad (48)$$

where $\chi_{ij}^{(1)}$ are $\chi_{ijk}^{(2)}$ are the (macroscopic) polarizability tensors. For any crystal with centro-symmetric structure the quadratic term of the polarizability vanishes. Thus, the SPDC effect exists only for birefringent media. If one assumes that $\chi_{ijk}^{(2)}(\mathbf{x})$ has the same value for all points within the crystal, one gets

$$\begin{aligned} H_{int} &\sim \int_V \mathbf{p}(\mathbf{x}, t) \cdot \mathbf{E}(\mathbf{x}, t) d^3x \\ &= \int_V \mathbf{p}^{lin}(\mathbf{x}, t) \cdot \mathbf{E}(\mathbf{x}, t) d^3x \\ &+ \int_V \mathbf{p}^{nl}(\mathbf{x}, t) \cdot \mathbf{E}(\mathbf{x}, t) d^3x, \end{aligned}$$

where \mathbf{p}^{lin} (\mathbf{p}^{nl}) is the linear (nonlinear) term of polarization. The nonlinear part of the Hamiltonian is

$$H^{NL} \sim \int_V \sum_{ijk} \chi_{ijk}^{(2)} E_i(\mathbf{x}, t) E_j(\mathbf{x}, t) E_k(\mathbf{x}, t) d^3x. \quad (49)$$

Electromagnetic field.—The quantized electric field can be expressed (in the interaction picture) as

$$\begin{aligned} \mathbf{E}(\mathbf{x}, t) &= \sum_{p=1}^2 \int d^3k \frac{i}{\sqrt{2\omega(2\pi)^3}} \\ &\times \hat{\boldsymbol{\epsilon}}(\mathbf{k}, p) a(\mathbf{k}, p) e^{i(\mathbf{k} \cdot \mathbf{x} - \omega t)} + h.c. \\ &= \mathbf{E}^{(+)}(\mathbf{x}, t) + \mathbf{E}^{(-)}(\mathbf{x}, t), \end{aligned} \quad (50)$$

where $\mathbf{E}^{(-)}(\mathbf{x}, t) = [\mathbf{E}^{(+)}(\mathbf{x}, t)]^\dagger$, and the summation is over two orthogonal linear polarizations, $h.c.$ denotes the hermitian conjugate of the previous term, and $\hat{\boldsymbol{\epsilon}}(\mathbf{k}, p)$ is a unit vector defining the linear polarization. The symbol $a(\mathbf{k}, p)$ denotes the annihilation operator of a monochromatic photon with wave vector \mathbf{k} , and polarization $\hat{\boldsymbol{\epsilon}}(\mathbf{k}, p)$. The principal commutation rule for such creation and annihilation operators is given by³⁴ $[a(\mathbf{k}, p), a^\dagger(\mathbf{k}', p')] = \delta_{p,p'} \delta^{(3)}(\mathbf{k} - \mathbf{k}')$, $[a^\dagger(\mathbf{k}, p), a^\dagger(\mathbf{k}', p')] = 0$ and $[a(\mathbf{k}, p), a(\mathbf{k}', p')] = 0$.

The relevant terms in the Hamiltonian.—One can neglect the depletion of the laser field and assume that the total field is $\mathbf{E}^{Laser}(\mathbf{x}, t) + \mathbf{E}(\mathbf{x}, t)$, where \mathbf{E}^{Laser} is a classical field. The quantum field \mathbf{E} describes the emitted photons. The down conversion takes place, thanks to only the terms in (49) of the form

$$\int_V \sum_{ijk} \chi_{ijk}^{(2)} E_i^{Laser} E_j^{(-)} E_k^{(-)} d^3x. \quad (51)$$

Simply, only $E^{(-)}$ contains the creation operators, and thus acting on the vacuum state $|\Omega\rangle$ can give rise to a two-photon state. Thus, we forget about all other terms and analyze only H^{NL} in the form of (51) plus its Hermitian conjugate.

Let us describe the laser field as a monochromatic wave $\hat{x} E_0 (e^{i(\mathbf{k}_0 \cdot \mathbf{x} - \omega_0 t - \phi)} + c.c.)$, where E_0 is the field amplitude.³⁵ Then, from (51), one gets for H^{NL}

$$\begin{aligned} &\sim \int_V \sum_{jk} \{ \chi_{3jk}^{(2)} E_0 [e^{i(\mathbf{k}_0 \cdot \mathbf{x} - \omega_0 t - \phi)} + c.c.] \\ &\times \sum_p \int d^3k f(\omega) \hat{\boldsymbol{\epsilon}}(\mathbf{k}, p) a^\dagger(\mathbf{k}, p) e^{-i(\mathbf{k} \cdot \mathbf{x} - \omega t)} \\ &\times \sum_{p'} \int d^3k' f(\omega') \hat{\boldsymbol{\epsilon}}(\mathbf{k}', p) a^\dagger(\mathbf{k}', p) e^{-i(\mathbf{k}' \cdot \mathbf{x} - \omega' t)} d^3x + h.c., \end{aligned} \quad (52)$$

³⁴ These new operators are linked with the ones discussed earlier by the relation $a^l = \sum_p \int d^3k g_{pk}^l a(\mathbf{k}, p)$.

³⁵ Since an arbitrary electromagnetic field is a superposition of the plane waves, starting with this trivial case it is very easy to get the general description.

with $f(\omega)$ being a factor dependent on ω . Its specific structure is irrelevant here. Extracting only those elements of the above expressions which contain \mathbf{x} and t , one sees that their overall contribution to H^{NL} is given by $\Delta(\pm\mathbf{k}_0 - \mathbf{k} - \mathbf{k}')e^{-i(\pm\omega_0 - \omega - \omega')t}$, where $\Delta(\dots) = \int_V d^3x e^{i(\pm\mathbf{k}_0 - \mathbf{k} - \mathbf{k}') \cdot \mathbf{x}}$. The terms with the time dependent factors, $e^{i(\omega_0 + \omega + \omega')t}$, average out in any time integration, and thus we can drop them. If we assume that our crystal is a cube $L \times L \times L$, then for $L \rightarrow \infty$, Δ approaches $\delta(\mathbf{k}_0 - \mathbf{k} - \mathbf{k}')$. Thus, emission of the photon pairs is possible only for the directions for which the condition $\mathbf{k}_0 \approx \mathbf{k} + \mathbf{k}'$ is met. Finally one has

$$H^{NL} \sim \sum_{\pm} \sum_{p,p'} \int d^3k \int d^3k' \Delta(\mathbf{k}_0 - \mathbf{k} - \mathbf{k}') A_{p,p'}^{eff} \times e^{-i(\omega_0 - \omega - \omega')t} a^\dagger(\mathbf{k}, p) a^\dagger(\mathbf{k}', p') + \text{h.c.}, \quad (53)$$

where $A_{p,p'}^{eff} = \sum_{j,k} E_0 \chi_{3jk}^{(2)} \hat{\epsilon}_j(\mathbf{k}, p) \hat{\epsilon}_k(\mathbf{k}', p')$ is the effective strength of the laser-crystal coupling. Furthermore, we shall replace the symbol $A_{p,p'}^{eff}$ by $F_o(\mathbf{k}_o)$.

The state of photons emitted in the SPDC process.—The pump-crystal coupling is weak. The evolution of the state $|\Psi_D(t)\rangle$ (in the interaction picture) is given by $i\hbar \frac{d}{dt} |\Psi_D(t)\rangle = H^{NL}(t) |\Psi_D(t)\rangle$. In the first order in the perturbation expansion

$$|\Psi_D(t)\rangle \simeq |\Psi_D(t_0)\rangle + \frac{1}{i\hbar} \int_{t_0}^t H^{NL}(t') |\Psi_D(t_0)\rangle dt'. \quad (54)$$

Put $t_0 = -\infty$, and take the vacuum state (no photons) $|\Omega\rangle$ as the initial state $|\Psi(0)\rangle$. Then, only in the term with the integral one can find creation of pairs of photons. It contains an integral of the following form: $\int_{-\infty}^{+\infty} dt' e^{it'(\omega + \omega' - \omega_0)}$ which is $2\pi\delta(\omega + \omega' - \omega_0)$. Thus, the two-photon component of the state, at $t = \infty$, is

$$\sum_{\pm} \sum_{p,p'} \int d^3k \int d^3k' F_o(\mathbf{k}_o) \Delta(\mathbf{k}_0 - \mathbf{k} - \mathbf{k}') \times \delta(\omega + \omega' - \omega_0) a^\dagger(\mathbf{k}, p) a^\dagger(\mathbf{k}', p') |\Omega\rangle, \quad (55)$$

and the frequencies of the emissions satisfy the relation³⁶ $\omega_0 = \omega + \omega'$.

Directions of emissions.—Since $\omega = |\mathbf{k}| \frac{c}{n(\omega, p)}$, where $\frac{c}{n(\omega, p)} = c(\omega, p)$ is the speed of light in the given medium, which depends on frequency and polarization, the condition for frequencies becomes $|\mathbf{k}_0|c(\omega_0) \simeq |\mathbf{k}|c(\omega, p) + |\mathbf{k}'|c(\omega', p')$. This, together with $\mathbf{k}_0 \simeq \mathbf{k}_s + \mathbf{k}_i$ fixes the possible emission directions, frequencies and polarizations. There are two types of SPDC. Type-I: both

photons of a pair have the same polarization; type-II: they have orthogonal polarizations.³⁷

Time correlations.—The probability of a detection of a photon, of say, the horizontal polarization H , at a detector situated at point \mathbf{x} and at time t , is proportional to $\eta \text{Tr} \rho(t) E_H^{(-)}(\mathbf{x}, t) E_H^{(+)}(\mathbf{x}, t)$, where η is the coefficient which characterizes the quantum efficiency of the detection process, ρ is the density operator, E_H is the horizontal component of the field in the detector. For the above relation to be true, we also assume that, only via the aperture of the detector enter the photons of a specified direction of the wave vector. For a pure state, this reduces to $p(\mathbf{x}, t, H) \simeq \langle \psi | E_H^{(-)} E_H^{(+)} | \psi \rangle$. The probability of a joint detection of two photons, of polarization H , at the locations \mathbf{x}_1 and \mathbf{x}_2 , and at the moments of time t and t' , is proportional to

$$p(\mathbf{x}_1, t; \mathbf{x}_2, t') \sim \langle \psi | E_H^{(-)}(\mathbf{x}_1, t) E_H^{(-)}(\mathbf{x}_2, t') \times E_H^{(+)}(\mathbf{x}_2, t') E_H^{(+)}(\mathbf{x}_1, t) | \psi \rangle. \quad (56)$$

If the detectors are very far away from each other, and from the crystal, then the photon field reaching them can be treated as free-evolving. We put into (56) the photon state (55). Let $t = t_1$ and $t' = t_2$, and $|\psi\rangle = |\psi(t = \infty)\rangle$, then (56) can be written down as

$$p(\mathbf{x}_1, t | \mathbf{x}_2, t') \simeq \langle \psi | E_H^{(-)}(\mathbf{x}_1, t) E_H^{(-)}(\mathbf{x}_2, t') \times E_H^{(+)}(\mathbf{x}_1, t) E_H^{(+)}(\mathbf{x}_2, t') | \psi \rangle. \quad (57)$$

To simplify the description, let us replace the annihilation and creation operators, which were used above, with new operators $a_i(\omega)$ and their conjugates, which describe “unidirectional” excitations of the photon field [i.e., we assume that the detectors see only the photons of a specified direction of propagation, a good assumption if the detectors are far from the crystal, and the apertures are narrow, see (Fearn and Loudon, 1987)]. The index i defines the direction (fixed) of the wave vector. The new operators satisfy commutation relation, which are a modification of those given above to the current specific case $[a_i(\omega), a_j^\dagger(\omega')] = \delta_{ij} \delta(\omega - \omega')$, $[a_i(\omega), a_j(\omega')] = 0$. If we choose just two propagation directions that fulfill the phase matching conditions, then effectively one can put

$$E_H^{(+)}(\mathbf{x}_i, t) = \int d\omega e^{-i\omega t} f_i(\omega) a_i(\omega)$$

with $i = 1, 2$, and where f_1 and f_2 are the frequency response functions of the filter-detector system. We assume that the maxima of the functions agree with the frequencies given by the phase matching conditions. Introducing a unit operator $\hat{I} = \sum_{i=0}^{\infty} |b_i\rangle \langle b_i|$, where $|b_i\rangle$ is

³⁶ One should add here a note that in reality this relation is not absolutely sharp. The molecular polarization was treated here phenomenologically. Still, once a more refined model is used the relationship is sharp enough, so that the deviations from perfect equality are beyond the resolution of the present measuring apparatus.

³⁷ If one has $\omega \simeq \omega'$ then we have a frequency degenerate PDC, and if $\hat{k} \simeq \hat{k}'$, then we have a co-linear one.

the basis states, into (57), we obtain

$$p(\mathbf{x}_1, t | \mathbf{x}_2, t') \simeq \langle \psi | E_H^{(-)}(\mathbf{x}_1, t) E_H^{(-)}(\mathbf{x}_2, t') \times \hat{I} E_H^{(+)}(\mathbf{x}_1, t) E_H^{(+)}(\mathbf{x}_2, t') | \psi \rangle. \quad (58)$$

Since $E_H^{(+)}$ contains only the annihilation operators, they transform the two-photon state $|\Psi\rangle$ into the vacuum state. Thus, Eq. (58) can be put as (Mollow, 1973)

$$p(\mathbf{x}_1, t | \mathbf{x}_2, t') \simeq \langle \psi | E_H^{(-)} E_H'^{(-)} | \Omega \rangle \langle \Omega | E_H^{(+)} E_H'^{(+)} | \psi \rangle, \quad (59)$$

where the primed expressions pertain to the moment of time t' and the position \mathbf{x}_2 . Thus we have $p(\mathbf{x}_1, t | \mathbf{x}_2, t') \simeq |A_{12}(t, t')|^2$, where $A_{12}(t, t') = \langle \Omega | E_H^{(+)}(\mathbf{x}_1, t) E_H'^{(+)}(\mathbf{x}_2, t') | \psi \rangle$. With the use of the new creation operators, the state $|\Psi\rangle$ can be approximated by

$$|\Omega\rangle + \int d\omega_1 \int d\omega_2 F_o \delta(\omega - \omega_1 - \omega_2) a_1^\dagger(\omega_1) a_2^\dagger(\omega_2) |\Omega\rangle. \quad (60)$$

With this one gets the following formula for the detection amplitude

$$A_{12}(t, t') = \langle \Omega | \int d\omega' e^{-i\omega't} f_2(\omega') a_2(\omega') \times \int d\omega e^{-i\omega t} f_1(\omega) a_1(\omega) \int d\omega_2 \int d\omega_1 \times F_o \delta(\omega_0 - \omega_1 - \omega_2) a_2^\dagger(\omega_2) a_1^\dagger(\omega_1) | \Omega \rangle. \quad (61)$$

Since the creation and annihilation operators for different modes commute, and since one can use $\langle \Omega | a_i(\omega') a_j^\dagger(\omega) | \Omega \rangle = \delta_{ij} \delta(\omega' - \omega)$, we get

$$A_{12}(t, t') = F_o e^{-i\omega_0 t'} \int d\omega e^{-i\omega(t-t')} f_2(\omega_0 - \omega) f_1(\omega), \quad (62)$$

and we have

$$p(\mathbf{x}_1, t | \mathbf{x}_2, t') \sim |A_{12}(t, t')|^2 \simeq \left| \int d\omega e^{-i\omega(t-t')} f_2(\omega_0 - \omega) f_1(\omega) \right|^2, \quad (63)$$

i.e., the probability depends on the difference of the detection times.

For instance, assume that: $f_1 = f_2 = f$, and that they are Gaussian, $f(\omega) = C e^{-\frac{(\omega_c - \omega)^2}{\sigma^2}}$, with the central frequency $\omega_c = \frac{1}{2}\omega_0$. Then we have $f_1(\omega) = f_2(\omega_0 - \omega) = f(\omega)$. The probability of detection of two photons at the moments t and t' reads

$$p(\mathbf{x}_1, t | \mathbf{x}_2, t') \sim \left| \int d\omega e^{-i\omega(t-t')} C^2 e^{-2\frac{(\omega_c - \omega)^2}{\sigma^2}} \right|^2 \sim e^{-\frac{\sigma^2}{2}(t-t')^2}. \quad (64)$$

If $\sigma \rightarrow \infty$ then the expression (64) approaches $\delta(t - t')$. We have perfect time correlation. For a realistic case of

final bandwidths, the degree of time correlation of the detection of the SPDC photons depends entirely on the frequency response of the detectors.

The output state of pulsed pump SPDC.—Since the pump pulse is a superposition of a monochromatic waves, the output state for this case is an integral of the monochromatic case over the momentum profile of the pulse: $|\psi_{pulse}\rangle = \int d^3\mathbf{k}_o |\psi(F_o(\mathbf{k}_o))\rangle$, where $|\psi(F_o(\mathbf{k}_o))\rangle$ is the state for in the monochromatic case with wave vector \mathbf{k} and field amplitude $F_o(\mathbf{k}_o)$. Since the frequency of the pulse and the wave vector are not strictly defined. If the pulse is too short the SPDC photons are less tightly correlated directionally.

The two photon state coming out of an SPDC can be approximated by

$$|\Psi\rangle = \int d\omega_0 F_o(\omega_0) \int d\omega_1 \int d\omega_2 \times \delta(\omega_0 - \omega_1 - \omega_2) a_1^\dagger(\omega_1) a_2^\dagger(\omega_2) |\Omega\rangle, \quad (65)$$

where we have replaced the effective pump amplitude by the spectral decomposition of the laser pulse $F_o(\omega_0)$. Since a pulse is a superposition of monochromatic waves, we therefore integrate over its spectrum.

Two-photon detection amplitude: the pulsed pump case.—If we have a pulsed pump we have to integrate the amplitude (62) over the frequency content of the pump (just like it is in the case of the state 65):

$$A(t, t') = \int d\omega_o F_o(\omega_o) e^{-i\omega_o t'} \int e^{-i\omega(t-t')} f_2(\omega_o - \omega) f_1(\omega) = \int dt_p \int dt_1 \int dt_2 F_o(t_p) f_1(t - t_p) f_2(t' - t_p). \quad (66)$$

where, e.g., $F_o(t)$ is the Fourier transformation (time profile) of $F_o(\omega)$. Namely, the time correlation of the detections is defined by the resolution of the respective filters, and the events happen at times dictated by the pulse.

2. Early SPDC interference experiments

One of the first phenomena observed using the SPDC sources was interference effect now called the Hong-Ou-Mandel dip (Hong, Ou, and Mandel, 1987), described in section III.D. Type-I down conversion was used therein. This allows both SPDC photons to be almost fully indistinguishable, due to the fact they possess the same polarization, and thus their spectral properties are symmetric. If the optical paths are identical, the alternative quantum processes are indistinguishable, and one has the dip. In a related experiment (Ou and Mandel, 1988b) with SPDC photons of slightly different central frequencies, one could observe the so-called spatial quantum beats phenomenon (beating in the coincidence rate depending on the relative optical paths). It should be pointed out that these two-photon interference effects are insensitive to the relative phase of the photons.

The Hong-Ou-Mandel interference experiment was since repeated many times [see, e.g., also (Walborn *et al.*, 2003a) for the multimode case]. It can also be observed with photons that are successively emitted from, e.g., a quantum-dot single-photon source (Santori *et al.*, 2002). Recently, Legero *et al.* (2004) demonstrated the fourth-order interference of two photons in the temporal regime.

First observations of Bell-type quantum interference for photon pairs generated by type-I SPDC were made by Shih and Alley (Alley and Shih, 1986; Shih and Alley, 1988), and Ou and Mandel (1988a). The photons of a down-converted pair were impinging a 50:50 BS, each into a different input port. Polarization of one of the photons was rotated by 90° . If the two photons are indistinguishable except that they are oppositely polarized (say, one is horizontally polarized, H , and the other vertically polarized, V), then after leaving the two output ports 1 and 2, the resulting two-photon state is $\frac{1}{\sqrt{2}}[\sqrt{2}|\psi^-\rangle_{12} + i(|H\rangle_1|V\rangle_1 + |H\rangle_2|V\rangle_2)]$. Thus in coincidence, behind two separated polarization analysers, detection effects only due to the first, entangled, component appear.³⁸ There was some controversy (see De Caro and Garuccio, 1994) whether such observation is a valid test of a Bell inequality. However, it turns out that if one takes into account the full process, one can derive a refined version of Bell's theorem which applies for this type of experiment (Popescu, Hardy, and Żukowski, 1997).

3. Various types of entanglement

Below we summarize several standard types of photonic entanglement, which can be obtained with SPDC sources.

Polarization entanglement.—The standard method to produce polarization-entangled photons is now the non-collinear type-II SPDC process (Kwiat *et al.*, 1995) and its principle is described in (Fig. 7) and the caption. The state emerging through the two beams A and B is a superposition of $|H\rangle|V\rangle$ and $|V\rangle|H\rangle$, namely,

$$\frac{1}{\sqrt{2}}(|H\rangle_A|V\rangle_B + e^{i\alpha}|V\rangle_A|H\rangle_B) \quad (67)$$

where the relative phase α is due to the birefringence. Using an additional birefringent phase shifter (or even slightly rotating the down-conversion crystal itself), the value of α can be set as desired, e.g., to 0 or π . A net phase shift of π may be obtained by a 90° rotation of a quarter wave plate in one of the paths. A half wave plate in one path can be used to change horizontal polarization to vertical and *vice versa*. One can thus produce any of the four Bell states in Eq. (17).

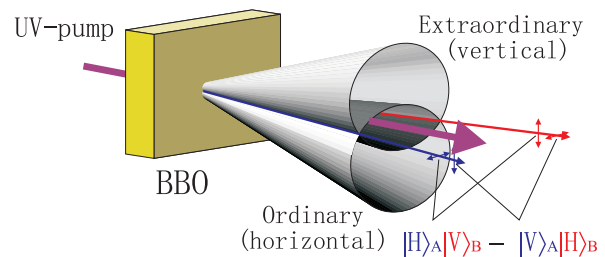


FIG. 7 Principle of type-II parametric down-conversion. Inside a nonlinear crystal (e.g., BBO), an incoming pump photon can decay spontaneously into two photons. Two down-converted photons arise polarized orthogonally to each other. Each photon is emitted into a cone, and the photon on the top cone is vertically polarized while its exactly opposite partner in the bottom cone is horizontally polarized. Along the directions where the two cones intersect, their polarizations are undefined; all that is known is that they have to be different, which results in polarization entanglement between the two photons in beams A and B.

The birefringence introduces complications. Since the ordinary and extraordinary photons have different velocities, and propagate along different directions, even though they become collinear outside the crystal, the resulting longitudinal and transverse walk-offs between the two terms in the state (67) are maximal for pair creation near the entrance face. This results in a relative time delay $\delta T = L(1/u_o - 1/u_e)$ (L is the crystal length, and u_o and u_e are the ordinary and extraordinary group velocities, respectively) and a relative lateral displacement $d = L \tan \rho$ (ρ is the angle between the ordinary and extraordinary beams inside the crystal). If for the coherence time, τ_c , of the down-converted light one has $\delta T \geq \tau_c$, then the terms in Eq. (67) become, in principle, distinguishable, and no two-photon polarization interference is observable. Similarly, if d is larger than the coherence width, the terms can become partially labeled by their spatial location. Fortunately, because the photons are produced coherently along the entire length of the crystal, one can completely compensate for the longitudinal walk-off (Rubin *et al.*, 1994). After the compensation, interference occurs pairwise between processes in which the photon pair is created at distances $\pm x$ from the middle of the crystal. The ideal compensation is therefore to use two crystals, one in each path, which are identical with the down-conversion crystal, but only half as long. If the polarizations are rotated by 90° (e.g., with a half wave plate), the retardations of the o and e components are exchanged and complete temporal indistinguishability is restored ($\delta T = 0$). The method provides optimal compensation for the transverse walk-off effect as well.

Using type-II SPDC, two-photon states of tunable purity and the degree of entanglement can be produced (White *et al.*, 1999; Peters *et al.*, 2004; Cinelli *et al.*, 2004). This extends the boundaries of experimentally accessible two-qubit Hilbert space of photons.

³⁸ This type of interference was recently demonstrated for two indistinguishable photons from quasi-independent sources (Pittman and Franson, 2003; Fatal *et al.*, 2004).

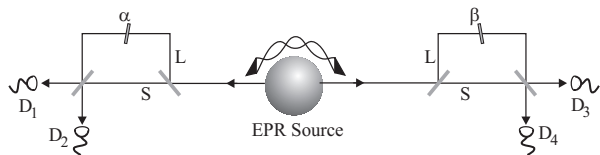


FIG. 8 A Franson-type experiment testing the interference of time-entangled photon pairs by measuring them with two remote unbalanced Mach-Zehnder-interferometers.

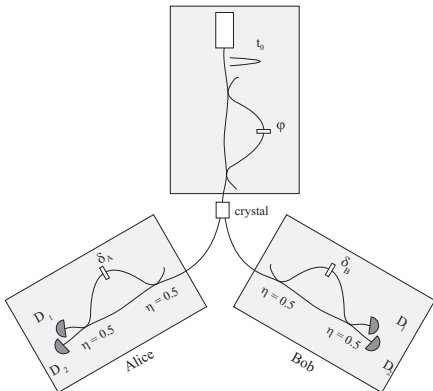


FIG. 9 Schematic of the pulsed time-entangled twin-photon source (Gisin *et al.*, 2002).

Temporal entanglement.—The two photons of an SPDC are tightly time correlated. Because of the spontaneous nature of the emission, if the crystal is pumped by a cw laser, the time of pair emission is undefined. Suppose that both photons enter two *identical* unbalanced Mach-Zehnder interferometers with the path-length difference, ΔL much longer than their coherence length (see Fig. 8). As it was shown by Franson (1989) the coincidence count rates at the outputs of both interferometers show a sinusoidal interference pattern, which depends on the sum of the local phase shifts. If coincidence gate is much shorter than ΔLc only the following processes contribute to the interference:

$$\frac{1}{\sqrt{2}} (|long\rangle_1|long\rangle_2 + e^{i\phi}|short\rangle_1|short\rangle_2), \quad (68)$$

where $|short\rangle$ and $|long\rangle$ denote the photon in short or long arm of the local interferometer. This is the principle of Franson-type interferometry (Franson, 1989). This type of interference was observed with high visibilities by Brendel *et al.* (1992) and Kwiat *et al.* (1993).

A pulsed-pump version of Franson-interferometry is called time-bin entanglement (Brendel *et al.*, 1999; Marcikic *et al.*, 2002; Gisin *et al.*, 2002), and is good for practical applications (see Fig. 9). A short, ultraviolet pump pulse is sent first through an unbalanced Mach-Zehnder interferometer (the pump interferometer), and next through a BBO crystal. In the interferometer the pulse is split by the first variable coupler (an optical fiber equivalent of a variable BS) into two pulses, one propa-

gating along the short path and another along the long path. If the pulse duration is shorter than ΔLc , the output from the second variable coupler is two pulses, well separated in time. This process transforms the state of the pump into a superposition $\alpha|short\rangle_p + \beta|long\rangle_p$. Then, if via SPDC a pump photon split into a pair, it is in the state

$$\alpha|short\rangle_1|short\rangle_2 + \beta|long\rangle_1|long\rangle_2. \quad (69)$$

The two entangled photons can be separated and subject to local measurements in unbalanced interferometers with ΔL identical as in the pump interferometer (For more details, see Gisin *et al.*, 2002). By varying the coupling ratio of the couplers and phases in the pump interferometer, all two-qubit entangled time-bin states can be generated. The coherence is build by the pump interferometer. A remarkable advantage of the time-bin entanglement is that it can be robustly distributed to a long distance in optical fibers—experimental distribution over 50 km in optical fibers was achieved (Marcikic *et al.*, 2004).

Path entanglement.—Entanglement experiments involving path-entanglement were proposed by Horne and Zeilinger (1986), and their feasible version by Żukowski and Pykacz (1988). Finally Horne, Shimony and Zeilinger (1989) showed that SPDC is an ideal source in case of such experiments. This was realized by Rarity and Tapster (1990). Due to the phase-matching relation, idler and single photons of given frequencies are correlated in emission directions (i.e., paths, or momenta). One can use apertures, see Fig. 10, to select only two spatial conjugate mode pairs (directions). The pairs of photons emerge via the apertures such that they are either in the upper a-mode ($a1$) and lower b-mode ($b2$), or in the lower a-mode ($a2$) and upper b-mode ($b1$). The resulting state is thus

$$|\Psi\rangle = \frac{1}{\sqrt{2}} (e^{i\phi_b}|a1\rangle|b2\rangle + e^{i\phi_a}|a2\rangle|b1\rangle). \quad (70)$$

The a -modes enter a BS via opposite inputs, so do b -modes. Behind the beamsplitters upper and lower paths cannot be distinguished, leading to two-photon interference, which depends on the sum relative phase shifts in a and b modes.

In the Rarity-Tapster experiment two particle interference fringes had 82% visibility. This is beyond the maximum predicted for any local realistic model of the experiment (see also section IV.D), however, lower than in polarization entanglement experiments. This is due to the difficulties of alignment and overlap of the four beams. For further discussion on the physics underlying this interferometer, see section IV.C.1.

B. Hyper-entangled photons

As it was shown earlier the SPDC photons are entangled in energy and momentum, and if suitably selected,

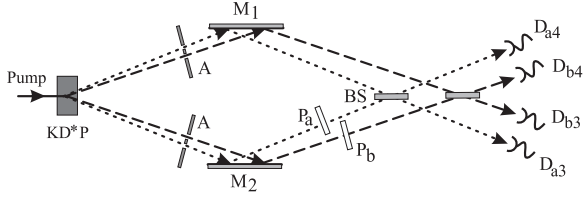


FIG. 10 The Rarity-Tapster experiment on momentum entanglement from a type-I SPDC (Rarity and Tapster, 1990). Two correlated pairs of modes are selected from the emission spectrum of a type-I down-conversion source using double apertures A. The different wavelengths are recombined on two BS. The detectors D_{a3} , D_{b3} , D_{a4} , and D_{b4} are used to measure the outputs from the BSs.

can be also entangled in polarization or path. If one selects pairs which are entangled not only in polarization but also in some other degree(s) of freedom, this specific entanglement is called hyper-entanglement (Kwiat, 1997). Hyper-entanglement may have interesting applications. These include hyper-entanglement assisted Bell-state analysis (Kwiat and Weinfurter, 1998; Walborn *et al.*, 2003b; Schuck *et al.*, 2006), entanglement purification (Simon and Pan, 2002), two-particle GHZ-type test of local realism (Chen *et al.*, 2003), implementations of single-photon two-qubit CNOT gate (Fiorentino *et al.*, 2004) and two-qubit swap gate (Fiorentino *et al.*, 2005), and deterministic quantum cryptography (Chen *et al.*, 2006d). In addition, hyper-entanglement can also be interpreted as entanglement of two higher-dimensional quantum systems (Chen *et al.*, 2003). This may be used in higher-dimensional quantum cryptography (e.g., Bechmann-Pasquinucci and Peres, 2000; Cerf *et al.*, 2002).

1. Polarization-path entanglement

The first polarization-path hyper-entanglement was independently realized by Barbieri *et al.* (2005) using type-I nonlinear crystal, and by Yang *et al.* (2005) using type-II nonlinear crystal. Polarization-path entanglement can be generated by a double pass of a pump laser through a BBO crystal (Chen *et al.*, 2003). A pump pulse passing through the crystal leads to a non-zero probability amplitude of creating a polarization-entangled photon pair in two spatial (path) modes d_A and u_B , for example $|\psi^-\rangle_{\text{pol}} = \frac{1}{\sqrt{2}}(|H\rangle_A |V\rangle_B - |V\rangle_A |H\rangle_B)$. If the pump is reflected and passes the crystal a second time, then another probability amplitude is non zero: for producing entangled pairs of photons in $|\psi^-\rangle_{\text{pol}}$, but now into the other two path modes u_A and d_B . Both pair-creation amplitudes can be equal by adjusting a focusing lens F. If there is perfect temporal overlap of modes R_A and L_A and of modes u_B and d_B , the path state of the pairs is $|\psi^-(\phi)\rangle_{\text{path}} = \frac{1}{\sqrt{2}}(|u\rangle_A |d\rangle_B - e^{i\phi} |d\rangle_A |u\rangle_B)$, where the

two orthonormal kets $|d\rangle$ and $|u\rangle$ denote the two path states of photons. By properly adjusting the distance between the mirror and the crystal such that $\phi = 0$, one gets

$$|\Psi\rangle = |\psi^-\rangle_{\text{pol}} \otimes |\psi^-(0)\rangle_{\text{path}}, \quad (71)$$

which is a two-photon state maximally entangled in both polarization and path.

2. Polarization-time entanglement

A more robust distribution of hyper-entanglement is possible with photon pairs which are entangled both in time (i.e., time-bin entanglement) and in polarization (Genovese and Novero, 2002; Chen *et al.*, 2006d). To create such polarization-time entanglement, a short, ultraviolet laser pulse is sent first through an unbalanced Mach-Zehnder interferometer (the pump interferometer), to have two pulses well separated in time; next they pass a BBO crystal. Assume that each pulse can create the following state: $\frac{1}{\sqrt{2}}(|H\rangle_1 |H\rangle_2 + |V\rangle_1 |V\rangle_2)$, thus after the “early” and “late” pulses pass the crystal, a polarization-time entangled two-photon state is created $|\Psi\rangle_{12} = \frac{1}{2}(|H\rangle_1 |H\rangle_2 + |V\rangle_1 |V\rangle_2) \otimes (|E\rangle_1 |E\rangle_2 + e^{i\phi} |L\rangle_1 |L\rangle_2)$. Here $|E\rangle$ (early time) and $|L\rangle$ (late time) are two time shifted states of photons (time shift beyond the coherence time makes them orthogonal). The phase shift ϕ can be adjusted by changing in the relative phase of the two pulses. Using a “time-path transmitter” introduced by Chen *et al.* (2006d), one can realize a transformation between polarization-path and polarization-time hyper-entanglement.

3. Entanglement in more degrees of freedom

In an experiment by Barreiro *et al.* (2005), besides the entanglement in polarization and in energy, photon pairs from a single nonlinear crystal were also entangled in orbital angular momentum. By pumping two contiguous BBO crystals with optical axes aligned in perpendicular planes, a two-photon $(2 \otimes 2) \otimes (3 \otimes 3) \otimes (2 \otimes 2)$ -dimensional hyper-entangled state was produced, approximately described by

$$\underbrace{(|HH\rangle + |VV\rangle)}_{\text{polarization}} \otimes \underbrace{(|rl\rangle + \alpha|gg\rangle + |lr\rangle)}_{\text{spatial}} \otimes \underbrace{(|EE\rangle + |LL\rangle)}_{\text{energy-time}}.$$

Here $|l\rangle$, $|g\rangle$ and $|r\rangle$ represent the paraxial spatial modes (Laguerre-Gauss) carrying $-\hbar$, 0, and $+\hbar$ orbital angular momentum, respectively (Allen *et al.*, 2003); α describes the orbital-angular-momentum spatial mode balance which is due the properties of the source (Torres *et al.*, 2003) and the selection via the mode-matching conditions.

C. Photonic entanglement in higher dimensions

Photonic entanglement in higher dimensions can in principle be generated by SPDC process in a form of generalization of path-entanglement into more than two conjugate pairs of beams (Zeilinger *et al.*, 1993), and analyzed with N -port BS (for a general theory of such devices see Reck *et al.*, 1994). As it was shown by Żukowski, Zeilinger and Horne (1997) such configuration can lead to new types of EPR correlations, and can be used as tests of local realism (which are more discriminating than two qubit tests, see [Kaszlikowski *et al.* (2000)]). However, such schemes usually require complex optical circuits.

A more practical route is as follows.³⁹ The spatial modes of the electromagnetic field carry orbital angular momentum. Orbital angular momentum eigenstates of photons are states of the electromagnetic field with phase singularities (doughnut modes). This can be utilized for observation of higher dimensional entanglement (Mair *et al.*, 2001; Vaziri *et al.*, 2002, 2003). This approach has advantages in certain quantum communication protocols (Vaziri *et al.*, 2002, Molina-Terriza *et al.*, 2004; Gröblacher *et al.*, 2006).

In the experiments, first it was confirmed that SPDC conserves orbital angular momentum of photons. This was done for pump beams carrying orbital angular momenta of $-\hbar$, 0, and $+\hbar$ per photon respectively. Next it was shown that the state of the down-converted photons is indeed a coherent superposition of the two-photon processes allowed by angular momentum conservation, in other words: that orbital angular momentum state of the pairs is entangled. Since the Laguerre-Gauss modes form an infinite basis, the SPDC pairs are in an entangled state given by

$$|\psi\rangle = C_{0,0}|0\rangle|0\rangle + C_{1,-1}|1\rangle|-1\rangle + C_{-1,1}|-1\rangle|1\rangle + C_{2,-2}|2\rangle|-2\rangle + C_{-2,2}|-2\rangle|2\rangle + \dots, \quad (72)$$

where the numbers in the brackets represent the indices l of the Laguerre-Gauss modes and the $C_{i,j}$ denote the corresponding probability amplitudes.

D. Twin-beam multi-photon entanglement

It is also possible to produce entangled states involving large numbers of photons, approaching the macroscopic domain. Such entanglement is related to experiments on twin beams (Smithey *et al.*, 1992) and should be called *bipartite* multi-photon entanglement. It should not be confused with multi-photon entanglement in which each photon represents a qubit, and can be individually manipulated.

The bipartite multi-photon entanglement can be generated via a standard SPDC, but with a strong pump pulse. The interaction time is increased by employing cavities both for the pump and the down-converted light. Such a stimulated SPDC (Lamas-Linares *et al.*, 2001; Simon and Bouwmeester, 2003) may show the onset of laser-like action for entangled photons (“entanglement laser”) in the sense that a (spontaneously created) photon pair in two polarization-entangled modes stimulate, inside a nonlinear gain medium, the emission of additional pairs.

A simplified Hamiltonian for the generation of polarization entangled SPDC photons is given by $H_{\text{SPDC}}^{\text{sim}} = i\kappa(a_H^\dagger b_V^\dagger - a_V^\dagger b_H^\dagger) + h.c.$ Horizontally (H) and vertically (V) polarized photons occupy two spatial modes (a and b); κ is a coupling constant that depends on the nonlinearity of the crystal and the intensity of the pump pulse. After the interaction time t the resulting photon state is given by $|\psi\rangle = e^{-itH_{\text{SPDC}}^{\text{sim}}} |0\rangle$, namely, (Kok and Braunstein, 2000; Lamas-Linares *et al.*, 2001; Simon and Bouwmeester, 2003)

$$|\psi\rangle = \frac{1}{\cosh^2 \tau} \sum_{n=0}^{\infty} \sqrt{n+1} \tanh^n \tau |\psi_n^-\rangle, \\ |\psi_n^-\rangle = \sum_{m=0}^n \frac{(-1)^m}{\sqrt{n+1}} |n-m, m; m, n-m\rangle, \quad (73)$$

where $|n-m, m; m, n-m\rangle$ denotes a number state in respectively modes a_H , a_V , b_H and b_V , and $\tau = \kappa t$ is the interaction parameter. To avoid multi-pair emission events most SPDC experiments are restricted to $\tau < 0.1$. By going to higher values, bipartite entangled states constituting of large numbers of photons are generated. The state $|\psi\rangle$ is a superposition of the states $|\psi_n^-\rangle$ of n indistinguishable photon pairs. Each $|\psi_n^-\rangle$ is an analog of a singlet state of two spin- $n/2$ particles, thus $|\psi\rangle$ is invariant under joint rotations of the polarization bases of both modes. The polarization of each beam is completely undetermined, but the polarizations of the two beams are always anti-correlated. The average photon pair number is $\langle n \rangle = 2 \sinh^2 \tau$.

From such states one can extract for example the following 2-pair term of Eq. (73):

$$|\psi_2^-\rangle = \frac{1}{\sqrt{3}} (|2, 0; 0, 2\rangle - |1, 1, 1, 1\rangle + |0, 2; 2, 0\rangle), \quad (74)$$

which can be treated as a singlet state of two (composite) spin-1 systems [see Howell *et al.* (2002) for a test of Bell’s inequality by entangled states of spin-1 systems].

The theory of entanglement laser was developed by Simon and Bouwmeester (2003). The basic principle of stimulated entanglement creation was first experimentally demonstrated in the few-photon regime (Lamas-Linares *et al.*, 2001). Later, twin-beam entanglement of up to 12 photons (Eisenberg *et al.*, 2004) was experimentally observed. A specific twin-beam entanglement is the so-called “high NOON” type (Bouwmeester, 2004) state

³⁹ For another realization of multi-dimensional photonic entanglement, i.e., the “pixel entanglement”, see (O’Sullivan-Hale *et al.*, 2005).

of two beams a and b (Dowling, 1998; Kok *et al.*, 2001, 2002):

$$|\text{NOON}\rangle = |N, 0; 0, N\rangle = \frac{1}{\sqrt{2}}(|N\rangle_a|0\rangle_b + |0\rangle_a|N\rangle_b). \quad (75)$$

It was experimentally realized for $N = 3$ (Mitchell, Lundeen, and Steinberg, 2004) and $N = 4$ (Walther *et al.*, 2004). The latter experiment demonstrated a fascinating feature of NOON states: the effective de Broglie wavelength of the multiphoton state is by $1/N$ shorter than the wavelength of a single photon (Jacobson *et al.*, 1995).

Bipartite multi-photon entanglement has many interesting applications including tests of foundations of quantum theory (Howell *et al.*, 2002), phase sensitive measurements (Holland and Burnett, 1993; Mitchell *et al.*, 2004) and quantum photolithography beyond the classical diffraction limit (Boto *et al.*, 2000; Kok *et al.*, 2001).

E. Multi-photon polarization entanglement

The original motivation to observe entanglement of more than two particles, with measurements on the particles performed at spatially separated stations, stems from the observation by GHZ that three-particle entanglement leads to a dramatic conflict between local realism and EPR's ideas with predictions of quantum mechanics (Greenberger *et al.*, 1989), see section IV.D.2. However, in 1989 no ready sources of three or more particle entanglement were available. Yurke and Stoler (1992a, 1992b) showed that in theory multiparticle entanglement effects should be in principle observable for particles originating from independent sources. A general method for making such an interference observable, and also to swap entanglement, was given by Żukowski *et al.* (1993), Żukowski *et al.* (1995), Rarity (1995) and Żukowski *et al.* (1999). This will be presented first, and later we shall show a series of experiments in which multi-photon entanglement was observed. Once one is able to entangle two photons that never interacted, one can construct very many types of entanglement (Zeilinger *et al.*, 1997), which can be utilized in very many ways (Bose *et al.*, 1998).

1. Entanglement construction

We basically have at hand only sources of two-particle entanglement. We shall show in detail how to swap entanglement of two pairs of particles (Żukowski, Zeilinger, and Weinfurter, 1995). The technique of, here, erasing which-source information, can be applied in many other configurations, e.g., in the case of a double pair emission from a single source, etc. It works even for totally independent emissions (provided they are synchronized).

Entangling two independent particles: the principle.—Figure 11 shows a configuration for obtaining interference effects for two pairs of particles originating from two independent sources. Assume that the sources in Fig. 11,

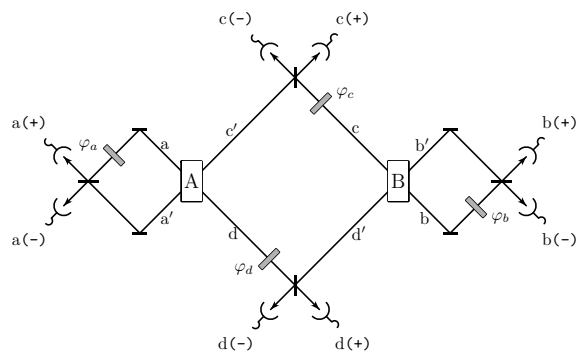


FIG. 11 Four-particle interference effects for two pairs of particles originating from two independent sources (Żukowski *et al.*, 1999).

A and B, each spontaneously emits a pair of particles in an entangled state (all particles are supposed to be identical) at nearly the same moment of time, and the states of the pairs are $|\Psi^A\rangle = \frac{1}{\sqrt{2}}(|a\rangle|d\rangle + |a'\rangle|c'\rangle)$ for source A, and $|\Psi^B\rangle = \frac{1}{\sqrt{2}}(|b'\rangle|d'\rangle + |b\rangle|c\rangle)$ for source B (the letters represent beams taken by the particles in Fig. 11, and $\langle e|f\rangle = \delta_{ef}$). The beams x and x' , where $x = a, b, c$ or d , are superposed at 50:50 beamsplitters. Behind the beamsplitters we place detectors in the output ports $x(\pm)$. In all unprimed beams one can introduce a phase shift of ϕ_x . The detector stations differ in their role: $a(\pm)$ and $b(\pm)$ observe radiation coming from one source only, and this is not so for stations $d(\pm)$ and $c(\pm)$. For instance, if a *single* particle is detected by $d(+)$, its origin may be uncertain. If it cannot be determined which source produced the particle which activated the detectors, say $d(+)$ and $c(+)$, then four-particle interference effects may occur.

Assume that detectors $a(+)$ and $b(+)$ also fired. Simultaneous firings of the four detectors can exhibit interference effects provided the two contributing processes—detection of the particles from source A in $d(+)$ and $a(+)$, and detection of the particles from source B in $c(+)$ and $b(+)$; detection of the particles from source A in $c(+)$ and $a(+)$, and detection of the particles from source B in $d(+)$ and $b(+)$ —are *indistinguishable* (all knowledge of the sources of the photons in $c(+)$ and $d(+)$ is erased). Note that depending on the phase shifts the detection at, e.g., $c(+)$ and $d(+)$, is a realization of a Bell-state measurement, which occurs if the two photons are in state $\frac{1}{\sqrt{2}}(|c'\rangle|d'\rangle + e^{i(\phi_c + \phi_d)}|c\rangle|d\rangle)$. Therefore the other two photons are due to this event in state: $\frac{1}{\sqrt{2}}(|b'\rangle|a'\rangle + e^{-i(\phi_c + \phi_d)}|b\rangle|a\rangle)$. This process is called *entanglement swapping*.

Enforcing source indistinguishability.—Imagine now that the sources of entangled states are two crystals pumped by independent pulsed lasers operating synchronously. Assume that the time separation between two pulses is much larger than all other time scales of the experiment, i.e., we study the radiation generated in

each crystal by a single pulse. We omit retardation effects by assuming equal optical paths. We assume that we pick the SPDC radiation with frequencies close to $\frac{1}{2}\omega_p^o$, where ω_p^o is the central frequency of the pulse. Suppose that the four SPDC photons are detected coincidentally (up to a few nanosecond window), one in each of the detectors $a(+)$, $b(+)$, $c(+)$, and $d(+)$. One could determine that photon detected at $d(+)$ came from crystal A (B) by noting the near simultaneity of the detection of photon $d(+)$ and one of the photons at $a(+)$ or $b(+)$ (the detection times of a true SPDC pair are tightly correlated). To ensure that the source of photons is unknowable the photons should be detected behind a filtering system (to be called later simply a filter) whose inverse of the bandwidth (coherence time) exceeds τ (pulse duration) by an order of magnitude. Then, the temporal separation of true SPDC pairs spreads to around 10τ and thereby prevents identifying the source of the photon at $d(+)$ by comparison of the arrival times. However, if the detections at, say, $b(+)$ and $c(+)$ are strictly time correlated one still concludes that the photons came from one crystal. One can again put a similar filter in front of the detectors $c(\pm)$ and as such, the which-way information is erased. Note that no filtering is required in front of the detectors $a(\pm)$ and $b(\pm)$.⁴⁰

One can estimate the maximal visibility expected for the interference process. The amplitude of the four-photon detections at, say, detectors $a(+)$, $b(+)$, $c(+)$ and $d(+)$ at times t_a , t_b , t_c , and t_d , is proportional to

$$e^{i(\phi_a+\phi_b+\phi_c+\phi_d)} A_{ad}(t_a, t_d) A_{cb}(t_c, t_b) + A_{b'd'}(t_b, t_d) A_{a'c'}(t_a, t_c), \quad (76)$$

where ϕ_i , $i = a, b, c, d$ is the local phase shift in the given beam. To get an overall probability of the process one has to integrate the square of the modulus of the amplitude over the detection times. Since typical time resolution of the detectors is of the order of nanoseconds, which is much longer than the coherence times of typical filters and the width of fs pump pulses, the integrations over time can be extended to infinity. The joint probability to have counts in the four detectors behaves as $1 - V_{(4)} \cos(\sum_{x=a,b,c,d} \phi_x)$ and the visibility $V_{(4)}$ is given by

$$V_{(4)} = \frac{\int d^4t |A_{ad}(t_a, t_d) A_{bc}(t_b, t_c) A_{b'd'}(t_b, t_d) A_{a'c'}(t_a, t_c)|}{\int d^4t |A_{ad}(t_a, t_d) A_{bc}(t_b, t_c)|^2}, \quad (77)$$

where $d^4t = dt_a dt_b dt_c dt_d$. Assume that the filter functions in all beams are of identical Gaussian form: $F_f(t) = e^{-\frac{1}{2}\omega_p^o t} |F_f(t)|$, whereas the pump beam is described by

$G(t) = e^{-i\omega_p^o t} |G(t)|$. Here ω_p^o is the central frequency of the pulse, and $|F|$ and $|G|$ functions are given by $\exp[-\frac{1}{2}(\omega - \Omega)^2/\sigma^2]$, where $\Omega = \frac{1}{2}\omega_p^o$ (for $|F|$) or ω_p^o (for $|G|$), and σ is the given spectral width. One gets:

$$V_{(4)} = \left[\frac{\sigma_p^2}{\sigma_p^2 + \sigma_F^2 \sigma_f^2 / (\sigma_p^2 + \sigma_F^2 + \sigma_f^2)} \right]^{1/2}, \quad (78)$$

where σ_p is the spectral width of the pulse, σ_f is the spectral width of the filters in beams a, a', d, d' , and the spectral width of the filters in c and d is σ_F . If one removes the filters in beams a, a', b and b' , the formula simplifies to $V_{(4)} = \left(\frac{\sigma_p^2}{\sigma_p^2 + \sigma_F^2} \right)^{1/2}$. Namely, narrow filters in paths a, a' and b, b' are not necessary to obtain high visibility (Żukowski *et al.*, 1999). The other filters, for detectors which observe radiation from both sources, should be always sufficiently narrow.

The influence of photon statistics.—The visibility of the four-particle fringes in the set-up of Fig. 11 can be impaired by the statistical properties of the emission process. The statistics of a single beam of a down converter is thermal-like. The state of idler-signal pairs emerging via a pair of (perfectly phase matched) pinholes is given by

$$|\psi\rangle = N^{-1} \sum_{m=0}^{\infty} z^m |m, s\rangle |m, i\rangle \quad (79)$$

where z is a number dependent on the strength of the pump, $|m, s\rangle$ ($|m, i\rangle$) denotes an m -photon state in the signal (idler) mode, and N is the normalization constant. It can be shown (Żukowski *et al.*, 1999) that visibility is reduced below 50% if $|z|^2 > (\sqrt{17} - 3)/8 \approx 0.140$. Thus, to have high visibility the ratio of the probability of *each pulse* to produce a single down converted pair to the probability of not producing anything must be less than 14%. This threshold is at quite high pump powers. Nevertheless, this puts a strong limitation as far as how many particles can be entangled using such methods. Simply, creation of entanglement for many particles requires more and more initial entangled pairs, thus one pumps stronger. However, strong pump leads to lower visibility of quantum interference, which may prohibit to observe the correlations due to the desired multi-photon entanglement.

Remarks.—Note that source indistinguishability in principle can also be achieved with an ultra-coincidence techniques, which does not require pulsed pump, but extremely good detection time resolution, ΔT , by order of magnitude sharper than the coherence time of the filtered SPDC radiation, and rejection of all events at $c(+)$ and $d(+)$ which are detected with time difference higher than, say, $2\Delta T$ [see Żukowski *et al.* (1993)]. In such a case the pumping lasers may be cw ones.⁴¹ However,

⁴⁰ This method also precludes the possibility of inferring the source of the photon from the frequency correlations. The frequency of the photons reaching $d(+)$ is better defined than the pumping pulse frequency, and it is the spread of the latter one that limits the frequency correlations of the idler-signal pair from one source.

⁴¹ A recent experiment reported by Halder *et al.* (2007), however,

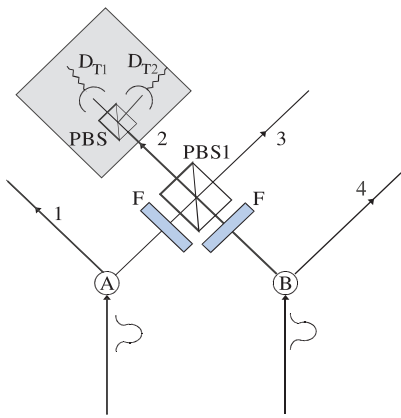


FIG. 12 A three- and four-photon polarization-entanglement source. The photon sources, A and B , pumped by short pulses. Here the PBS1 is a rotated PBS which transmits 45° polarization and reflects -45° polarization, F is a narrow filter, and D_{T1} and D_{T2} are two single-photon detectors.

such techniques are difficult to use in case of SPDC, due to lack of sufficiently time resolving detectors.

The methods described above call for femtosecond pulsed laser as a pump. Unfortunately, femtosecond pulse pumped SPDC shows relatively poor quantum interference visibilities (Keller and Rubin, 1997). The following methods were tested to lead to increase the quantum interference visibility in femtosecond pulse pumped type-II SPDC: (i) to use a thin nonlinear crystal (Sergienko *et al.*, 1999), (ii) to use narrow-band spectral filters in front of detectors, as shown above (Grice and Walmsley, 1997; Grice *et al.*, 1998; Di Giuseppe *et al.*, 1997), or (iii) to use an interferometric technique (Branning *et al.*, 1999, 2000) without spectral and amplitude post-selection (Kim *et al.*, 2001). The first two methods necessarily reduce the intensity of the entangled photon pairs significantly and cannot achieve perfect overlap of the two-photon amplitudes in principle. For the theoretical and experimental details of the last method, see (Kim *et al.*, 2001).

2. First proposal

In 1990's many proposals were made for observations of multi-photon entanglement (Żukowski *et al.*, 1993; Żukowski, Zeilinger and Weinfurter (1995); Zeilinger *et al.*, 1997; Pan and Zeilinger, 1998; see also section V.F.2),

achieved this using single-photon detectors of a time resolution ~ 70 ps, which is much shorter than the coherence length (~ 350 ps) of the photons in the experiment. In this way, photon timing can be obtained by the detection times, and pulsed sources can be replaced by cw sources, which do not require any synchronization (see section VII.E.4). Yet, the Halder *et al.* experiment has a much lower rate of fourfold coincidences.

or involving atoms (Cirac and Zoller, 1994; Haroche, 1995). Also three nuclear spins within a single molecule have been prepared such that they locally exhibit three-particle correlations (Lloyd, 1998; Laflamme *et al.*, 1998).

The idea of observing photonic GHZ entanglement, later put into practice, was given by Zeilinger *et al.* (1997) and by Pan and Zeilinger (1998), see Fig. 12. Assume that sources A and B simultaneously emit a photon pair each. Pairs in beams x, y (1, 3, and 2, 4) are in identical polarization states $\frac{1}{\sqrt{2}}(|H_x, H_y\rangle + |V_x, V_y\rangle)$. The state of the four particles, after passage of 2 and 3 via PBS1, if the sources of the photons are indistinguishable (which can be secured using the methods of section V.E.1), reads

$$\frac{1}{2}(|H_1, H_2, H_3, H_4\rangle + |V_1, V_2, V_3, V_4\rangle + |H_1, H_3, V_3, V_4\rangle + |V_1, V_2, H_2, H_4\rangle) \quad (80)$$

Only for the superposition $|H_1, H_2, H_3, H_4\rangle + |V_1, V_2, V_3, V_4\rangle$, which is a GHZ state, leads to four-fold coincidence. Therefore, four-fold coincidences can reveal four-particle GHZ correlations.

The scheme in Fig. 12 also allows one to generate *unconditional* three-particle GHZ states using a method based on the notion of entangled entanglement (Krenn and Zeilinger, 1996). For example, one could analyze the polarization state of photon 2 by passing it through a PBS selecting 45° and -45° polarizations. Then the polarization state of the remaining three photons 1, 3 and 4 will be projected into $\frac{1}{\sqrt{2}}(|H_1, H_3, H_4\rangle + |V_1, V_3, V_4\rangle)$, if, and only if, detector D_{T1} detects a *single* photon. A similar superposition, however with a minus sign, is obtained once detector D_{T2} detects a single photon. The detection of photon 2 excludes the last two terms in Eq. (80), and projects the remaining three photons into a spatially separated and freely propagating GHZ state. However, the scheme works only if both sources emit a pair each, and there are no two-pair (and more) emissions from one source.

3. Experimental realizations

Three-particle GHZ correlations were observed in an experiment by Bouwmeester *et al.* (1999a). One of the main complications of other experiments, namely, the creation of two pairs of photons by a single source, was turned into an advantage. Figure 13 is a schematic of the setup. Pairs of polarization-entangled photons are generated by a short pulse of ultraviolet (UV) light (≈ 200 fs, $\lambda = 788$ nm from a frequency-doubled, mode-locked Ti:Sapphire laser), which passes through a BBO crystal. The probability per pulse to create a single pair in the desired modes was of the order of a few 10^{-4} . Each photon pair is created in the state $\frac{1}{\sqrt{2}}(|H_a, V_b\rangle - |V_a, H_b\rangle)$ (the relative phase is irrelevant, as long as it is the same for both pairs).

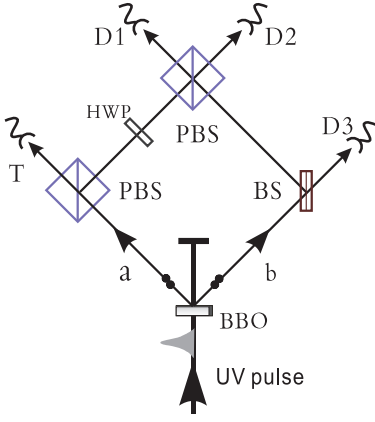


FIG. 13 Schematic drawing of the experimental setup for creating GHZ entanglement of three spatially separated photons (Bouwmeester *et al.*, 1999a). The UV pulse incident on the BBO crystal produces two pairs of entangled photons. Conditioned on the registration of one photon at the trigger detector T, the three photons registered at D_1 , D_2 , and D_3 exhibit the desired GHZ correlations.

Extending the above technique, entanglement among more particles was observed. For the four-photon entanglement, see (Pan *et al.*, 2001a; Zhao *et al.*, 2003a; Eibl *et al.*, 2003); the five-photon polarization entanglement was observed by Zhao *et al.* (2004). Very recently, six-photon entanglement in graph states (see section VIII.C) was also observed by Lu *et al.* (2007).

F. Photonic polarization entanglement analyzers

The preparation and measurement of Bell states are essential for many quantum information processing protocols, such as quantum dense coding (Bennett and Wiesner, 1992; Mattle *et al.*, 1996), quantum teleportation (Bennett *et al.*, 1993; Bouwmeester *et al.*, 1997; Boschi *et al.*, 1998), and entanglement swapping (Żukowski *et al.*, 1993; Pan *et al.*, 1998). After having discussed the photonic entanglement creation, below we present the existing photonic polarization entanglement analyzers (i.e., Bell-state and GHZ-state analyzers).

1. Bell-state analyzer

According to the Bell-state measurement circuit in Fig. 4(a), a full Bell-state measurement necessitates nonlinear optical interactions at a single-photon level so as to realize the CNOT gate. Actually, it is proved that the full Bell-state measurement is impossible with only linear optics (Vaidman and Yoran, 1999; Lütkenhaus *et al.*, 1999). The existing Bell-state analyzer for photonic polarization entanglement (Weinfurter, 1994; Braustein and Mann, 1995; Michler *et al.*, 1996) involves practically realizable procedures, by which one can readily identify

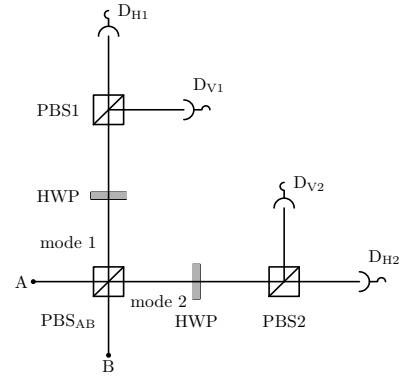


FIG. 14 A modified Bell-state analyzer (Pan and Zeilinger, 1998). Two indistinguishable photons enter the Bell-state analyzer from input ports A and B. D_{H1} , D_{V1} , D_{H2} , and D_{V2} are four photon-counting detectors. The angle between the half-wave plate axis and the horizontal direction is 22.5° such that it corresponds to a 45° rotation of the polarization.

two of the maximally entangled states of any number of photons (Pan and Zeilinger, 1998).

The Bell-state analyzer first suggested by Weinfurter *et al.* is based on the two-photon interference effect at a 50:50 BS and can distinguish two of the four Bell states via two-fold coincidence analysis. Here we introduce a modified version of the Bell-state analyzer, which can directly be generalized to the N -particle case (Pan and Zeilinger, 1998); the basic elements of the experimental setup are just PBS and half-wave plates.

Consider the arrangement of Fig. 14. Two identical photons enter our Bell-state analyzer from modes A and B, respectively. Of course, these two photons A and B arrive at PBS_{AB} simultaneously so that their spatial wavefunctions overlap each other. Noting the property of PBS in Fig. 2 and using the coincidence between detectors in mode 1 and in mode 2, one is ready to see that two Bell states $|\phi^+\rangle_{12}$ and $|\phi^-\rangle_{12}$ can be identified. Specifically, if we observe a coincidence either between detectors D_{H1} and D_{H2} or D_{V1} and D_{V2} , then the incident state was $\frac{1}{\sqrt{2}}(|H_A\rangle|H_B\rangle + |V_A\rangle|V_B\rangle)$. On the other hand, if we observe coincidence between detectors D_{H1} and D_{V2} or D_{V1} and D_{H2} , then the incident state was $\frac{1}{\sqrt{2}}(|H_A\rangle|H_B\rangle - |V_A\rangle|V_B\rangle)$. The other two incident Bell states will lead to no coincidence between detectors in mode 1 and in mode 2. Such states are signified by some kind of superposition of $|H_A\rangle|V_B\rangle$ and $|V_A\rangle|H_B\rangle$. This concludes the demonstration that we can identify two of the four Bell states using the coincidence between modes 1 and 2. Actually, one can identify *any* two of the four Bell states using similar technique (Pan and Zeilinger, 1998).

A recent teleportation experiment (van Houwelingen *et al.*, 2006) exploited a novel Bell-state analyzer for time-bin qubits allowing the detection of three out of four Bell states with linear optics, two detectors, and no auxiliary

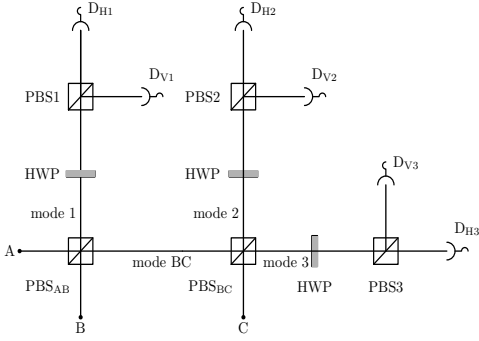


FIG. 15 A GHZ-state analyzer (Pan and Zeilinger, 1998). Three photons incident one each in modes A, B, and C will give rise to distinct 3-fold coincidence if they are in the GHZ-states $|\Phi_0^+\rangle$ or $|\Phi_0^-\rangle$.

photons. Yet, the theoretical success rate of this scheme is still 50%. There are several theoretical proposals (e.g., see Scully *et al.*, 1999; DelRe *et al.*, 2000; Vitali *et al.*, 2000; Lloyd *et al.*, 2001) for complete Bell-state measurement relevant to photonic manipulation. Complete Bell-state measurement was realized for ions (Riebe *et al.*, 2004; Barrett *et al.*, 2004), and for photons (Kim, Kulik, and Shih, 2001) using nonlinearity and can also be performed probabilistically with linear optics, as realized by Zhao *et al.* (2005b), and by Walther and Zeilinger (2005). Another novel route is the hyper-entanglement assisted Bell-state analysis (Kwiat and Weinfurter, 1998; Walborn *et al.*, 2003b), which has been experimentally realized (Schuck *et al.*, 2006).

2. GHZ-state analyzer

The above scheme can directly be generalized to the N -particle case. Making use of its basic idea, one can easily construct a type of GHZ-state analyzer (Pan and Zeilinger, 1998) by which one can immediately identify two of the 2^N maximally entangled GHZ states.

For example, in the case of three identical photons, the eight maximally entangled GHZ states are given by

$$|\Phi_0^\pm\rangle = \frac{1}{\sqrt{2}}(|H\rangle|H\rangle|H\rangle \pm |V\rangle|V\rangle|V\rangle), \quad (81)$$

$$|\Psi_1^\pm\rangle = \frac{1}{\sqrt{2}}(|V\rangle|H\rangle|H\rangle \pm |H\rangle|V\rangle|V\rangle), \quad (82)$$

$$|\Psi_2^\pm\rangle = \frac{1}{\sqrt{2}}(|H\rangle|V\rangle|H\rangle \pm |V\rangle|H\rangle|V\rangle), \quad (83)$$

$$|\Psi_3^\pm\rangle = \frac{1}{\sqrt{2}}(|H\rangle|H\rangle|V\rangle \pm |V\rangle|V\rangle|H\rangle), \quad (84)$$

where $|\Psi_i^\pm\rangle$ designates the GHZ states where the polarization of photon i is different from the other two. Consider now the setup of Fig. 15 and suppose that three photons enter the GHZ analyzer, each one from modes A, B and C, respectively. A suitable arrangement can be

realized such that the photon coming from mode A and the one coming from mode B overlap at PBS_{AB} and, thus they are correspondingly transformed into mode 1 and into mode BC. Let us further suppose that the photons from mode BC and mode C overlap each other at PBS_{BC} . Thus, following the above demonstration for the case of the Bell-state analyzer, it is easy to find that one can observe three-fold coincidence between modes 1, 2 and 3 only for the state of Eq. (81). For the other states, there are always two particles in the same mode. We can thus distinguish the two states $\frac{1}{\sqrt{2}}(|H\rangle|H\rangle|H\rangle \pm |V\rangle|V\rangle|V\rangle)$ from the other six GHZ states.

Furthermore, after the states of Eq. (81) pass through the HWP, using three-fold coincidence we can readily identify the relative phase between states $|H\rangle|H\rangle|H\rangle$ and $|V\rangle|V\rangle|V\rangle$. This is because only the initial state $|\Phi_0^+\rangle$ leads to coincidence between detectors D_{H1} , D_{H2} and D_{H3} (or $H_1V_2V_3$, $V_1H_2V_3$, $V_1V_2H_3$). On the other hand, only the state $|\Phi_0^-\rangle$ leads to coincidence between detectors D_{H1} , D_{H2} and D_{V3} (or $H_1V_2H_3$, $V_1H_2H_3$, $V_1V_2V_3$). Consequently, states $|\Phi_0^\pm\rangle$ are thus identified by coincidences between all three output modes 1, 2, and 3. They can be distinguished because behind the half-wave plates $|\Phi_0^+\rangle$ results in one or three horizontally, and zero or two vertically polarized photons, while $|\Phi_0^-\rangle$ results in zero or two horizontally polarized photons and one or three vertically polarized ones.

The GHZ-state analyzer has many possible applications. For example, the three photons entering via the modes A, B and C, respectively, could each come from one entangled pair. Then projection of these three photons using the GHZ-state analyzer onto the GHZ state $|\Phi_0^+\rangle$ or $|\Phi_0^-\rangle$ implies that the other three photons emerging from each pair will be prepared in a GHZ state. It is clear that the scheme can readily be generalized to analyze entangled states consisting of more than three photons by just adding more PBSs and half-wave plates.

Finally we would like to note that in all these schemes the principle of quantum erasure (Scully *et al.*, 1991) has been used in a way that, behind the Bell- and GHZ-state analyzer, at least some of the photons registered cannot be identified anymore as to which source they came from. This implies very specific experimental schemes, because the particles might have been created at different times. Practical quantum erasure has been successfully used in the experiments on quantum teleportation (section VII.B), entanglement swapping (section VII.C) and multi-photon entanglement (see especially section V.E.1).

VI. FALSIFICATION OF REALISTIC WORLD VIEW

The initial atomic-cascade experiments testing Bell's inequalities (Freedman and Clauser, 1972; Aspect *et al.*, 1982a, 1982b) falsified Bell's inequalities as constraints on correlations of microsystems—thus a local realistic world-view was challenged. However, this falsification

was up to certain loopholes—which are due to experimental imperfections, and still allow to build local realistic models for the data obtained in the experiments (alas, not for ideal quantum predictions). There are two principal loopholes. Locality loophole is present in experiments which do not have random and fast switching of the local measurement settings. In such a case one of the assumptions behind Bell inequalities—independence of Alice’s results on Bob’s settings, and *vice versa*—is not enforced. Efficiency loophole emerges due to low collection and detection efficiency of the particles in Bell test since in such a case for qubits one has three possible local outcomes, ± 1 or no count; for efficiency lower than about 83% [see, e.g., (Garg and Mermin, 1987; Eberhard, 1993)] one can show that one cannot derive (generalized) CHSH-type inequality that is violated by quantum predictions.

The Aspect *et al.* experiments addressed the locality loophole, by including fast switching of local polarization analyzers (via acousto-optical modulators). Weihs *et al.* (1998) and Peng *et al.* (2005) addressed the locality loophole with more refined techniques which also included random switching. Meanwhile, there were many ideas to close the detection loophole, see, e.g., (Eberhard, 1993; Kwiat *et al.*, 1994; Simon and Irvine, 2003). The detection loophole was closed in an ion-trap experiment by Rowe *et al.* (2001). However, this experiment had big problems with the locality loophole.

An important line of research was opened once the drastic non-classicality of the GHZ multiparticle correlations was discovered. Thus, there is a series of experiments which test local realism with such correlations—here one more problem was to be solved—one does not have physical processes that lead directly to GHZ correlations. Thus new quantum engineering methods had to be invented and applied. We shall concentrate here on such multi-photon experiments; however, we shall also present some two-photon experiments from the last ten years.

A. Testing Bell’s inequalities with photons

To close the locality loophole, one must freely and rapidly choose the directions of local analyzers, and to register the particle, in such way that it is impossible for any information about the setting and the detection to travel via any (possibly unknown) causal channel to the other observer before he, in turn, chooses the setting and finishes measurement (Fig. 16). Selection of analyzer directions has to be completely unpredictable. This necessitates a physical random number generator. A numerical pseudo-random number generator would not do: its state at any time is predetermined. Furthermore, to achieve a complete independence of both observers, one should avoid any common context, as would be conventional use of coincidence circuits. Individual events should be registered on both sides completely indepen-

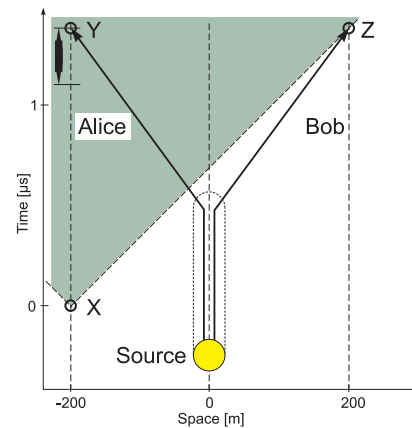


FIG. 16 Spacetime diagram of the Bell experiment by Weihs *et al.* (1998). Selecting a random analyzer direction, setting the analyzer, and finally detecting a photon constitute the measurement process. This process on Alice’s side must fully lie inside the shaded region which is invisible to Bob’s during his own measurement. For the present setup this means that the decision about the setting has to be made after point “X” if the corresponding photons are detected at spacetime points “Y” and “Z”, respectively. In the experiment the measurement process (indicated by a short black bar) including the choice of a random number took less than only one-tenth of the maximum allowed time. The vertical parts of the kinked photon world lines emerging from the source represent the fiber coils at the source location, which are obviously irrelevant to the locality argument.

dently, and compared only long after the measurements are finished. This requires independent and highly accurate time bases on both sides.

The above requirements were experimentally realized by Weihs *et al.* (1998) and Peng *et al.* (2005). In the former, the observers “Alice” and “Bob” (Fig. 17) were spatially separated by 400 m across the Innsbruck university science campus. The individual measurements were finished within a time shorter than $1.3 \mu\text{s}$, which is the the distance of the two observation stations in light seconds. The polarization entangled photon pairs were distributed to the observers through optical fibers. A typical observed value of of the left hand side of the CHSH inequality was 2.73 ± 0.02 . In 10 s 14 700 coincidence events were collected. This corresponds to a violation of the local realistic threshold of 2 by 30 standard deviations. In the Hefei experiment, the polarization entangled photon pairs were distributed in free space to Alice and Bob stations, which were spatially separated by 10.5 km. The measured result of S_{Bell} is 2.45 ± 0.09 . The violation of the Bell-CHSH inequality was by 5 standard deviations.

B. GHZ paradox in the laboratory

In a series of experiments the GHZ correlations have been realized with visibility high enough to allow one to

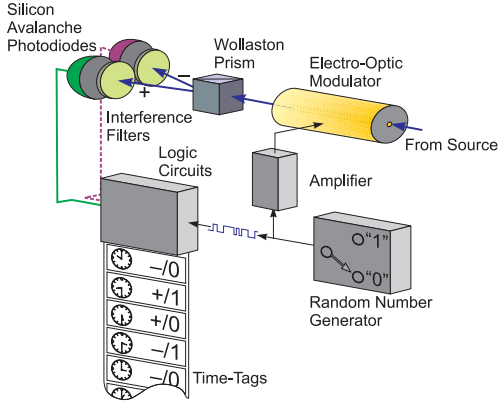


FIG. 17 One of the two observer stations. A random number generator is driving the electro-optic modulator. Silicon avalanche photodiodes are used as detectors. A “time tag” is stored for each detected photon together with the corresponding random number “0” or “1” and the code for the detector “+” or “-” corresponding to the two outputs of the polarizer. See Weihs *et al.* (1998).

refute the notion of EPR’s elements of reality (modulo the usual loopholes).

1. Three-photon test

The standard reasoning of the GHZ theorem using the three-photon GHZ entangled state was given earlier. The laboratory realization of the GHZ paradox was done by Pan *et al.* (2000). The aim of the experiment was to get the following state

$$|\Delta\rangle = \frac{1}{\sqrt{2}}(|H\rangle_1 |H\rangle_2 |H\rangle_3 + |V\rangle_1 |V\rangle_2 |V\rangle_3), \quad (85)$$

and to demonstrate that the (necessarily imperfect) GHZ correlations violate local realism. Thus, one has to achieve multiphoton interference with high enough visibility.

The GHZ state (85) satisfies the eigenequations as

$$\begin{aligned} \hat{x}_1 \hat{y}_2 \hat{y}_3 |\Delta\rangle &= -|\Delta\rangle, & \hat{y}_1 \hat{x}_2 \hat{y}_3 |\Delta\rangle &= -|\Delta\rangle, \\ \hat{y}_1 \hat{y}_2 \hat{x}_3 |\Delta\rangle &= -|\Delta\rangle, & \hat{x}_1 \hat{x}_2 \hat{x}_3 |\Delta\rangle &= |\Delta\rangle, \end{aligned} \quad (86)$$

where \hat{x} denotes the observable discriminating between $|45^\circ\rangle$ and $|135^\circ\rangle$ polarizations, whereas \hat{y} discriminates between heft and right circular polarizations. In both cases the ascribed eigenvalues are, respectively, 1 and -1 .

Thus, the demonstration of the conflict between local realism and quantum mechanics for GHZ entanglement consists of four experiments. The experimental values for $\hat{x}_1 \hat{y}_2 \hat{y}_3$, $\hat{y}_1 \hat{x}_2 \hat{y}_3$, and $\hat{y}_1 \hat{y}_2 \hat{x}_3$ in the experiment followed the values predicted by quantum physics in a fraction of 0.85 ± 0.04 of all cases. Then the $\hat{x}_1 \hat{x}_2 \hat{x}_3$ experiment was performed with results shown in Fig. 18. The experimental results confirmed the quantum predictions, within

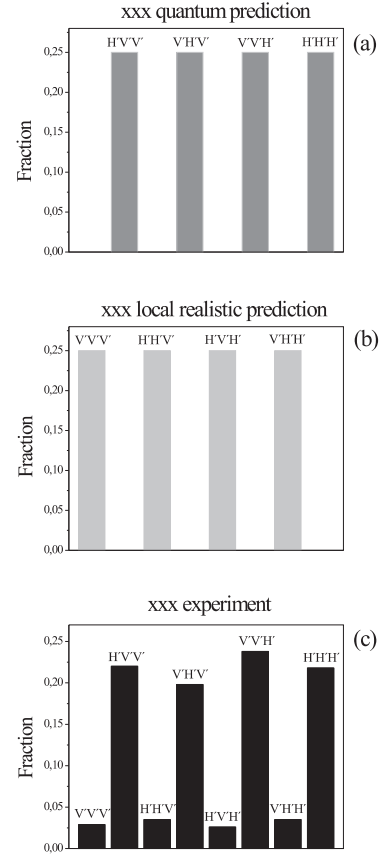


FIG. 18 Predictions of quantum mechanics (a) and of local realism (b), and observed results (c) for the $\hat{x}_1 \hat{x}_2 \hat{x}_3$ experiment of Pan *et al.* (2000).

an experimental uncertainty. Since the average visibility of $(71 \pm 4)\%$ in these experiments clearly surpasses the minimum of 50%, necessary for a violation of local realism in three-particle GHZ experiments (Mermin, 1990b; Roy and Singh, 1991; Żukowski and Kaszlikowski, 1997; Ryff, 1997), the observed correlations were in clear conflict with local realism (but still leaving the locality and detection-efficiency loopholes open), and allow a GHZ-type analysis—which directly refutes the EPR concept of elements of reality.

2. Four-photon test

The realization of a high intensity source of four-photon GHZ entanglement (Pan *et al.*, 2001a, see also a related experiment by Eibl *et al.*, 2003), allowed Zhao *et al.* (2003a) to report the first four-photon GHZ-type laboratory falsification of local realism. The experiment provided a sufficient experimental evidence for the existence of genuine four-photon entanglement. The observed correlations can be linked with the following state

$$\frac{1}{\sqrt{2}}(|H\rangle_1 |V\rangle_2 |V\rangle_3 |H\rangle_4 + |V\rangle_1 |H\rangle_2 |H\rangle_3 |V\rangle_4). \quad (87)$$

For this GHZ experiment, the optimal two-setting-per-observer Bell inequality is the one by Ardehali (1992). Namely, for the Bell operator

$$\hat{A} = \frac{1}{2}(\hat{x}_1\hat{x}_2\hat{x}_3 - \hat{x}_1\hat{y}_2\hat{y}_3 + \hat{y}_1\hat{x}_2\hat{y}_3 + \hat{y}_1\hat{y}_2\hat{x}_3)(\hat{\sigma}_a + \hat{\sigma}_b) + \frac{1}{2}(\hat{y}_1\hat{y}_2\hat{y}_3 + \hat{x}_1\hat{y}_2\hat{x}_3 + \hat{x}_1\hat{x}_2\hat{y}_3 - \hat{y}_1\hat{x}_2\hat{x}_3)(\hat{\sigma}_a - \hat{\sigma}_b), \quad (88)$$

where $\hat{\sigma}_a = \frac{1}{\sqrt{2}}(\hat{x} + \hat{y})$ and $\hat{\sigma}_b = \frac{1}{\sqrt{2}}(\hat{x} - \hat{y})$ correspond to measurements of two (orthogonal) pairs of elliptic polarizations, one can find the following local realistic bound

$$\left| \langle \hat{A} \rangle_{\text{local realism}} \right| \leq 2. \quad (89)$$

This was found to be violated, as $\left| \langle \hat{A} \rangle_{\text{measured data}} \right| = 4.433 \pm 0.032$. This is a violation of the inequality (89) by over 76 standard deviations. Note that the experiment involved the measurement settings different from the three-particle one.

Quantum mechanics predicts the maximal violation of the inequality (89) by a factor of $2\sqrt{2}$. Hence, the threshold visibility to violate (89) is given by the inverse of this factor: $1/2\sqrt{2} \simeq 35.4\%$. The average visibility observed in the experiment, 78.4%, greatly exceeds the threshold. Further, it was shown (Uffink, 2002; Seevinck and Svetlichny, 2002; Yu *et al.*, 2003) that if $\left| \langle \hat{A} \rangle \right| > 4$, which was the case, one has an unambiguous evidence for genuine four-particle entanglement (such value is inexplicable by any hybrid model using 3 or less photon entanglement).

C. Two-observer GHZ-like correlations

One may ask: Can the conflict between quantum mechanics and local realism arise for two-particle systems, for the definite predictions, and for the whole ensemble? Namely, can the GHZ reasoning be reduced to a two-party (thus two space-like separated regions) case while its all-versus-nothing feature is still retained? If so, one can then refute local realism in the simplest and the most essential irreducible way. Further, since the EPR reasoning involved only two particles, such a refutation would be an even more direct counterargument against the EPR ideas than the three-particle one.

In a recent debate (Cabello, 2001a, 2001b, 2003; Lvovsky, 2002; Marinatto, 2003; Chen *et al.*, 2003) it has been shown that an all-versus-nothing violation of local realism does exist for two-particle four-dimensional entangled systems (Chen *et al.*, 2003). In this new refutation of local realism, one recovers EPR's original situation of two-party perfect correlations, but with much less complexity. However, this becomes possible with a new approach for defining elements of reality, which nevertheless strictly follows the EPR criteria (Chen *et al.*, 2003).

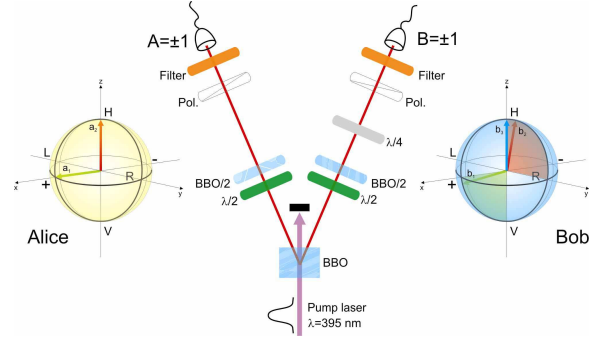


FIG. 19 Experimental setup for testing the Leggett-type inequality (47). As usual, the required polarization-entangled singlet state $|\Psi^-\rangle_{AB} = \frac{1}{\sqrt{2}}[|H\rangle_A|V\rangle_B - |V\rangle_A|H\rangle_B]$ was generated by pumping 2-mm-thick type-II BBO crystal with a pulsed frequency-doubled Ti:sapphire laser (180 fs) at $\lambda = 395$ nm wavelength and ~ 150 mW optical c.w. power. The arrows in the Poincaré spheres indicate the measurement settings of Alice's and Bob's polarizers for the maximal violation of inequality (47). Note that setting \mathbf{b}_2 lies in the y - z plane and therefore a quarter-wave plate has to be introduced on Bob's side. The coloured planes indicate the measurement directions for various difference angles φ for the Leggett-type and CHSH inequalities. (Gröblacher *et al.*, 2007)

A crucial point of the two-observer GHZ-like theorem is the use of a two-photon hyper-entanglement (Chen *et al.*, 2003). Due to the specific properties of the hyper-entanglement, nine variables for each party can be regarded as simultaneous EPR elements of reality. The nine variables can be arranged in three groups of three, and the three variables of each group can be measured by one and the same apparatus. This eliminates the necessity of an argument based on non-contextuality as it is not necessary to assume any of these variables to be independent of experimental context.

After successfully creating a two-photon hyper-entangled state in Eq. (71), see section V.B, Yang *et al.* (2005; see also a slightly oversimplified version by Cinelli *et al.*, 2005) experimentally demonstrated the two-photon hyper-entanglement GHZ-type paradox. The actual experimental configuration was suggested by Chen *et al.* (2003), and it involves only linear optics.

D. Experimental test of a nonlocal realism

The Leggett-type inequality (see section IV.E) refuting certain nonlocal realistic theories was tested very recently by Gröblacher *et al.* (2007) using the experimental setup shown in Fig. 19. In the experiment Gröblacher *et al.* observed maximal coincidence count rates (per 10 s), in the H/V basis, of around 3,500 with single count rates of 95,000 (Alice) and 105,000 (Bob), 3,300 coincidences in the $\pm 45^\circ$ basis (75,000 singles at Alice and 90,000 at Bob), and 2,400 coincidences in the R/L basis (70,000 singles at Alice and 70,000 at Bob). The reduced count

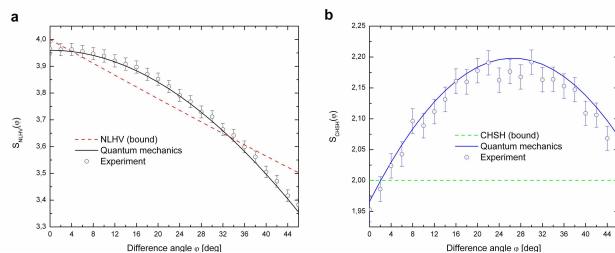


FIG. 20 Experimental violation of the inequalities for nonlocal hidden-variable theories and for local realistic theories. (a) Dashed line indicates the bound of inequality (47) for the investigated class of nonlocal hidden-variable theories. The solid line is the quantum theoretical prediction reduced by the experimental visibility. The shown experimental data were taken for various difference angles φ (on the Poincaré sphere) of local measurement settings. The bound is clearly violated for $4^\circ < \varphi < 36^\circ$. Maximum violation is observed for $\varphi_{max} \approx 20^\circ$. (b), At the same time, no local realistic theory can model the correlations for the investigated settings as the same set of data also violates the CHSH inequality. The bound (dashed line) is overcome for all values φ around φ_{max} , and hence excludes any local realistic explanation of the observed correlations in (a). The solid line is the quantum prediction for the observed experimental visibility. Error bars indicate standard deviations. (Gröblacher *et al.*, 2007)

rates in the R/L basis are due to additional retarding elements in the beam path. The two-photon visibilities are approximately $99.0 \pm 1.2\%$ in the H/V basis, $99.2 \pm 1.6\%$ in the $\pm 45^\circ$ basis and $98.9 \pm 1.7\%$ in the R/L basis, which is the highest reported visibility for a pulsed SPDC entanglement source. Such a high two-photon visibility is well beyond the threshold of 97.4% which is required for testing the Leggett-type inequality. So far, no experimental evidence against the rotational invariance of the singlet state exists, and as such the rotation averaged correlation functions in inequality (47) was replaced with their values measured for one pair of settings (in the given plane).

Figure 20 summarizes the experimental violation of the inequalities for nonlocal hidden-variable theories (the Leggett-type inequality) and for local realistic theories (the CHSH inequality). The observed $S_{NLHV} = 3.8521 \pm 0.0227$, which violates inequality (47) by 3.2 standard deviations. At the same time, $S_{CHSH} = 2.178 \pm 0.0199$, which violates the CHSH inequality by ~ 9 standard deviations. The Gröblacher *et al.* experiment thus excluded a class of important nonlocal hidden-variable theories.

E. Quantum vs. noncontextual hidden variables

As it was explained earlier the Bell-Kochen-Specker theorem (Bell, 1966; Kochen and Specker, 1967) states that noncontextual hidden-variable theories are incompatible with quantum mechanics. So far, two groups reported experimental results (Michler *et al.*, 2000a; Huang

et al., 2003) pointing toward falsification of noncontextual hidden-variable theories. In particular, following an experimentally feasible scheme suggested by Simon *et al.* (2000) the experiment by Huang *et al.* was performed with a single individual system (i.e., a single photon carrying path and polarization information). Also the actual realization of the experiment by Cinelli *et al.* (2005), mentioned above, puts it into the class of tests of non-contextual hidden variables.

VII. QUANTUM COMMUNICATION

Quantum communication ultimately aims at absolutely secure transfer of classical or quantum information. As the fastest information carrier in nature, photons, with very weak coupling to the environment, are the obvious choice for quantum communication tasks, especially the long-distance ones. Hence, the ability of manipulating the quantum features (such as coherence and entanglement) of photons is a precious resource.

We will review several breakthroughs in the field of quantum communication⁴². By exploiting entanglement one can efficiently encoding classical messages (Bennett and Wiesner, 1992; section VII.A), transfer quantum information to a remote location (Bennett *et al.*, 1993; section VII.B), entangle two remote particles that have no common past (Żukowski *et al.*, 1993; section VII.C), and purify less entangled states of a larger ensemble into more entangled states of a smaller ensemble (Bennett *et al.*, 1996b; Deutsch *et al.*, 1996; Pan *et al.*, 2001b; section VII.D).

Needless to say, one of the ultimate dreams is long-distance or even global (10^3 - 10^4 km) quantum communication. As a combination of the ideas of entanglement purification and swapping, the quantum repeater protocol (Briegel *et al.*, 1998), see section VII.E, provides a way of beating decoherence and photon losses when attempting to create remote high-quality entanglement. Thus, it enables long-distance quantum communication. In section VII.F we discuss the road towards satellite-based quantum communication and its first step, i.e., free-space distribution of entangled photon pairs to the mutual distance of 10 km, which are well beyond the effective thickness of the atmosphere.

A. Quantum dense coding

One can encode two bits on two qubits in such a way that each qubit carries a single bit. For qubits represented by polarization states of two photons one may have: HH , HV , VH , and VV . The idea of quantum dense coding,

⁴² Except quantum cryptography, which has been extensively reviewed by Gisin *et al.* (2002)

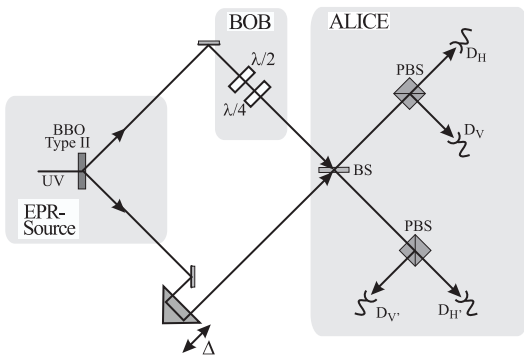


FIG. 21 Experimental set-up for quantum dense coding (Mattle *et al.*, 1996).

introduced by Bennett and Wiesner (1992) is that, by manipulating only *one* of the two particles in a Bell state, one can encode two bits of information.

The procedure runs as follows:

Step 1. Sharing maximal entanglement. A maximally entangled qubit pair (say, in the state $|\psi^+\rangle_{AB}$) is first shared by Alice and Bob (Fig. 21). They agree in advance that $|\psi^-\rangle_{AB}$, $|\phi^-\rangle_{AB}$, $|\phi^+\rangle_{AB}$, and $|\psi^+\rangle_{AB}$ (say) respectively represent the binary numbers 00, 01, 10, and 11.

Step 2. Coding of message. According to the value Bob wants to transmit to Alice, Bob performs one out of four possible unitary transformations (identity operation \hat{I} , \hat{x} , \hat{y} , and \hat{z}) on his qubit B alone.⁴³ The four operations transform, in an one-to-one way, the original state $|\psi^+\rangle_{AB}$, respectively, into $|\psi^+\rangle_{AB}$, $|\phi^+\rangle_{AB}$, $|\phi^-\rangle_{AB}$, and $|\psi^-\rangle_{AB}$. One has four distinguishable messages. Once this is done, he sends his qubit to Alice.

Step 3. Decoding of message. Upon reception, Bob performs the Bell-state measurement, hence reads out the encoded information.

The overall effect of the quantum dense coding thus doubles the information capacity of the transmission channel, while actually one sends only one physical qubit. This more efficient way of coding information is to be contrasted with the Holevo (1973) result that maximum one bit can be encoded on a single qubit *in isolation*. Entanglement allows to encode information entirely in the relative properties of the pair of qubits, i.e. their correlations.

The first experimental realization of quantum dense coding was reported by the Innsbruck group (Mattle *et al.*, 1996). The preparation of the polarization entangled photon pairs, the single-qubit operations at Bob's station, and Alice's Bell-state analyzer can all be done

⁴³ The operations are represented here by Pauli matrices. They are not only hermitian, but also unitary. We use here a shorthand notation, $\sigma_x = \hat{x}$ *etc.* It is assumed that the “computational” basis is the basis of \hat{z} .

with techniques presented in the previous sections. In the Innsbruck experiment, two $(|\psi^\pm\rangle_{AB})$ out of the four Bell states could be distinguished and as such, transmission of three different messages per two-state photon was realized,⁴⁴ enabling an increase of the channel capacity to $\log_2 3 \simeq 1.58$ bits.

In a more recent experiment, Schuck *et al.* (2006) realized a complete deterministic linear-optical Bell-state analyzer with the help of hyper-entanglement (polarization entanglement plus the intrinsic time-energy entanglement in SPDC). With this new possibility, the dense coding protocol was then implemented and achieved a channel capacity of 1.18 ± 0.03 bits per photon, which still can be increased by appropriate coding.

B. Quantum teleportation

The fascinating possibility of quantum teleportation was discovered by Bennett, Brassard, Crépeau, Jozsa, Peres, and Wootters (1993). Quantum teleportation is indeed not only a critical ingredient for quantum computation (Gottesman and Chuang, 1999; Knill, Laflamme, and Milburn, 2001) and communication, its experimental realization allows new studies of the fundamentals of quantum theory. In this section we survey the experimental realizations⁴⁵ (Bouwmeester *et al.*, 1997; Boschi *et al.*, 1998; Pan *et al.*, 1998, 2003a; Zhao *et al.*, 2004; Zhang *et al.*, 2006c) of quantum teleportation with photonic qubits and the related experimental “tricks”.

1. The protocol

The idea of quantum teleportation is illustrated in the Fig. 22(a). Suppose a photon (or any other particle) 1, the state of which Alice wants to teleport to Bob, is in a general polarization state $|\chi\rangle_1 = \alpha|H\rangle_1 + \beta|V\rangle_1$ (unknown to Alice). The trivial idea that Alice performs certain measurement on $|\chi\rangle_1$ by which she would obtain all the information necessary for Bob to reconstruct the state is ruled out: an experiment on qubit can give one only one bit of information. Enough to determine which state can be ruled out, but insufficient to reconstruct the actual state - to this end we need infinitely many measurements on identical copies of the state. The projection postulate makes it impossible to fully determine the state of a single quantum system. The no-cloning principle ex-

⁴⁴ The states $|\psi^\pm\rangle_{AB}$ carried two different values, while $|\phi^\pm\rangle_{AB}$ the third.

⁴⁵ Experimental advances with physical systems other than photonic qubits include quantum teleportation of continuous-variable states (Furusawa *et al.*, 1998), the complete quantum teleportation using nuclear magnetic resonance (Nielsen, Knill, and Laflamme, 1998), and deterministic quantum teleportation with atoms (Riebe *et al.*, 2004; Barret *et al.*, 2004).

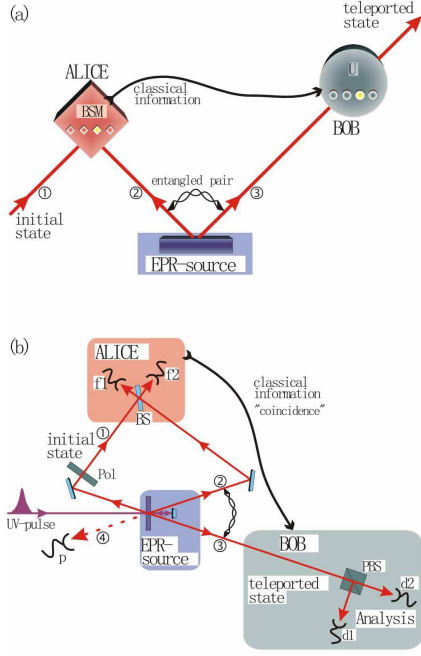


FIG. 22 (a) Principle of quantum teleportation. Alice has particle 1, in an initial state which she wants to teleport to Bob. Alice and Bob also share an ancillary entangled pair of particles 2 and 3 emitted by an EPR source. Alice then performs a Bell-state measurement on the initial particle and one of the ancillaries, projecting them also onto an entangled state. After she has sent the result of her measurement as classical information to Bob, he can perform a unitary transformation (U) on the other ancillary particle resulting in it being in the state of the original particle. (b) Setup of the Innsbruck teleportation experiment (Bouwmeester *et al.*, 1997). A pulse of ultraviolet light passing through a non-linear crystal creates the ancillary pair of entangled photons 2 and 3. After retroreflection during its second passage through the crystal the ultraviolet pulse creates another pair of photons, one of which will be prepared in the initial state of photon 1 to be teleported, the other one serves as a trigger indicating that a photon to be teleported is under way. Alice then looks for coincidences after a BS where the initial photon and one of the ancillaries are superposed. Bob, after receiving the classical information that Alice obtained a coincidence count in detectors f1 and f2 identifying $|\psi^-\rangle_{12}$, knows that his photon 3 is in the initial state of photon 1 which he then can check using polarization analysis with the PBS and the detectors d1 and d2. The detector P provides the information that photon 1 is under way.

cludes the possibility to have more high-fidelity copies than the original one.

Still, according to Bennett *et al.* there is a way out. Suppose that an ancillary pair of photons 2 and 3 is shared by Alice and Bob, and it is in the polarization entangled state $|\psi^-\rangle_{23}$. The entire system, comprising Alice's unknown particle 1 and the entangled pair, is in a product state, $|\chi\rangle_1|\psi^-\rangle_{23}$. By expanding the state of

Alice's particles 1 and 2 in the Bell basis one has

$$|\chi\rangle_1|\psi^-\rangle_{23} = \frac{1}{2} [|\psi^-\rangle_{12} (-\alpha|H\rangle_3 - \beta|V\rangle_3) + |\psi^+\rangle_{12} (-\alpha|H\rangle_3 + \beta|V\rangle_3) + |\phi^-\rangle_{12} (\alpha|V\rangle_3 + \beta|H\rangle_3) + |\phi^+\rangle_{12} (\alpha|V\rangle_3 - \beta|H\rangle_3)]. \quad (90)$$

Now, if Alice performs a Bell-state measurement on her two particles, with respect to the above basis, then the four possible outcomes are equally likely regardless of the unknown state $|\chi\rangle_1$. However, once particles 1 and 2 are projected into one of the four entangled states, particle 3 is instantaneously projected into one of the four pure states in Eq. (90). They can be rewritten into the following form

$$-|\chi\rangle_3, \quad -\hat{z}|\chi\rangle_3, \quad \hat{x}|\chi\rangle_3, \quad \hat{x}\hat{z}|\chi\rangle_3, \quad (91)$$

where the hatted symbols represent the respective Pauli operators, which act as unitary transformations. Each of these possible resultant states for Bob's particle 3 is related in a one-to-one way to the original state $|\chi\rangle_1$ which Alice wants to teleport. In the case of the first (singlet) outcome, the state of particle 3 is the same as the initial state of particle 1 except for an irrelevant phase factor, so Bob does not need do anything further to produce a replica of Alice's unknown state. In the other three cases, Bob could accordingly apply one of the unitary transformations in Eq. (91) to convert the state of particle 3 into the original state of particle 1, after receiving via a classical communication channel a two-bit information on which of the Bell-state measurement results was obtained by Alice. After Bob's unitary operation, the final state of particle 3 becomes an exact replica of Alice's unknown state, $|\chi\rangle_1$. The same state of Alice's particle 1 is irrecoverably erased by the Bell-state measurement. The Bell-state measurement does not reveal any information on the properties of any of the particles prior to the measurement. This is the very reason why quantum teleportation using entanglement works, while any measurement on one-particle superpositions would fail. This is why quantum teleportation escapes the verdict of the no-cloning theorem.

The transfer of quantum information from particle 1 to particle 3 can happen over arbitrary distances. In this process it is even not necessary for Alice to know where Bob is. Furthermore, as quantum teleportation is a linear operation applied to $|\chi\rangle_1$, it works for mixed states or entangled states as well; the initial state $|\chi\rangle_1$ can be completely unknown not only to Alice but to anyone. Here a fascinating case it that $|\chi\rangle_1$ could even be quantum mechanically completely undefined at the time the Bell-state measurement takes place. This is the case when, as already remarked by Bennett *et al.* (1993), particle 1 itself is a member of an entangled pair. This ultimately leads to entanglement swapping (Zukowski *et al.*, 1993; Bose *et al.*, 1998). Quantum teleportation does not violate causality as two bits of classical information, which are sent at a speed not greater than the speed of light, are absolutely necessary to conclude the process.

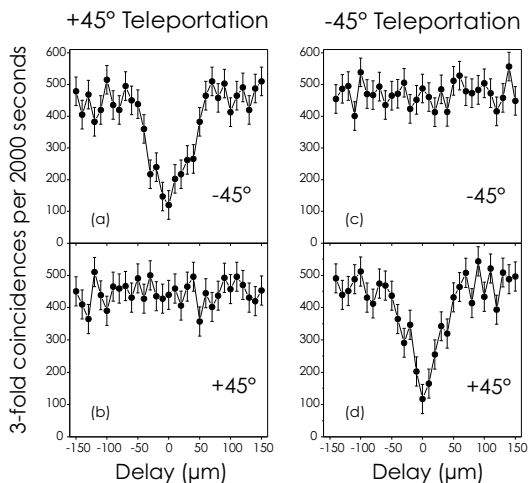


FIG. 23 Measured three-fold coincidence rates $d1f1f2$ (-45°) and $d2f1f2$ ($+45^\circ$) in the case that the photon state to be teleported is polarized at $+45^\circ$ (a and b) or at -45° (c and d). The coincidence rates are plotted as function of the delay (in μm) between the arrival of photon 1 and 2 at Alice’s BS [see Fig. 22(b)]. The three-fold coincidence rates are plotted after subtracting the spurious three-fold background contribution. These data, together with similar ones for other polarisations, confirm teleportation for an arbitrary state. (Bouwmeester *et al.*, 1997)

Generally speaking, the basic criteria (Bouwmeester *et al.*, 1999b) to constitute a *bona fide* teleportation should be: (1) the experimental scheme is capable of teleporting any state that is designed to teleport, (2) a fidelity better than $2/3$ (Massar and Popescu, 1995), (3) for future applications, at least in principle, the scheme should be extendible to long-distances.

2. Experimental teleportation of photonic states

Figure 22(b) is a schematic of the Innsbruck experimental setup of Bouwmeester *et al.* (1997). To demonstrate the very principle of teleportation it is sufficient to identify one of the four Bell states [here $|\psi^-\rangle_{12}$, i.e., the case where particle 3 is instantaneously projected into $|\chi\rangle_3$, see Eq. (90)].⁴⁶ This is exactly what was accomplished by detecting a two-fold coincidence behind a 50:50 BS in the Innsbruck experiment.

To experimentally demonstrate that an arbitrary unknown quantum state can be teleported, it is sufficient to show that the scheme works for all the mutually orthogonal axes of the polarization (Poincaré) sphere. The experimental results for teleportation of photon 1 polarized under $+45^\circ$ (-45°) is shown in the left (right) col-

⁴⁶ If one chooses to identify only one of the four Bell states, teleportation is successfully achieved in a quarter of the cases.

umn of Fig. 23: teleportation works for a complete basis for polarization states.

What is the main difficulty in the task of performing experimentally quantum teleportation? The Bell-state analysis relies on the interference of two independently created photons. One, therefore, has to guarantee behind the beamsplitter the information which photon came for which source is completely erased. This can be done using the methods of Żukowski *et al.* described in section V.E.1.⁴⁷ In the Innsbruck teleportation experiment UV pulses with a duration of 200 fs were used to create the photon pairs. By using narrow bandwidth filters ($\Delta\lambda = 4$ nm) in front of the detectors registering photons 1 and 2, the resulting coherence time of about 500 fs can be obtained and is sufficiently longer than the pump pulse duration. As it was shown in section V.E.1, this warrants high visibility of the multiphoton interference. Furthermore, single-mode fiber couplers acting as spatial filters were used to guarantee good mode overlap of the detected photons.

3. Teleportation onto freely propagating qubits

In the original teleportation experiment teleportation events were happening at random. For teleportation to happen the ultraviolet pulse passing through the crystal must first result in an emission of the ancillary EPR pair, and then after reflection must create a pair, which is used to prepare the state to be teleported and the trigger which indicates the presence of this state. However, as both processes are spontaneous, this is very rare. In most cases only one of the processes occurs. Even worse, one may have a double emissions, and a double emission in the second process leads to a the possibility of an event of three fold coincidence in $f1-f2-p$. This looks like a good teleportation event in which Bob failed to detect the teleported qubit. But this is not the case. Thus Bob can be sure that teleportation happened only when he additionally detects his photon, but..., this leads to its destruction⁴⁸. To remedy this, Pan *et al.* (2003a) realized an experiment in which teleporation events were happening with very high probability. This means that the teleportation process has an unconditional high-fidelity, and that after an admissible ththree fold $f1-f2-p$ event one has with high probability a copy of the original state at Bob’s location (that is a “freely propagating qubit”).

⁴⁷ To meet the condition of temporal overlap, the emission time of photon 2 was varied in small steps by changing the delay between the first and the second down conversion event by translating the retroreflection mirror [Fig. 22(b)].

⁴⁸ For this reason, the Innsbruck teleportation experiment has been called a “postselected” teleportation (Braunstein and Kimble, 1998), while the word “conditional” would be more appropriate as photon 3 is not selected depending on its state (Bouwmeester *et al.*, 1998; Bouwmeester *et al.*, 1999b).

Most applications of quantum teleportation include the subsequent manipulation of the teleported photon. Thus a freely propagating output state, which is teleported with high fidelity, is strongly desired. Possible solutions (Braunstein and Kimble, 1998; Kok and Braunstein, 2000) could include the discrimination of one- and two-photon events at detector p [Fig. 22(b)], a quantum non-demolition measurement of the photon number in mode 3, or the introduction of an unbalanced coupling between modes 1-4 relative to modes 2-3. Due to the lack of appropriate technology, none of the proposed schemes has so far been realized.

In the Vienna teleportation experiment (Pan *et al.*, 2003a), a freely propagating teleported quantum state was achieved [see Fig. 22(b)]. The main point is to reduce the number of unwanted f1-f2 coincidence counts. This was accomplished by attenuating the beam 1 by a factor of $\gamma/p \geq 200$, while leaving the modes 2-3 unchanged. Then a three-fold coincidence f1-f2-p occurs with probability γp^2 due to successful teleportation and with significantly lower probability $(\gamma p)^2$ one has a spurious coincidence. Thus, for sufficiently low γ it is not necessary anymore to actually detect the teleported photon 3 and a freely propagating teleported beam of qubits emerges. In essence, the entangled ancillary pair is provided much more frequently than the photon to be teleported. Thus when a qubit which is to be teleported arrives the teleportation machinery is almost always ready.

To demonstrate a non-conditional teleportation, a series of neutral filters were inserted in mode 1 to show that the probability of a successful teleportation conditioned on an f1-f2-p three-fold coincidence increases with decreasing filter transmission γ . The experimental data indeed shows that probability of success increases with decreasing γ . The preparation of a freely propagating teleported quantum state was shown to have a high (non-conditional) fidelity of 0.85 ± 0.02 , which is well above the classical limit $2/3$.

4. Teleportation of a qubit encoded in one of EPR particles

The quantum teleportation scheme presented above allows a state carried by a particle that arrives at Alice's station to be teleported with the use of an independently created EPR pair of two auxiliary particles. In this three-particle protocol the quantum state of the initial particle does not have to be specified in any way. However, if the quantum state that Alice wishes to transfer is prepared by some device that performs a unitary operation on a given input particle prepared in a "blank" state (such a device could be, for example, a quantum computer) there is a way to perform the transmission of the quantum state from Alice to Bob using only a two-particle protocol, by utilizing one of the EPR particles as the carrier of the qubit which is to be teleported. This protocol has been proposed by Popescu (1995) and was experimentally realized in Rome (Boschi *et al.*, 1998). As the protocol

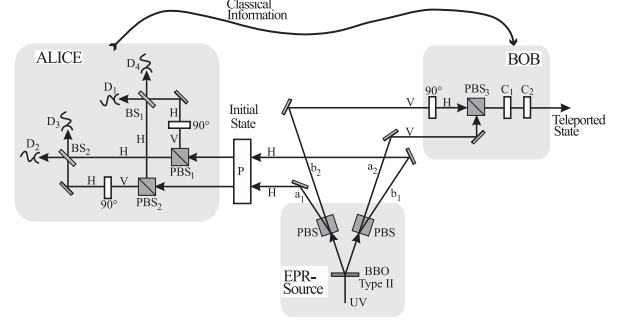


FIG. 24 Experimental setup for the “two-particle scheme” of quantum teleportation (Boschi *et al.*, 1998).

does not involve interference of photons from two separate emissions, only the EPR pair is manipulated, it avoids many difficulties. For instance, it is very easy to perform a full Bell-state measurement. However, if one aims at teleporting a state of an independent qubit, one would have to somehow transfer its state into the Alice's particle of the EPR pair.

The main idea (see the experimental setup in Fig. 24) is to use both the spatial and polarization degrees of freedom of photons. One emulates the particle which carries the to-be-teleported-qubit with the use of an additional degree of freedom of an EPR particle sent to Alice. The first step is to produce two EPR photons entangled in their directions of propagation, i.e., entangled in momentum, but each with a well-defined polarization. Thus one starts with

$$\frac{1}{\sqrt{2}} (|a_1\rangle|a_2\rangle + |b_1\rangle|b_2\rangle) |H\rangle_1 |V\rangle_2. \quad (92)$$

The area in Fig. 24 indicating the EPR source shows how this can be achieved. On the way to Alice photon 1 is intercepted by the Preparer P who changes the polarization from H to an arbitrary quantum superposition

$$|\chi\rangle_1 = \alpha|H\rangle_1 + \beta|V\rangle_1. \quad (93)$$

This is the quantum state that Alice will transmit to Bob. The Preparer affects the polarization in both paths a_1 and b_1 in the same way. The total state $|\Phi\rangle$ of the two photons is now

$$|\Phi\rangle = \frac{1}{\sqrt{2}} (|a_1\rangle_1 |a_2\rangle_2 + |b_1\rangle_1 |b_2\rangle_2) |\chi\rangle_1 |V\rangle_2. \quad (94)$$

which is a formal analogue of the initial state in Eq. (90).

Next, Alice performs a Bell-state measurement on her (single) particle. The four “Bell states” are represented by the following correlated polarization-path states of the photon:

$$\begin{aligned} |\bar{\psi}^\pm\rangle_1 &= \frac{1}{\sqrt{2}} (|a_1\rangle_1 |V\rangle_1 \pm |b_1\rangle_1 |H\rangle_1), \\ |\bar{\phi}^\pm\rangle_1 &= \frac{1}{\sqrt{2}} (|a_1\rangle_1 |V\rangle_1 \pm |b_1\rangle_1 |H\rangle_1). \end{aligned} \quad (95)$$

The measurement of photon 1 with respect to this basis can in principle be achieved with 100% success rate (A photon detection by D_1 , D_2 , D_3 , or D_4 corresponds directly to a projection onto one of the four Bell states; see Fig. 24).

Since, in terms of the four single-photon Bell states, one has

$$\begin{aligned} |\Phi\rangle = & \frac{1}{2} [|\bar{\psi}^+\rangle_1 (\beta|a_2\rangle + \alpha|b_2\rangle) |H\rangle_2 \\ & + |\bar{\psi}^-\rangle_1 (\alpha|a_2\rangle + \beta|b_2\rangle) |H\rangle_2 \\ & + |\bar{\phi}^+\rangle_1 (\alpha|a_2\rangle - \beta|b_2\rangle) |H\rangle_2 \\ & + |\bar{\phi}^-\rangle_1 (\beta|a_2\rangle - \alpha|b_2\rangle) |H\rangle_2, \end{aligned} \quad (96)$$

the final step of the protocol is that Alice informs Bob which detector clicked. With this information Bob can reproduce the initial polarization state by transforming the momentum superposition of photon 2 (see Eq. (96)) into the same superposition in polarization, and next applying the polarization transformations which represent the unitary corrections, which depend on the two-bit information sent by Alice, needed to reproduce the teleported state.

5. Various approaches to teleportation

It is fair to say that each teleportation experiment has its own advantages and disadvantages [for a comparison between various methods, see Bouwmeester *et al.* (1999b)]. Quantum teleportation of continuous-variable states (Furusawa *et al.*, 1998) is hard to extend to the long-distance case, because of the unavoidable dispersion of squeezed-states during the distribution of entanglement. This consequently leads to a fast degrading of the quality of squeezed-state entanglement. Quantum teleportation using nuclear magnetic resonance (Nielsen *et al.*, 1998) or atoms (Riebe *et al.*, 2004; Barret *et al.*, 2004) has an obvious advantage in that the input quantum state can be, in principle, teleported with an efficiency of 100%. Yet, it is difficult (if not impossible) to implement it over long distances. An essential criterion of teleportation is to be able to teleport any independent quantum state coming from outside. This is obviously not possible in the Rome experiment, where the initial photon has to be entangled from the beginning with the final one. The Innsbruck teleportation technique with its later improvements enables one to aim at a long-distance teleportation (Marcicic *et al.*, 2003; Ursin *et al.*, 2004) and more complicated schemes (Zhao *et al.*, 2004; Zhang *et al.*, 2006c).

6. More involved teleportation schemes

a. Open-destination quantum teleportation A more involved scheme in multi-party quantum communication is the so-called open-destination teleportation (Karlsson

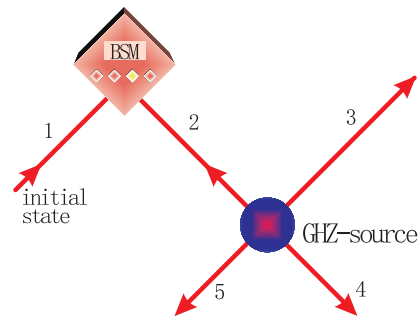


FIG. 25 The basic idea of open-destination teleportation (Zhao *et al.*, 2004)

and Bourennane, 1998). An unknown quantum state of a single particle is first teleported onto a N -particle coherent superposition. At a later stage the teleported state can be readout at any of the N particles, by performing a projection measurement on the remaining $N - 1$ particles. Such a teleportation scheme was demonstrated for $N = 3$ by Zhao *et al.* (2004). This was the first experiment in which one was able to manipulate five photonic qubits.

Figure 25 shows the basic idea. A GHZ entanglement source emits a four-photon maximally entangled state, say,

$$|\Phi\rangle_{2345} = \frac{1}{\sqrt{2}} (|H\rangle_2|H\rangle_3|H\rangle_4|H\rangle_5 + |V\rangle_2|V\rangle_3|V\rangle_4|V\rangle_5) \quad (97)$$

Photon 1 is in an unknown polarization state $|\chi\rangle_1 = \alpha|H\rangle_1 + \beta|V\rangle_1$. By performing a joint Bell-state measurement on photons 1 and 2 one can follow the usual teleportation protocol to transfer the information on the initial state of photon 1 to a multi-particle superposition, which takes form $|\chi\rangle_{345} = \alpha|H\rangle_3|H\rangle_4|H\rangle_5 + \beta|V\rangle_3|V\rangle_4|V\rangle_5$. This is actually a three-qubit encoding. Moreover, by performing later a polarization analysis on any *two* of the three photons 3, 4 and 5 in the $45^\circ/135^\circ$ basis one can convert the remaining photon into the initial state of photon 1.

In contrast to the original teleportation scheme, after the encoding operation the destination of teleportation is left open until we perform a polarization measurement (“decoding”) on two of the remaining three photons. This implies that, even though photons 3, 4 and 5 are far apart, one can still choose which particle should act as the carrier of the teleportation output. No prior agreement on the final destination of the teleportation is necessary.

The required (conditional) four-photon GHZ entanglement was generated using the techniques of sections V.E.2 and VI.B.2. The measured fidelities of teleportation from photon 1 to photon 5 and from photon 1 to photon 4 for $+/-$ linear and R/L circular polarization states were $\sim 0.80 \pm 0.04$, well above the classical limit of $2/3$.

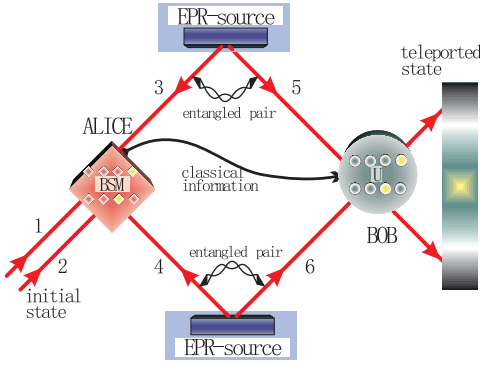


FIG. 26 Basic idea of two-qubit quantum teleportation (Zhang *et al.*, 2006c).

b. Quantum teleportation of composite two-qubit states
Teleportation of single qubits, as reviewed above, is insufficient for certain large-scale realizations of quantum information processing. In a recent experiment (Zhang *et al.*, 2006c), teleportation of two-qubit states was realized with a six-photon interferometer.

In the two-qubit teleportation, Alice wants to send an unknown state of a composite system, qubits 1 and 2:

$$|\chi\rangle_{12} = \alpha |H\rangle_1 |H\rangle_2 + \beta |H\rangle_1 |V\rangle_2 + \gamma |V\rangle_1 |H\rangle_2 + \delta |V\rangle_1 |V\rangle_2 \quad (98)$$

to a distant receiver, Bob (Fig. 26). Before teleportation Alice and Bob share two ancillary entangled photon pairs (photon pairs 3-5 and 4-6) which are prepared in the Bell state, say, $|\phi^+\rangle = (|HH\rangle + |VV\rangle)/\sqrt{2}$. The two-qubit teleportation scheme then works as follows: (1) Following the standard teleportation protocol, Alice first teleports the state of photon 1 to photon 5 by consuming entangled pair 3-5. The result of this step is $|\chi\rangle_{52}$. (2) Similarly, Alice can also teleport the state of photon 2 to photon 6 by consuming entangled pair 4-6. After successful implementation of the two steps, the original two-qubit state $|\chi\rangle_{12}$ is teleported to qubits 5 and 6 in $|\chi\rangle_{56}$, realizing the most general two-qubit teleportation.

The teleportation of two-qubit states was realized by teleporting the two photonic qubits individually. Thus, neither the two original qubits nor the teleported qubits have to be in the same place. Such a flexibility is desired in distributed quantum information processing such as quantum telecomputation (Grover, 1997) and quantum state sharing (Cleve *et al.*, 1999). Moreover, the way of teleporting each qubit of a composite system individually can be easily generalized to teleport an N -qubit composite system.

In the two-qubit teleportation experiment (Zhang *et al.*, 2006c), to have enough six-photon coincidence rate, various efforts (e.g., the high-intensity UV laser and better collection efficiency) were made to significantly improve the brightness and stability of the entangled photon sources. On average 10^5 photon pairs per second

were observed from each EPR source. This is almost 5 times brighter than the source achieved in the five-photon experiment (Zhao *et al.*, 2004). As a result, in total 10 six-photon events per minute were registered. This is two orders of magnitude higher than any former photonic teleportation experiments could have achieved.

The two-qubit teleportation protocol was implemented for three different initial states $|X\rangle_A = |H\rangle_1 |V\rangle_2$, $|X\rangle_B = (|H\rangle_1 + |V\rangle_1)(|H\rangle_2 - i|V\rangle_2)/2$ and $|X\rangle_C = (|H\rangle_1 |V\rangle_2 - |V\rangle_1 |H\rangle_2)/\sqrt{2} = |\psi^-\rangle$. The measured fidelity for $|X\rangle_A$ ($|X\rangle_B$) is 0.86 ± 0.03 (0.75 ± 0.02). The measurement of the fidelity of the $|X\rangle_C$ teleportation can be converted into local measurements on individual qubits by using the identity

$$|\psi^-\rangle \langle \psi^-| = \frac{1}{4}(\hat{I} - \hat{x}\hat{x} - \hat{y}\hat{y} - \hat{z}\hat{z}). \quad (99)$$

Each of these local measurements took about 60 hours. And the experimental fidelity of the $|X\rangle_C$ teleportation was measured to be 0.65 ± 0.03 . All the measured fidelities are well beyond the state estimation limit of 0.40 (Hayashi *et al.*, 2005) for a two-qubit system. Particularly, the fact that the $|X\rangle_C$ teleportation has fidelity greater than $1/2$ already proves that there exists entanglement (Bennett *et al.*, 1996b; Horodecki *et al.*, 1997) between photon 5 and photon 6 that never interacted before. In this sense, the $|X\rangle_C$ teleportation can be reinterpreted as a two-stage realization of entanglement swapping.

C. Entanglement swapping

As it was mentioned, entanglement swapping (Żukowski *et al.*, 1993) provides a method of entangling of two particles that never interacted or even have no common past. It can also be interpreted as teleportation of entanglement, i.e., teleportation of undefined states (Bennett *et al.*, 1993). We would like to mention that one of the original motivations of entanglement swapping is the so called “event-ready detection” of the entangled particles, a concept suggested by John Bell (Clauser and Shimony, 1978; Bell, 1987). Entanglement swapping, together with entanglement purification, is a key element of the quantum repeater protocol (Briegel *et al.*, 1998; Dür *et al.*, 1999; see also section VII.E) and opens up a way to speed up the distribution of entanglement for massive particles (Bose *et al.*, 1998).

Consider the arrangement of Fig. 27. We have two EPR sources. Assume that each source emits a pair of entangled photons in the state, say, $|\psi^-\rangle$ so that the total state of the four photons is $|\Psi\rangle_{1234} = |\psi^-\rangle_{12} |\psi^-\rangle_{34}$. While pairs 1-2 and 3-4 are entangled, there is no entanglement of any of the photons 1 or 2 with any of the photons 3 or 4. Next, one performs a Bell-state measurement on photons 2 and 3. Due to the expansion

$$|\Psi\rangle_{1234} = \frac{1}{2}(|\psi^+\rangle_{14} |\psi^+\rangle_{23} - |\psi^-\rangle_{14} |\psi^-\rangle_{23} - |\phi^+\rangle_{14} |\phi^+\rangle_{23} + |\phi^-\rangle_{14} |\phi^-\rangle_{23}), \quad (100)$$

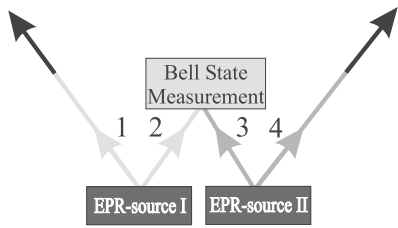


FIG. 27 Principle of entanglement swapping.

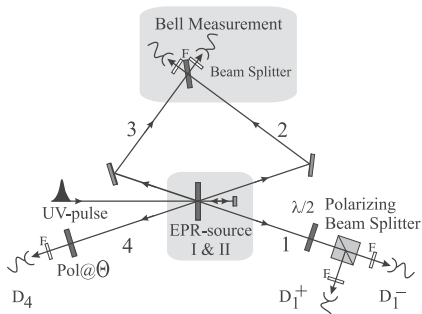


FIG. 28 Experimental setup of entanglement swapping (Pan *et al.*, 1998). The entangled photon pairs 1-2 and 3-4, and the Bell-state measurement identifying the $|\psi^-\rangle_{23}$ state are similar to the Innsbruck teleportation experiment. As a consequence of the Bell-state measurement the two remaining photons 1 and 4 will be projected onto an entangled state. To analyse their entanglement one looks at coincidences between detectors $D1^+$ and $D4$, and between detectors $D1^-$ and $D4$, for different polarization angles Θ . By rotating the $\lambda/2$ plate in front of the PBS one can also analyze photon 1 in a different orthogonal polarization basis which is necessary to obtain statements for relative polarization angles between photons 1 and 4. Note that, since the detection of coincidences between detectors $D1^+$ and $D4$, and $D1^-$ and $D4$ are conditioned on the detection of the $|\psi^-\rangle_{23}$ state, one is looking at 4-fold coincidences. Narrow bandwidth filters (F) are positioned in front of each detector.

this measurement always projects photons 1 and 4 also onto a Bell state. For example, if the result of the Bell-state measurement of photons 2 and 3 is $|\psi^-\rangle$, then the resulting state for photons 1 and 4 is also $|\psi^-\rangle$. In all cases photons 1 and 4 emerge entangled despite the fact that they never interacted in the past. In Fig. 27 entangled particles are indicated by the same line darkness. Note that particles 1 and 4 become entangled after the Bell-state measurement on particles 2 and 3.

The process of entanglement swapping also gives a means to define that an entangled pair of photons, 1 and 4, is available. As soon as Alice completes the Bell-state measurement on particles 2 and 3, we know that photons 1 and 4 are on their way ready for detection in an entangled state. In this way one has the possibility to perform an event-ready test of Bell's inequality (Żukowski *et al.*, 1993).

Figure 28 is a schematic drawing of the Pan *et al.* (1998) experimental setup. As in the Innsbruck teleportation experiment, only the anti-symmetric Bell-state $|\psi^-\rangle_{23}$ was identified experimentally. Afterwards, according to the entanglement swapping scheme, photon 1 and 4 should be projected into the same entangled state $|\psi^-\rangle_{14}$. This entanglement was verified by analyzing the polarization correlations between photons 1 and 4 conditioned on coincidences between the detectors of the Bell-state analyzer. At the variable polarization direction Θ , the correlations should show two sine curves as a function of Θ which are 90° out of phase. The observed sinusoidal behavior (the interference pattern) of the coincidence rates has a visibility of 0.65 which clearly surpasses the 0.5 limit of a classical value. A later experiment (Pan *et al.*, 2001a) resulted with visibility of ~ 0.79 , which is sufficient for violating Bell's inequality for photons 1 and 4, even though these two photons never interacted directly. Such a test was performed by Jennewein *et al.* (2002) and the inequality was violated by the factor of 1.211 ± 0.045 , i.e., by 4.6 standard deviations.

Experimental entanglement swapping is a further demonstration of teleportation, i.e., teleportation of quantum mechanically undefined state. A test of Bell's inequality involving swapping entanglement has some appealing feature, except from being an “event-ready” one. We could even perform it in a delayed-choice mode, as suggested by Peres (2000) and realized by Jennewein *et al.* (2002). In such an experiment one delays the instant of time at which the Bell-state measurement is performed on photons 2 and 3. Thus entanglement between photons 1 and 4 in subensembles associated with a specific result for 2 and 3, is revealed, *a posteriori*, after they have already been measured and may no longer exist.

D. Beating noisy entanglement

So far, significant experimental progress has been achieved only in small-scale realizations of quantum information processing. However, serious problems occur in bringing quantum information processing to technologically useful scales. This is primarily due to the unavoidable decoherence [For general aspects on decoherence, we refer to the excellent reviews (see, e.g., Zurek, 2003; Schlosshauer, 2004)] caused by the coupling between the quantum system and the environment. In quantum communication, it is the noisy quantum channel that degrades the quality of entanglement between two particles the more the further they propagate. Yet, the implementation of any of the quantum communication schemes (as reviewed above) over large distances requires that two distant parties share entangled pairs with high quality. In addition, during quantum computation the coherence of a quantum system also decreases exponentially with the increase of operation time. This would consequently lead to the failure of quantum algorithms. It is therefore necessary to overcome the unfavorable de-

coherence in any realistic large-scale realization of quantum information processing.

The main tool to overcome the noise in the quantum communication channel is entanglement purification, proposed by Bennett *et al.* (1996a, 1996b, 1996c) and Deutsch *et al.* (1996). The linear-optical implementation of entanglement purification was suggested and then experimentally demonstrated by Pan *et al.* (2001b, 2003b). Quantum repeaters (Briegel *et al.*, 1998; Dür *et al.*, 1999), based on entanglement purification and entanglement swapping, provide an efficient way to generate highly entangled states between two distant locations. Remarkably, the quantum repeater protocol tolerates general errors on the percent level, which is reachable using entanglement purification based on linear optics (Pan *et al.*, 2001b, 2003b). A recent study (Dür and Briegel, 2003) shows that entanglement purification can also be used to increase the quality of logic operations between two qubits by several orders of magnitude. In essence, this implies that the threshold for tolerable errors in quantum computation is within reach using entanglement purification and linear optics.

In this section we will review the basic idea of entanglement purification and its linear-optical implementation. The experimental demonstration is certainly a significant step toward ultimate long-distance quantum communication. Before going into details, we would like to mention that there are other ways to beat decoherence by quantum error-correcting codes (Shor, 1995; Bennett *et al.*, 1996c; Steane, 1996, 1998; Calderbank and Shor, 1996; Laflamme *et al.*, 1996) and decoherence-free subspace of Hilbert space (Palma *et al.*, 1996; Duan and Guo, 1997; Zanardi and Rasetti, 1997; Lidar *et al.*, 1998; Zanardi, 1999; Bacon *et al.*, 1999; Kempe *et al.*, 2001). Experimental realization of decoherence-free subspaces with photons was reported by Kwiat *et al.* (2000), Altepeter *et al.* (2004), and Bourennane *et al.* (2004), and applications of decoherence-free subspace were demonstrated for an optical quantum-computing algorithm (Mohseni *et al.*, 2003) and for fault-tolerant quantum cryptography (Zhang *et al.*, 2006d).

Quantum error correction paves the way to protect a fragile unknown quantum state by encoding the state into a multiparticle entangled state. Then the subsequent measurements, i.e., the so-called decoding processes, can find out and correct the error during the quantum operations. Several quantum error correction protocols have been experimentally demonstrated in the NMR (Cory *et al.*, 1998; Knill *et al.*, 2001) and ion-trap (Chiaverini *et al.*, 2004) systems. Although the quantum error correction protocols are primarily designed for large-scale quantum computing, a similar idea is to implement error-free transfer of quantum information through a noisy quantum channel (Bouwmeester, 2001; Wang, 2004). Such an error-rejection protocol for error-reduced transfer of quantum information through a noisy quantum channel was experimentally verified (Chen *et al.*, 2006c). Yet, up to now optical implementation of quantum error-

correcting codes still remains an experimental challenge.

1. Entanglement concentration

Before introducing the generic entanglement purification, we first discuss its special case, i.e., entanglement concentration⁴⁹ which aims to obtain with a nonzero probability, a maximal entanglement from two nonmaximally entangled *pure states*. There are two methods to achieve this. The first is the so-called Procrustean method (Bennett *et al.*, 1996b). It requires that the photon pairs are all in a pure non-maximally entangled state, say, $|\Psi\rangle_{\text{nonmax}} = \alpha|H\rangle|V\rangle + \beta|V\rangle|H\rangle$, where α and β are two *known* coefficients that satisfy $|\alpha|^2 + |\beta|^2 = 1$. In this case, the scheme only involves local filtering operations (Gisin, 1996; Horodecki *et al.*, 1996) on single pairs. Second, the Schmidt decomposition scheme (Bennett *et al.*, 1996b) works for photon pairs that are all in a pure but *unknown* non-maximally entangled state $|\Psi\rangle_{\text{nonmax}}$. In practice, this scheme is difficult to implement as it requires simultaneous collective measurements on many photons.

Experimentally, the Procrustean method has been demonstrated very recently (Kwiat *et al.*, 2001). The Schmidt decomposition scheme becomes practically feasible after the proposal of a linear-optical implementation of entanglement concentration (Zhao *et al.*, 2001; Yamamoto *et al.*, 2001) was suggested. Two independent experiments (Yamamoto *et al.*, 2003; Zhao *et al.*, 2003b) were reported for linear-optical entanglement concentration. The experiment by Zhao *et al.* realized a prototype of quantum repeater by using local filtering and entanglement swapping, thus providing a practical toolbox for future realization of long-distance quantum communication.

2. Entanglement purification

The underlying idea of entanglement purification is to use several copies of a state whose entanglement is not sufficient for quantum information processing. Using local operations and classical communication (LOCC) it is sometimes possible to obtain fewer copies of particles in a state which is closer to a maximally entangled state. A sketch showing the working principle of entanglement

⁴⁹ We emphasize that, though only the general scheme can be used to purify arbitrary mixed states, both local filtering and entanglement concentration are of interest in their own rights. This is because, on the one hand, both methods provide a way to generate maximally entangled states, which is different from the general scheme where only highly entangled states are generated. On the other hand, with the help of local filtering any inseparable state can be purified (Horodecki *et al.*, 1997), while the general scheme alone only works for the cases where the entanglement fidelity F is larger than $1/2$ (Bennett *et al.*, 1996a).

purification is illustrated in Fig. 29(a). The purification procedure works as follows (Bennett *et al.*, 1996a, 1996c; Deutsch *et al.*, 1996).

1. Prepare all entangled pairs in the “working state”, i.e., the two-qubit Werner state (Werner, 1989),

$$\rho(F) = F|\psi^-\rangle\langle\psi^-| + \frac{(1-F)}{3}(|\psi^+\rangle\langle\psi^+| + |\phi^+\rangle\langle\phi^+| + |\phi^-\rangle\langle\phi^-|), \quad (101)$$

which is a rotationally symmetric mixture of the four Bell states. If the state is not a Werner state, then apply a depolarizing procedure, called random bilateral rotation, that converts it back into $\rho(F)$ without changing its fidelity $F = \text{tr}[|\psi^-\rangle\langle\psi^-|\rho(F)]$ (with respect to $|\psi^-\rangle$).

2. Choose randomly two less entangled pairs from the ensemble ρ . One member of each pair is sent to Alice, the other to Bob. Denote the first pair as the source pair, and the second one as target pair. Alice applies the unitary transformation \hat{y} to her two qubits. This for each pair gives a transformation $|\psi^\pm\rangle \leftrightarrow |\phi^\mp\rangle$ (irrelevant phase factors will be ignored.) Thus, the resulting state is $\rho(F)$ with $|\psi^-\rangle$ and $|\phi^+\rangle$ exchanged.
3. Alice and Bob bilaterally apply a CNOT operation to their pairs of qubits.
4. Alice and Bob measure their target qubits in the computational basis (i.e., 0/1 basis) and broadcast their results. If their results agree, they keep the source particles, and otherwise they discard them. One can easily see that this is equivalent to projecting the initial states onto the subspace in which either both the sources and the targets are $|\phi\rangle$ states or both are $|\psi\rangle$ states. The output state has a new fidelity F' with respect to $|\phi^+\rangle$

$$F' = \frac{F^2 + (1-F)^2/9}{F^2 + 2F(1-F)/3 + 5(1-F)^2/9}, \quad (102)$$

and the other three Bell states are not equally distributed. For $1 > F > 1/2$, one has $F' > F$, i.e., the fidelity after this operation increases.

5. Repeating step 1 to convert the output state into the Werner state $\rho(F')$ such that the process can be continued.

Thus, if the process is successful, Alice and Bob are left with a single pair in a Werner state $\rho(F')$ with larger fidelity $F'(F)$ if $F > 1/2$.⁵⁰ Iterating the procedure as

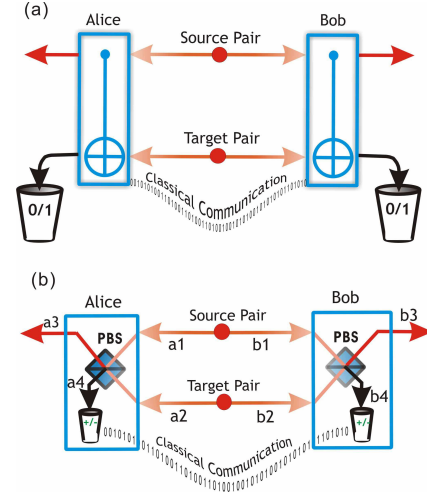


FIG. 29 Schematic drawings showing the principles of entanglement purification based on the CNOT operations (a) and on linear-optical elements (b). In the latter case the CNOT operations are replaced by two polarizing beam splitters (Pan *et al.*, 2001b).

many times as it is necessary, they can reach a fidelity as close to one as they wish, but at the expense of wasting many pairs.

From a practical point of view, the most important drawback of the above scheme is that it requires the CNOT operation. Although certain quantum logic gates have been experimentally demonstrated for atoms and ions (Raimond *et al.*, 2001; Leibfried *et al.*, 2003; for optical CNOT gate, see section VIII.B), there is at present no implementation of the CNOT gate that could realistically be used for purification in the context of long-distance quantum communication, in which the tolerable error rates caused by the CNOT operation must not exceed a few percent (Briegel *et al.*, 1998; Dür *et al.*, 1999). This is far outside the range of the present implementations. Fortunately, a linear-optical entanglement purification protocol (Pan *et al.*, 2001b, 2003b) solves the problem precisely, see below.

3. Linear-optical entanglement purification

a. Theory The linear-optical purification scheme [shown in Fig. 29(b)] will be presneted discussing a specific example.⁵¹ The working state in the linear-optical entan-

⁵⁰ In reality there will be imperfections in all local operations. Further consideration using some explicit models (Briegel *et al.*, 1998; Dür *et al.*, 1999) shows that there is a minimum value of the original fidelity of the state F_{\min} for which purification is possible; there is also a maximum achievable fidelity F_{\max} due to the imperfections in local operations.

⁵¹ This special example corresponds to eliminating single bit-flip errors. However, the same method would also apply to the general mixed states ρ_{ab} , provided that they contain a sufficiently large fraction $F > 1/2$ of photon pairs in a maximally entangled state (say, $|\phi^+\rangle_{ab}$). In short, this can be understood as follows. Using the linear-optical purification method, one can first purify away single bit-flip errors. Phase errors can then be transformed

glement purification is

$$\rho_{ab} = F|\phi^+\rangle_{ab}\langle\phi^+| + (1-F)|\psi^-\rangle_{ab}\langle\psi^-|, \quad (103)$$

where $|\psi^-\rangle_{ab}$ is an unwanted admixture; a and b indicate the particles at Alice's and Bob's locations, respectively. We choose this specific form of ρ_{ab} just for the convenience of discussion.

The linear optical purification scheme is very similar to the original one (Bennett *et al.*, 1996a, 1996c; Deutsch *et al.*, 1996). The main difference [compare Fig. 29(a) and Fig. 29(b)] is that now each CNOT gate is replaced by a PBS. As we mentioned in section III.C, the function of the PBS implies that finding one photon in each output mode corresponds to a projection onto the subspace spanned by $|H\rangle_1|H\rangle_2$ and $|V\rangle_1|V\rangle_2$.

Alice and Bob start by randomly choosing two pairs from the ensemble ρ_{ab} . Each of them then superimposes their photons on a PBS. An essential step in our purification scheme is to select those cases where there is exactly one photon in each of the four spatial output modes, which we refer to as ‘‘four-mode cases’’. As just explained, this corresponds to a projection onto the subspace where the two photons at the same experimental location (Alice's or Bob's) have equal polarization. Note that the polarizations at the two different locations do not have to be the same.

From Eq. (103) it follows that the original state $\rho_{a_1b_1} \cdot \rho_{a_2b_2}$ of the two pairs can be seen as a probabilistic mixture of four pure states: with a probability of F^2 , pairs 1 and 2 are in the state $|\phi^+\rangle_{a_1b_1} \cdot |\phi^+\rangle_{a_2b_2}$, with equal probabilities of $F(1-F)$ in the states $|\phi^+\rangle_{a_1b_1} \cdot |\psi^-\rangle_{a_2b_2}$ and $|\psi^-\rangle_{a_1b_1} \cdot |\phi^+\rangle_{a_2b_2}$, and with a probability of $(1-F)^2$ in $|\psi^-\rangle_{a_1b_1} \cdot |\psi^-\rangle_{a_2b_2}$. Among these, the cross combinations $|\phi^+\rangle_{a_1b_1} \cdot |\psi^-\rangle_{a_2b_2}$ and $|\psi^-\rangle_{a_1b_1} \cdot |\phi^+\rangle_{a_2b_2}$ never lead to four-mode cases. Namely, by selecting only four-mode cases one can eliminate the contribution of the cross terms.

Consider now the other two remaining combinations $|\phi^+\rangle_{a_1b_1} \cdot |\phi^+\rangle_{a_2b_2}$ and $|\psi^-\rangle_{a_1b_1} \cdot |\psi^-\rangle_{a_2b_2}$. For the state $|\phi^+\rangle_{a_1b_1} \cdot |\phi^+\rangle_{a_2b_2}$, selecting four-mode cases behind the two PBS results in the state

$$\frac{1}{\sqrt{2}}(|H\rangle_{a_3}|H\rangle_{a_4}|H\rangle_{b_3}|H\rangle_{b_4} + |V\rangle_{a_3}|V\rangle_{a_4}|V\rangle_{b_3}|V\rangle_{b_4}) \quad (104)$$

with the probability 50%. Alice and Bob can then generate maximal two-photon entanglement between the output modes a_3 and b_3 out of the four-photon entanglement by performing polarization measurements on each of the two photons in a_4 and b_4 in the $+/-$ basis and comparing their measurement results. If the measurement results at a_4 and b_4 are equal, i.e., $|+\rangle|+\rangle$ or $|-\rangle|-\rangle$ (opposite, i.e.,

$|+\rangle|-\rangle$ or $|-\rangle|+\rangle$), then the remaining two photons at a_3 and b_3 are left in the state $|\phi^+\rangle_{a_3b_3}$ ($|\phi^-\rangle_{a_3b_3}$). In the $|\phi^-\rangle_{a_3b_3}$ case either Alice or Bob could simply perform a local phase flip operation on his or her remaining photon to convert the state $|\phi^-\rangle_{a_3b_3}$ back into $|\phi^+\rangle_{a_3b_3}$. Therefore, starting from the initial state $|\phi^+\rangle_{a_1b_1} \cdot |\phi^+\rangle_{a_2b_2}$ Alice and Bob will get the state $|\phi^+\rangle_{a_3b_3}$ whenever there is exactly one photon in each output mode.

In the $|\psi^-\rangle_{a_1b_1} \cdot |\psi^-\rangle_{a_2b_2}$ case, following the same procedure Alice and Bob will project the remaining two photons a_3 and b_3 into the state $|\psi^+\rangle_{a_3b_3}$ with a probability of 50%. Since the probabilities to have a $|\phi^+\rangle_{a_1b_1} \cdot |\phi^+\rangle_{a_2b_2}$ and a $|\psi^-\rangle_{a_1b_1} \cdot |\psi^-\rangle_{a_2b_2}$ incident are F^2 and $(1-F)^2$, respectively, after performing the purification procedure (*selection of four-mode cases, measurements in modes a_4 and b_4 in the $+/-$ basis, and local operations conditional on the measurement results*) Alice and Bob will finally create a new ensemble described by the density operator

$$\rho'_{ab} = F'|\phi^+\rangle_{ab}\langle\phi^+| + (1-F')|\psi^-\rangle_{ab}\langle\psi^-|, \quad (105)$$

with a larger fidelity $F' = F^2/[F^2 + (1-F)^2]$ (for $F > 1/2$) of pairs in the desired state than before the purification.

b. Experiment To experimentally demonstrate the linear optical purification scheme (the experimental setup is shown in Fig. 30), one needs to process two photon pairs which are in the mixed state (103). This was achieved by first preparing the two photon pairs in the state $|\phi^+\rangle_{ab}$ (with a high signal to noise ratio of 30:1 in the $+/-$ basis) and then sending the photons a_1 and a_2 through a half-wave plate ($\lambda/2$), whose angle is randomly set at either $+\delta$ or $-\delta$. The experiment used a double-pass configuration, in which each pass an entangled photon pair in the state $|\phi^+\rangle_{ab}$ was created.

While the above purification method works ideally for the case where there is (at most) only one pair of photons in each of the input modes a_1 - b_1 and a_2 - b_2 , with a probability of the same order of magnitude two photon pairs will be emitted into the same mode pair because of the spontaneous nature of SPDC. This case would also contribute four-mode cases in the real experiment. Interestingly, if the position of the reflection mirror $\Delta 1$ is fixed and the amplitudes of these two four-mode contributions arrive at the two PBS simultaneously, then the two amplitudes will have a fixed relative phase (denoted by ϕ_4) and thus be in a coherent superposition $|H\rangle_{a_3}|V\rangle_{a_4}|H\rangle_{b_3}|V\rangle_{b_4} + e^{i\phi_4}|V\rangle_{a_3}|H\rangle_{a_4}|V\rangle_{b_3}|H\rangle_{b_4}$. Adjusting the position of $\Delta 1$ such that $\phi_4 = 0$ and further performing a polarization measurement in the mode pair a_4 - b_4 in the $+/-$ basis, the two remaining photons in a_3 - b_3 will always be converted into the state $|\phi^+\rangle_{a_3b_3}$, which is exactly the desired maximally entangled state. In essence, this implies that the presence of the double pair emission into the same mode pair does not at all prevent one from carrying out the purification protocol,

into bit-flip errors by a 45° polarization rotation and treated in a subsequent purification step. This is why it is sufficient to verify the purification effect for the mixed state described in Eq. (103) in an experimental demonstration of the scheme.

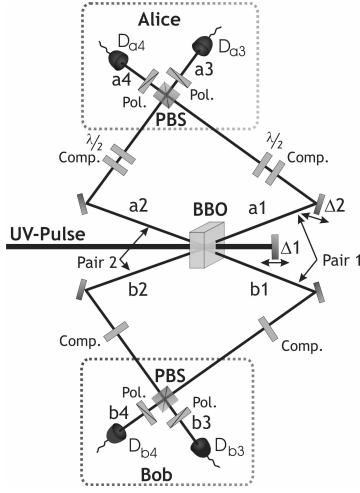


FIG. 30 Experimental set-up for entanglement purification (Pan *et al.*, 2003b). A pulse of UV light passes through a BBO crystal twice to produce two polarization-entangled photon pairs, i.e., the pair 1 in a1-b1 and the pair 2 in a2-b2. Four compensators (Comp.) are used to offset the birefringent effect caused by the BBO crystal during parametric down-conversion. The photons in the modes b1 and b2 further pass through a half-wave plate ($\lambda/2$) to simulate the noise that reduces the entanglement quality. We then send the two pairs through the corresponding PBS to perform entanglement purification. By adjusting the positions of the delay mirrors $\Delta 1$ and $\Delta 2$, one can achieve that the photons at the same experimental station arrive at their PBS simultaneously. Detecting exactly one photon in each of the four outputs (a3, a4, b3 and b4) behind a 45° polarizer (Pol.), one can verify the success of the purification scheme.

but rather makes the scheme more efficient (Simon and Pan, 2002).

To achieve $\phi_4 = 0$, Pan *et al.* exploited the two-photon hyper-entangled state $\frac{1}{2}(|H\rangle_a|H\rangle_b + |V\rangle_a|V\rangle_b)(|a1\rangle|b1\rangle + e^{i\phi_2}|a2\rangle|b2\rangle)$ (Simon and Pan, 2002; Chen *et al.*, 2003). This corresponds to the case where one and only one entangled pair is created after the pump pulse passing through the BBO crystal twice, that is, the entangled photon pair is emitted into a superposition of the mode pairs a1-b1 and a2-b2. The relative phase ϕ_2 of the two spatial modes is determined also by $\Delta 1$. Since the two relative phases ϕ_4 and ϕ_2 satisfy the relation $\phi_4 = 2\phi_2$, and hence if $\phi_2 = 0$, then $\phi_4 = 0$ (Simon and Pan, 2002). The case $\phi_2 = 0$ was achieved by the method used in the experimental test of two-photon GHZ-type theorem (Yang *et al.*, 2005).

In order to have a fixed phase of $\phi_4 = 0$, phase stabilization was maintained throughout the whole measurement. To achieve this, the setup was built onto an aluminium platform to avoid sound resonance; a feedback air-condition was used to avoid the thermal expansion of the interferometer; a plastic housing around the setup avoided the air flow. At the same time, the two-fold coincidence of a4-b4 acted as a phase monitor. In this

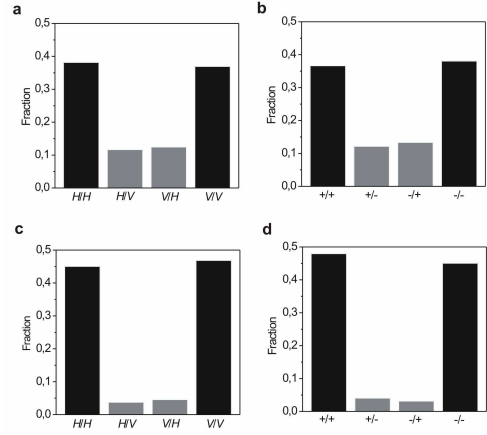


FIG. 31 Experimental results. (a) and (b) show the experimentally measured fractions both in the H/V and in the $+/-$ bases for the original mixed state. (c) and (d) show the measured fractions of the purified state in the modes a3 and b3 both in the H/V and in the $+/-$ bases. Compared with the fractions in (a) and (b), our experimental results shown in (c) and (d) both together confirm the success of entanglement purification. (Pan *et al.*, 2003b)

way, the phase could be kept stable for several hours. With emphasis we note that, opposed to the earlier multi-photon experiments, here the interferometric precision and stability are required at the scale of the wavelength, which is much smaller than coherence stability. This was a major experimental challenge.

Having achieved perfect spatial and temporal overlap and having fixed the relative phase ϕ_4 to zero, one is then ready to demonstrate entanglement purification. In the first purification experiment, the mixed state as in (103) with fidelity of $F = 0.75$ was prepared. The preparation was confirmed by the experimentally measured fractions both in the H/V and in the $+/-$ bases, as shown in Figs. 31(a) and 31(b), respectively. The measured results in Fig. 31(c) and 31(d) together prove the significant improvement of entanglement fidelity, with the fidelity $F' = 0.92 \pm 0.01$ of the purified sub-ensemble. In a second experiment entanglement purification was performed for the mixed state with $F = 0.80$. After purification, the observed entanglement fidelity for the sub-ensemble in the modes a3 and b3 is about 0.94 ± 0.01 . Both experiments verified the purification scheme. It is worth noting that in both experiments, the visibilities of the original mixed states are 50% and 60%, respectively. After one-step purification the visibilities of the new ensembles are 84% and 88%, which are well above the threshold to violate Bell's inequality. Such a Bell experiment with purified less-entangled states has already been performed by Walther *et al.* (2005a). In this experiment, the initial poorly entangled photons, not being able to violate Bell's inequality, were created by a controllable decoherence. After purification, $S_{\text{Bell}} = 2.29 \pm 0.13$ was

measured, which violates Bell’s inequality by 2.2 standard deviations.

Needless to say, the above methods to achieve perfect spatial-temporal overlap and phase stabilization provide the necessary techniques for experimental investigations of schemes in linear-optical quantum information processing. A slight modification of the purification setup can be used for testing two-photon GHZ-type theorem (Chen *et al.*, 2003; Yang *et al.*, 2005) and measuring de Broglie wavelength of a non-local four-photon state (Walther *et al.*, 2004), to mention a few. More importantly, Pan *et al.* also estimated the accuracy of local operations at the PBS, which is better than 98%, or equivalently an error probability of at most 2%. Entanglement purification with such a high accuracy is important not only for quantum communication, but also for quantum computation, as we mentioned at the beginning of this section. Moreover, with linear optics the accuracy of single photon operations on polarization and spatial degrees of freedom can be extremely high, with errors as low as 10^{-6} or even less. These facts, together with the experimental realization of high-fidelity teleportation (Pan *et al.*, 2003a), implies that the threshold of tolerable error rates in quantum repeaters can be achieved. This opens the door to realistic long-distance quantum communication.

E. Quantum repeater: towards long-distance quantum communication

The central problem of quantum communication is to generate nearly perfect entangled states between distant sites. While photons are ideal quantum information carriers for long-distance quantum communication task, it is more advantageous to exploit entanglement-based⁵² quantum communication protocols due to photon losses in the transmission channel. Then another problem (decoherence) arises due to the noisy quantum channel which degrades the quality of entanglement between spatially separated photons as they propagate. Both the photon losses and the decrease in the quality of entanglement scale exponentially with the length of the communication channel. Fortunately, the quantum repeater protocol (Briegel *et al.*, 1998; Dür *et al.*, 1999) enables to establish high-quality long-distance entanglement in the communication time increasing only polynomially with transmission distance.

⁵² The bottleneck for long-distance quantum communication is the scaling of the error probability with the channel length. Thus, for quantum communication using optical fibers and single photons as a quantum channel, both the absorption losses and the depolarization errors scale exponentially with the channel length. After propagating a few channel attenuation lengths, the state of the photon or the photon itself will therefore be destroyed almost with certainty.

The following, among others, criteria (see also DiVincenzo, 2000) have to be met for a feasible implementation of long-distance quantum communication:

1. Faithful transmission of photonic qubits between sepecific locations.
2. Localized qubits as quantum memory with long coherence time at each communication node.
3. The ability to interconvert localized and photonic qubits.
4. The ability to perform local (collective) operations on n (≥ 1) qubits (with error rates not exceeding a few per cent for quantum repeater protocol).

Entanglement purification can ensure faithful transmission of entangled photons. As it is difficult to store photons for a reasonably long time, quantum memory for photons (see section VII.E.3) is crucial for ensuring polynomial scaling in the communication efficiency as all entanglement purification protocols must be probabilistic. There are several candidates for localized qubits. For instance, one may use atomic internal states to store local information. Then interconverting the atomic and photonic qubits requires the strong coupling between atoms and photons via high-finesse cavities, which, in spite of the recent significant experimental advances (Raimond *et al.*, 2001; Leibfried *et al.*, 2003), still remains an experimental challenge. In this aspect, atomic-ensemble based schemes (Duan *et al.*, 2001, 2002; Chen *et al.*, 2007; Jiang *et al.*, 2007; Zhao *et al.*, 2007) are very promising.

Below we shall present the original idea of quantum repeater and a few promising technologies to implement it.

1. Original theoretical proposal

In classical communication, the problem of exponential attenuation can be overcome by using repeaters at certain points in the channel, which amplify the signal and restore it to its original shape. In analogy to a fault-tolerant quantum computing (Nielsen and Chuang, 2000; Bouwmeester *et al.*, 2001; Preskill, 1999), the quantum repeater proposal is a cascaded entanglement purification protocol for communication systems. Thus, it is entanglement that is “amplified” by quantum repeater.

The quantum repeater protocol comprises three elements (Briegel *et al.*, 1998; Dür *et al.*, 1999):

1. A method for creation of entanglement between particles at distant nodes, which uses auxiliary particles at intermediate “connection points” and a *nested purification protocol*.
2. Entanglement purification with imperfect means.

3. A protocol for which the time needed for entanglement creation scales polynomially whereas the required material resources per connection point grow only logarithmically with the distance.

The nested purification protocol works as follows. First we divide the long channel into \mathcal{N} segments with connection points (i.e., auxiliary nodes) in between. We then create \mathcal{N} elementary EPR pairs of fidelity F_1 between the nodes A & C_1 , C_1 & C_2 , \dots , $C_{\mathcal{N}-1}$ & B . The number \mathcal{N} is chosen such that $F_{\min} < F_1 \leq F_{\max}$. For simplicity, assume that $\mathcal{N} = L^n$ for some integer n . On the first level, we simultaneously connect the pairs (initial fidelity F_1) at all the checkpoints except at $C_L, C_{2L}, \dots, C_{\mathcal{N}-L}$. As a result, we have \mathcal{N}/L pairs of length L and fidelity F_L between A & C_L , C_L & C_{2L} and so on. To purify these pairs, we need a certain number M of copies that we construct in parallel fashion. We then use these copies on the segments A & C_L , C_L & C_{2L} etc., to purify and obtain one pair of fidelity $\geq F_1$ on each segment. This last condition determines the (average) number of copies M that we need, which will depend on the initial fidelity, the degradation of the fidelity under connections, and the efficiency of the purification protocol. The total number of elementary pairs involved in constructing one of the more distant pairs of length L is LM . On the second level, we connect L of these more distant pairs at every checkpoint C_{kL} ($k = 1, 2, \dots$) except at $C_{L^2}, C_{2L^2}, \dots, C_{\mathcal{N}-L^2}$. As a result, we have \mathcal{N}/L^2 pairs of length L^2 between A & C_{L^2} , C_{L^2} & C_{2L^2} , and so on of fidelity $\geq F_L$. Again, we need M parallel copies of these long pairs to repurify up to the fidelity $\geq F_1$. The total number of elementary pairs involved in constructing one pair of length L^2 is thus $(LM)^2$. We iterate the procedure to higher and higher levels, until we reach the n th level. As a result, we have obtained a final pair between A & B of length \mathcal{N} and fidelity $\geq F_1$. In this way, the total number R of elementary pairs will be $(LM)^n$, namely,

$$R = \mathcal{N}^{\log_L M + 1}. \quad (106)$$

Thus, the resources grow polynomially with the distance N .

Obviously, there are error mechanisms in the quantum repeater protocol: decoherence induced by the environment, imperfect operations and measurements, and decrease of fidelity in entanglement swapping due to non-ideal entanglement. Choosing a generic error model for imperfect operations and measurements, one can estimate the maximum attainable fidelity F_{\max} and the minimum required fidelity F_{\min} . Region for error parameters where purification is possible are of the order of some percent, implying that the scheme tolerates general errors on the percent level. Remarkably, the temporal resources to implement the quantum repeater protocol are also polynomially growing with the number of segments N and thus with the distance.

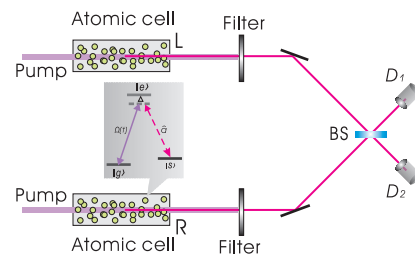


FIG. 32 Schematic setup for generating entanglement between the two atomic ensembles L and R in the DLCZ scheme (Duan *et al.*, 2001). The inset shows the relevant level structure of the atoms in the ensemble with $|g\rangle$, the ground state, $|s\rangle$, the metastable state for storing a qubit, and $|e\rangle$, the excited state. The transition $|g\rangle \rightarrow |e\rangle$ is coupled by the classical laser with the Rabi frequency Ω , and the forward scattering Stokes light comes from the transition $|e\rangle \rightarrow |s\rangle$. For convenience, off-resonant coupling with a large detuning Δ is assumed.

2. Implementation with atomic ensembles and linear optics

In the following we shall briefly review physical realizations⁵³ of quantum repeater based on atomic ensembles (as localized memory qubits) and linear optics (manipulating flying photonic qubits).

Duan, Lukin, Cirac and Zoller (DLCZ, 2001, 2002) proposed a promising implementation of quantum repeater by using atomic ensembles as local memory qubits, which have collectively enhanced coupling to light even without the aid of high-finesse cavities. This elegant scheme was believed to incorporate entanglement swapping, built-in entanglement purification and quantum memory together into a single unit.

Figure 32 is a schematic setup for entangling the two atomic ensembles (optically-thick atomic cell of N_a identical atoms) L and R which are spatially separated within the channel attenuation length. A pair of metastable lower states $|g\rangle$ and $|s\rangle$ can correspond to hyperfine or Zeeman sublevels of electronic ground state of alkali atoms. Long lifetimes for relevant coherence have been observed both in a room-temperature dilute atomic gas (Phillips *et al.*, 2001) and in a sample of cold trapped atoms (Liu *et al.*, 2001).

All the atoms are initially prepared in the ground state $|g\rangle$. A sample is illuminated by a short, off-resonant laser pulse that induces Raman transitions into the states $|s\rangle$. We are particularly interested in the forward-scattered Stokes light (the signal mode \hat{a}) which are uniquely correlated with the excitation of the symmetric collective atomic mode $\hat{S} \equiv (1/\sqrt{N_a}) \sum_i |g\rangle_i \langle s|$, where the sum-

⁵³ Other physical implementations include the quantum repeater based on solid-state photon emitters (Childress *et al.*, 2005, 2006) and a hybrid quantum repeater using bright coherent light and electronic- and nuclear-spins (van Loock *et al.*, 2006).

mation is taken over all the atoms. The light-atom interaction generates, after the interaction time t_Δ , a two-mode (\hat{a} and \hat{S}) squeezed state of the with the squeezing parameter r_c proportional t_Δ . If t_Δ is very small, the two-mode squeezed state can be written in the perturbative form

$$|\zeta\rangle = |0_a\rangle|0_p\rangle + \sqrt{p_c}\hat{S}^\dagger\hat{a}^\dagger|0_a\rangle|0_p\rangle + O(p_c), \quad (107)$$

where $p_c = \tanh^2 r_c \ll 1$ is the small excitation probability and $O(p_c)$ represents the terms with more excitations whose probabilities are equal or smaller than p_c^2 ; $|0_a\rangle$ and $|0_p\rangle$ are, respectively, the atomic and optical vacuum states with $|0_a\rangle \equiv \bigotimes_i |g\rangle_i$. For large N_a , the collectively enhanced signal-to-noise ratio may greatly enhances the efficiency of the scheme.

Now we show how to use this setup to generate entanglement between two distant ensembles L and R using the configuration shown in Fig. 32. Here, two laser pulses excited both ensembles simultaneously, and the whole system is described by the state $|\zeta\rangle_L \otimes |\zeta\rangle_R$, where $|\zeta\rangle_L$ and $|\zeta\rangle_R$ are given by Eq. (107) with all the operators and states distinguished by the subscript L or R. The forward scattered Stokes signal from both ensembles is combined at the BS and a photodetector click in either D1 or D2 measures the combined radiation from two samples, $\hat{a}_+^\dagger\hat{a}_+$ or $\hat{a}_-^\dagger\hat{a}_-$ with $\hat{a}_\pm = (\hat{a}_L \pm e^{i\varphi}\hat{a}_R)/\sqrt{2}$. Here, φ denotes an unknown difference of the phase shifts in the two-side channels. Conditional on the detector click, we should apply \hat{a}_+ or \hat{a}_- to the whole state $|\zeta\rangle_L \otimes |\zeta\rangle_R$, and the projected state of the ensembles L and R is nearly maximally entangled with the form [neglecting $O(p_c)$ terms]

$$|\Psi_\varphi\rangle_{LR}^\pm = \left(\hat{S}_L^\dagger \pm e^{i\varphi}\hat{S}_R^\dagger\right)/\sqrt{2}|0_a\rangle_L|0_a\rangle_R. \quad (108)$$

The probability for getting a click is given by p_c for each round, so we need repeat the process about $1/p_c$ times for a successful entanglement preparation, and the average preparation time is given by $T_0 \sim t_\Delta/p_c$.

The entanglement generation (as well as entanglement connection) in the DLCZ scheme is based on single-photon interference at photodetectors,⁵⁴ which was first proposed to entangle single atoms (Cabrillo *et al.*, 1999; Bose *et al.*, 1999). However, to have stable single-photon interference, a long-distance interferometric stability has to be kept; otherwise, the fluctuations of the relative phase φ caused by the environment would wash out the coherence (i.e., entanglement) in Eq. (108). For instance, to maintain path length phase stabilities at the level of $\lambda/10$ (λ : wavelength) for single photons, typically of

$\lambda \sim 1 \mu\text{m}$, generated from atomic ensembles (Eisaman *et al.*, 2005) requires the fine control of timing jitter at a sub-femtosecond level, which is almost an experimentally forbidden task (Holman *et al.*, 2005). For more detailed analysis on phase-stability problem of the DLCZ scheme, we refer to (Chen *et al.*, 2007).

The above phase-stability problem could be overcome by interfering two photons, one coming from each remote ion or atom in cavity (Bose *et al.*, 1999; Browne *et al.*, 2003; Feng *et al.*, 2003; Simon and Irvine, 2003). However, this improved robust entanglement creation requires difficult techniques and are unscalable to many communication nodes. A robust implementation of quantum repeater using several atomic-ensemble-based technology and linear optics does exist (Chen *et al.*, 2007; Jiang *et al.*, 2007; Zhao *et al.*, 2007) and eliminates the stringent requirement of long-distance phase stabilization with help of two-photon interference.

Though the DLCZ scheme does not fulfil the criteria for long-distance quantum communication, it does provide a promising mechanism for a fully controllable single-photon source based on atomic ensembles, which seems to be much easier for experimental demonstrations. The idea is easy to understand as following. The atomic ensemble generates a correlated state in Eq. (107), which is an exact analogy of SPDC. By measuring the forward signal mode with a single-photon detector, and conditional on a detector click, the collective atomic mode is projected to a single-excitation state. Such excitations can be stored for a reasonably long time in the ground-state manifold of the atoms. On demand the single-atomic excitation can be transferred to a single photon at any desired time (still within the storage time) with the method described in the next section with fully controllable properties: the emitted single-photon pulse is directed to the forward direction; the emission time is controllable by the repumping time; and the pulse shape is controllable by varying the time dependence of the Rabi frequency of the repumping pulse.

So far, significant advance has been achieved along this line. Controllable generation, storage and retrieval of single photons with tunable frequency, timing and bandwidth have been demonstrated (Chou *et al.*, 2004; Eisaman *et al.*, 2004, 2005; Chanelière *et al.*, 2005). Furthermore, a deterministic single-photon source was demonstrated using measurement-based feedback protocol (Matsukevich *et al.*, 2006b; Laurat *et al.*, 2006; Chen *et al.*, 2006b). We anticipate that these exciting research efforts will develop technology useful for those atomic ensemble based quantum information schemes.

3. Quantum state transfer between matter and photons: quantum memory

Both for long-distance quantum communication and large-scale optical quantum computing (see section VIII), the technique of quantum state transfer between mat-

⁵⁴ Another attractive protocol due to Childress *et al.* (2005, 2006) also uses single-photon interference at photodetectors and thus suffers from the phase-stability problem. Moreover, local collective operations such as active error corrections are required, which are currently hard to do with high enough precision.

ter and photons is indispensable. Here the matter itself should have a long storage time. This makes atoms a strong candidate for localized photonic information carrier as the coherence of atomic internal states can be maintained for a quite long time with the current technology. The early proposal (Cirac *et al.*, 1997; van Enk, Cirac, and Zoller, 1997) along this line uses strong coupling of photons and single atoms in high-finesse cavities.

The basic idea of quantum light memory is to transfer a photonic state to the excitations in atomic internal states so that it can be stored, and after the storage of a programmable time, it should be possible to read out the excitations to photons without change of the quantum state. The experimentally challenging technology at the interface of photons and single atoms motivated search for alternative routes to matter-light quantum interfaces. Along this line, theoretical ideas on quantum light memory has been proposed (Kozhokin *et al.*, 2000; Lukin *et al.*, 2000; Fleischhauer and Lukin, 2000, 2002; Duan *et al.*, 2001; Duan, Cirac, and Zoller, 2002; Chen *et al.*, 2007), and the relevant experimental advances (Kash *et al.*, 1999; Phillips *et al.*, 2001; Liu *et al.*, 2001; Schori *et al.*, 2002; Julsgaard *et al.*, 2004; van der Wal *et al.*, 2003; Bajcsy *et al.*, 2003; Matsukevich and Kuzmich; 2004) are significant.

For the future applications in optical quantum networking, quantum light memory with reversible mapping between photonic and atomic states is highly desirable technology and was proposed by Fleischhauer, Lukin and coworkers (Lukin *et al.*, 2000; Fleischhauer and Lukin, 2000, 2002; Duan *et al.*, 2001; Duan, Cirac, and Zoller, 2002; Chen *et al.*, 2007). As this proposal enables storing light in a free-space atomic ensembles (i.e., without the aid of high-Q cavity), its experimental realization is relatively easy. Below we briefly give the basic idea of the atomic ensemble based quantum memory.

The atomic-ensemble-based quantum memory consists of a coherently driven atomic ensemble ($N \gg 1$ atoms) of large optical thickness with the level structure shown in the inset of Fig. 33. The $|c\rangle$ - $|e\rangle$ transition is coherently driven by a classical field of Rabi frequency $\Omega(t)$, and the $|b\rangle$ - $|e\rangle$ transition is coupled to a quantized single-mode (the multimode case is similar) light field (described by an annihilation operator \hat{a}) with a coupling constant g . Under the two-photon resonance (i.e., the two detunings for the two transitions shown in the inset of Fig. 33 are both equal to Δ), the classical driving field can induce transparency for the quantized light field and a substantial group-velocity reduction, even the complete stop of the light (for reviews, see Lukin and Imamoglu, 2001; Lukin, 2003; Fleischhauer *et al.*, 2005).

The Hamiltonian of the whole system (N atoms plus the quantized light field) reads in a frame rotating at the optical frequency $H = \hbar\Omega(t)\hat{S}_{ec} + \hbar g\sqrt{N}\hat{a}\hat{S}_{eb} + H.c.$, where $\hat{S}_{ec} = \sum_i^N |e\rangle_{ii}\langle c|$, $\hat{S}_{eb} = \frac{1}{\sqrt{N}} \sum_i^N |e\rangle_{ii}\langle b|$ and $H.c.$ means Hermitian conjugate. This Hamiltonian has particular zero-energy eigenstates, the so-called “dark states”. When the atom number is much larger than

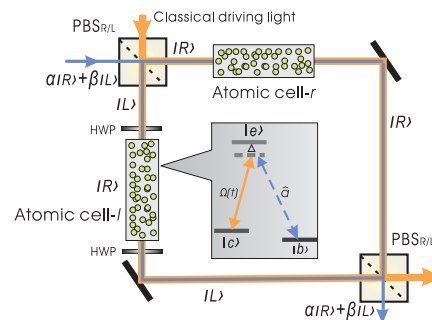


FIG. 33 Quantum memory for photonic polarization qubits. Two identical ensembles are identically driven by a classical field, which is equally right- and left-circularly polarized. Classical and quantized light fields are feed into the first PBS_{R/L} (“rotated” PBS which reflects left-circular photons and transmits right-circular photons) and will leave at two different outputs of the second PBS_{R/L}. Two half-wave plates (HWP) functioning as $|R\rangle \leftrightarrow |L\rangle$ are placed along the $|L\rangle$ -output of the first PBS_{R/L}. As the atomic cell- r (cell- l) works as quantum memory for single photons with right-circular (left-circular) polarization via the adiabatic transfer method, the whole setup is then quantum memory of any single-photon polarization states. The inset shows the relevant level structure of the atoms, with the ground state $|b\rangle$, the metastable state $|c\rangle$ for storage, and the excited state $|e\rangle$. (Chen *et al.*, 2007a)

the photon number, the dark states represent elementary excitations of bosonic quasiparticles, i.e., the dark-state polaritons. For more details on this concept, see (Lukin *et al.*, 2000; Fleischhauer and Lukin, 2000, 2002; Sun *et al.*, 2003).

By adiabatically changing $\Omega(t)$ between the two limiting cases ($\Omega(t) \ll g\sqrt{N}$, or $\Omega(t) \gg g\sqrt{N}$) one can coherently map dark-state polariton states onto either purely atom-like states where the photons are stored, or purely photon-like states which corresponds to the release of the stored photons. In principle, quantum memory based on this adiabatic transfer method is reversible, preserves pulse shape of the stored photons (Fleischhauer and Lukin, 2000; 2002) and may have efficiency very close to unity. The storage time can be very long as there is no excited atomic state in the dark-state subspace. The original quantum memory was proposed for storing a coherent superposition of photon-number states; two atomic ensembles can be entangled by storage of two entangled light fields (Lukin *et al.*, 2000). For many optical quantum information protocols, quantum information is carried by photons with polarization encoding. Quantum memory for photonic polarization qubits was proposed by Chen *et al.* (2007; see Fig. 33).

The atomic-ensemble-based quantum memory has an important application in realizing high-efficiency photon counting (James and Kwiat, 2002; Imamoglu, 2002). The idea is as follows. First, one maps the quantum state of a propagating light pulse onto metastable atomic collective excitations. Afterwards, the number of atoms in the

m -excitation atomic state is exactly equal to that of the number of incoming photons. By monitoring the resonance fluorescence induced by an additional laser field that couples only to the metastable excited state, the number of atoms in m -excitation atomic state can be measured with an efficiency exceeding 99% even with a photon collection/detection efficiency as low as 10%. The state-selective fluorescence technique used in the proposal is a method for quantum state measurement with efficiency approaching 100% developed for trapped ions (for a comprehensive review, see Leibfried *et al.*, 2003).

4. Quantum interference of independent photons

Interference of photons emerging from independent sources (Mandel, 1983; Paul, 1986) has no classical analogue and can be understood only by the interference of probability amplitudes of multi-particle detection events. The use of such independent sources might provide conceptual advantages for experiments on the foundations of quantum physics (Yurke and Stoler, 1992a, 1992b). Quantum interference of independent photons is also practically vital for modern quantum information processing ranging from quantum communication (in particular, quantum repeater) to linear-optical quantum computing (see section VIII). These quantum information schemes tacitly assume stable interference between two independently emitted photons. To fulfil this, it is important to assure that there exists no possibility whatsoever for the coherence properties of the light emitted by either source to be influenced by the other. Therefore, the operation of one source must not in any way rely on the working of the other source. Such a configuration addresses exactly the needs for practical quantum communication and computation schemes. In the case of long-distance quantum communication any common optical elements shared by the sources and thus any dependence would impede the working of the scheme over large distances due to dispersion or losses. A key point here is thus that “truly independent sources require the use of independent but synchronized fs laser[s]” (de Riedmatten *et al.*, 2003). Two recent experiments, one performed in Hefei (Yang *et al.*, 2006) and another in Vienna (Kaltenbaek *et al.*, 2006), successfully realized such technique using synchronized femto-second (fs) lasers.

Since the 1960s, interference of light from independent sources has been addressed in many experiments, see, e.g., (Javan *et al.*, 1962; Magyar and Mandel, 1963; Pfleegor and Mandel, 1967; Radloff, 1971). However, in these early experiments, the observed effects could “not readily be described in terms of one photon from one source interfering with one from the other” (Pfleegor and Mandel, 1967).

All following experiments involving the interference between single photons employed the well-known Hong-Ou-Mandel interference effect (section III.D), which utilizes the bosonic nature of photons: Two indistinguishable

photons that enter a 50:50 BS via different input ports will always be detected in one output port. Such two-photon interference was first reported (Hong *et al.*, 1987) for photon pairs emerging from an SPDC source. The first interference of separately generated photons was observed by Rarity *et al.* (1996) (see also Kuzmich *et al.*, 2000) by measuring the Hong-Ou-Mandel-type interference of an SPDC photon and an attenuated part of the very same laser beam pumping the SPDC process. Further related experiments provided gradual progress with respect to the independence of the utilized sources. A first step was the interference of two triggered single photons created via SPDC by the same pump pulse passing twice through the very same SPDC crystal in the Innsbruck teleportation experiment (Bouwmeester *et al.*, 1997). Further contributions used photons generated by two mutually coherent time-separated pulses from the same mode-locked laser in one SPDC crystal (Keller *et al.*, 1998) and, later, generated in one quantum dot (Santori *et al.*, 2002).

In realistic realization of quantum repeaters (Briegel *et al.*, 1998) one has to achieve entanglement swapping (see section VII.C) with synchronized entangled photon sources among all distributed segments. For the SPDC entanglement source, the UV laser pulses in each distributed segment must be synchronized. One natural solution is to split a single UV laser pulse into N beams and then distribute them to each segment (de Riedmatten *et al.*, 2003). However, such a naive solution is not a scalable scheme. This is because the maximal output power of a single laser is technically limited and the efficiency of the scheme will thus exponentially decrease with the number of segments.

A practical solution is to utilize synchronized pump lasers to prepare entangled pairs in each segment and then to connect these pairs via entanglement swapping. Yang *et al.* (2006) achieved such an entanglement swapping with independent entangled photon pairs that are created by two synchronized fs lasers.⁵⁵ The Hefei synchronization experiment implemented passive technique to synchronize two Ti:sapphire lasers by coupling both laser pulses in two intersecting laser cavities sharing the same Kerr medium (an additional Ti:sapphire crystal). The two lasers were synchronized with a timing jitter less than 2 fs and kept on synchronizing over 24 hours. The short pulse duration and little timing jitter are sufficient to ensure the perfect interference of two independent photons produced by synchronized laser pulses. In particular, Yang *et al.* demonstrated entanglement swapping with independent entangled photon pairs (pair 1-2 and 3-4, where photons 2 and 3 are subject to a Bell-state measurement, see Fig. 27), created from two synchro-

⁵⁵ Usually, fs laser uses either active synchronization with an electrical feedback device (Ma *et al.*, 2001), or passive synchronization by nonlinear coupling mechanism (De Barros and Becker, 1993).

nized but mutually incoherent fs lasers. The observed Bell inequality violation for the entangled pair 1-4 after entanglement swapping is $S_{\text{Bell}} = 2.308 \pm 0.095$ which violates the classical limit of 2 by 3.2 standard deviations, confirming the quantum nature of entanglement swapping.

In the Vienna synchronization experiment (Kaltenbaek *et al.*, 2006), each of the two separate sources consists of an SPDC crystal pumped optically by a pulsed fs laser and provides triggered single photons. To enable interference the two photons registered behind the BS cannot be distinguished in any way. For triggered single photons generated via SPDC, the initial sharp time correlation of SPDC photon pairs poses a problem without frequency filtering: the times of registration of the trigger photons provide temporal distinguishability of the photon registrations behind the BS. Short pump pulses and spectral filters narrower than the bandwidth of these pulses in the paths of the photons give the desired indistinguishability (Żukowski *et al.*, 1995).

Additional timing information is contained in the time difference between the independent pulses pumping the two SPDC crystals. In principle, one could compensate this again by filtering. For pulses without any time correlation this would, however, require extremely narrow filters and eventually result in prohibitively low count rates. Synchronizing the pulses of the two independent pumps increases the probability of joint emission events and hence the count rates. The fact that one needs to actively synchronize the sources is a direct unavoidable consequence of their independence. The active synchronization method implemented in Vienna involves only electronic communication (10 kHz bandwidth) about the relative pulse timing between the independently running femtosecond lasers. No optical elements whatsoever are shared by the pumps. The laser pulses were synchronized via electronic feedback loops up to a relative timing jitter of 260 ± 30 fs using the commercially available SynchrolockTM system from Coherent Inc.

F. Free-space entanglement distribution

Optical fibre and free-space links have proven potential for low-loss distribution of photons over long distances. Entangled photons have been distributed in optical fibre for long-distance fundamental tests or quantum cryptographic applications (Gisin *et al.*, 2002); the longest distance up to 50 km has been achieved so far (Marcikic *et al.*, 2004). While the experimental progress in this area has been rapid, theoretical studies have shown that Earth-bound fibre and free-space quantum communication based on current technology cannot surpass on the order of 100 km (Waks *et al.*, 2002).

Another promising way to realize long-distance quantum communication is to exploit satellite-based free-space distribution of single photons or entangled photon pairs (Aspelmeyer *et al.*, 2003b). In the scheme, the

photonic quantum states are first sent through the atmosphere, then reflected from one satellite to another and finally sent back to the Earth. Since the effective thickness of the atmosphere is on the order of 5-10 km (i.e., the whole atmosphere is equivalent to 5-10 km ground atmosphere) and in the outer space the photon loss and decoherence is negligible, with the help of satellites one can achieve global free-space quantum communication as long as the quantum states can still survive after penetrating the atmosphere.

Along this line, important experimental progress has been made very recently in the free-space distribution of attenuated laser pulses (over 23.4 km, see Kurtsiefer *et al.*, 2002) and entangled photon pairs (over 600 m, see Aspelmeyer *et al.*, 2003a). However, on the one hand, quantum cryptography experiments with attenuated laser pulses suffer from an eavesdropping loophole known as the beamsplitter attack (Gisin *et al.*, 2002). In this respect, entanglement-based schemes are preferable. On the other hand, while the achieved distance in the previous entanglement distribution experiment (Aspelmeyer *et al.*, 2003a) is only on the order of 600 m which is far below the effective thickness of the atmosphere, the achieved low transmission efficiency ($\sim 10^{-3}$) would not enable a sufficient link efficiency over large distances, which is, however, required for satellite-based free-space quantum communication (Aspelmeyer *et al.*, 2003b). Thanks to two recent free-space entanglement distribution experiments (Fig. 34) performed separately in Vienna (Resch *et al.*, 2005) and in Hefei (Peng *et al.*, 2005), the difficulties encountered in satellite-based free-space quantum communication can in principle be overcome.

In the Vienna experiment, polarization-entangled photons are distributed using a free-space optical link over a distance of 7.8 km through the heart of Vienna: the source of entangled photons is placed inside a 19th-century observatory, Kuffner Sternwarte (Alice), and a receiving station is 7.8 km away on the 46th floor of a modern skyscraper, Millennium Tower (Bob). Detection of one photon (by Alice) from the entangled pairs constitutes a triggered single photon source for Bob, hence only the triggered single photons were sent through the free-space link. With no direct time-stable connection, the two stations found coincidence counts in the detection events by calculating the cross-correlation of locally-recorded time stamps shared over a public internet channel. For this experiment, the quantum channel was maintained for a total of 40 minutes during which time a coincidence lock found approximately 60000 coincident detection events. The polarization correlations in those events yielded a Bell parameter $S_{\text{Bell}} = 2.27 \pm 0.019$, which violates the CHSH inequality by 14 standard deviations.

In the Hefei experiment, the source of entangled photons (as well as the Sender) is located on the top of Dashu Mountain in Hefei of China, with an elevation of 281 m, and two receivers (Alice and Bob) are located at the western campus of USTC and at Feixi of Hefei, respectively. The direct distance between the two receivers is

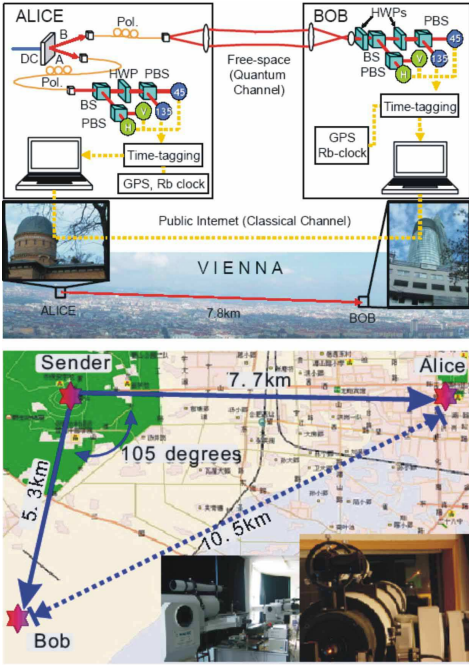


FIG. 34 The layouts for free-space entanglement distribution experiments performed in Vienna (upper panel; Resch *et al.*, 2005) and in Hefei (lower panel; Peng *et al.*, 2005).

about 10.5 km. The distances from the Sender to Alice and from the Sender to Bob are 7.7 km and 5.3 km, respectively. One of the two entangled photons passes through nearly half part of Hefei city, experiencing an extremely challenging environment above the city. The two receivers are not in sight with each other due to the existence of many buildings between them. In the Bell experiment under the space-like separation condition, $S_{\text{Bell}} = 2.45 \pm 0.09$ was measured, which is a violation of the Bell-CHSH inequality by 5 standard deviations. This result firmly confirms that the entanglement can still survive after the two entangled photons have passed through the noisy ground atmosphere with a distance beyond the effective thickness of the aerosphere. Peng *et al.* also performed a cryptography experiment, with 2435 bits of final secure key obtained within 4 minutes. This corresponds an average key distribution rate of 10 bit/second. Note that, using a high-intensity entangled photon source (Kurtsiefer *et al.*, 2001), one can easily increase the average key distribution rate to a few hundreds per second. The link efficiency of entangled photon pairs achieved in the Hefei experiment is about a few percent, which is well beyond the threshold required for satellite-based free-space quantum communication.

VIII. QUANTUM COMPUTING

A quantum computation can be considered as a physical process that transforms an input quantum state into

an output state and as such, it respects quantum laws. The “information flow” in quantum computing process is carried by qubits (of course, quantum computing with quNits or continuous quantum variables should in principle possible) which are subject to a designed unitary evolution. Due to the superposition principle, quantum computing is featured by Feynman’s quantum parallelism. The fact that qubits can be in coherent superposition and entangled states gives the extraordinary power to a quantum computer to outperform its classical counterpart. For more aspects on quantum computation, we refer to the textbooks by Nielson and Chuang (2000), by Bouwmeester *et al.* (2001) and by Preskill (1999).

Mathematically, a quantum computer consisting of N qubits can be regarded as a quantum devices realizing a unitary transformation \hat{U} which maps the initial states of the N qubits to a final state to be read out. To perform general transformations relies on the ability to engineer arbitrary interactions between the qubits. Fortunately, this task can be greatly simplified by the following powerful theorem for universal quantum computation (Barenco *et al.*, 1995a 1995b; Lloyd, 1995):

- Any unitary transformation of an N -qubit system can be implemented with single-qubit operations and quantum controlled-NOT (CNOT) gates or equivalent two-qubit gates.

These gates are known as *universal quantum logic gates*,⁵⁶ each of which is an elementary device performing a fixed unitary operation on selected qubits in a fixed period of time. Given the ability to perform the gates belonging to the set of universal quantum logic gates, we will be able to perform any computation (unitary operations on the quantum register) by simply applying them in a specified sequence. The central problem of quantum computing is then to design these computational sequences (quantum algorithms) depending on specific tasks and to implement them with specific quantum systems.

A. Criteria for optical quantum computing

The physical implementations of quantum computation preferably use localized systems like atoms in high-finesse cavities (Raimond *et al.*, 2001), ions (Schmidt-Kaler *et al.*, 2003; Leibfried *et al.*, 2003) or solid-state de-

⁵⁶ Two examples of universal sets of gates are $\{\hat{U}_{\text{CNOT}}^{(2)}, \hat{U}_z^{(1)}(\varphi), \hat{U}_x^{(1)}(\pi/4)\}$ and $\{\hat{U}_\pi^{(2)}, \hat{U}_z^{(1)}(\pi/4), \hat{U}_x^{(1)}(\varphi)\}$. Here $\hat{U}_{\text{CNOT}}^{(2)} = |H\rangle\langle H| \otimes \hat{I} + |V\rangle\langle V| \otimes \hat{x}$ is the CNOT gate; $\hat{U}_{\text{CPhase}}^{(2)} = |H\rangle\langle H| \otimes \hat{I} + |V\rangle\langle V| \otimes \hat{z}$ is the controlled-phase (CPhase) gate; two single-qubit gates are $\hat{U}_z^{(1)}(\varphi) = e^{-i\varphi\hat{z}}$ ($|H\rangle \rightarrow e^{i\varphi/2}|H\rangle$ and $|V\rangle \rightarrow e^{-i\varphi/2}|V\rangle$); $\hat{U}_x^{(1)}(\theta) = e^{-i\theta\hat{x}}$ ($|H\rangle \rightarrow \cos\theta|H\rangle - i\sin\theta|V\rangle$ and $|V\rangle \rightarrow -i\sin\theta|H\rangle + \cos\theta|V\rangle$); $\varphi \in [0, 2\pi)$.

vices (Loss and DiVincenzo, 1998; Makhlin *et al.*, 2001), for which significant progress has been made. However, the main focus of this section will be quantum computing (the usual circuit model based on quantum logic gates, or measurement-based model based on cluster states) with photons, a surprising possibility discovered by Knill, Laflamme, and Milburn (2001). This breakthrough, together with many subsequent theoretical and experimental advance, opens up an exciting future of manipulating multi-photon states with profound applications.

Before presenting these specific advances, let us give a set of *criteria for quantum computing with photons* while keeping in mind the DiVincenzo criteria (DiVincenzo, 2000):

1. *Encoding qubits with the degree of freedom that is easy to implement high-precision single-qubit operations and robust against various noises.*
2. *Nontrivial two-qubit gates (CNOT, Controlled-phase,...); for one-way quantum computing, the ability to prepare a sufficiently large cluster state.*
3. *Ideal single-photon detection (if not, the scheme should be photon-loss tolerant).*
4. *Quantum memory being able to store single photons for a reasonably long time and to read them out on demand.* This requirement simply stems from the fact that photons fly at the speed of light! Moreover, it is also crucial for the scalability as two-qubit gates for photons cannot be implemented with unit probability.

B. Linear-optical two-qubit logic gates

Photons are natively robust against decoherence and easy to do single-qubit operations. However, because it is very difficult to achieve the necessary logic operations between two individual photonic qubits and to store them for a reasonably long time, the application of photon states has thus been limited primarily in the field of quantum communication. Surprisingly, Knill, Laflamme and Milburn (2001), using the dual-rail encoding [for polarization encoding, see (Spedalieri *et al.*, 2006)], has shown that nondeterministic two-qubit logic operations can be performed using linear optical elements, additional photons (ancilla) and postselection based on the output of single-photon detectors. They further demonstrated that the success rate of the logic gates can be arbitrarily close to one by using more additional ancilla and detectors. This implies that the nondeterministic two-qubit logic gate based on linear optics can be used as a basic block for quantum information protocols, even for efficient quantum computation. A novel aspect of linear-optical quantum computing is that, despite the lack of the photon-photon interaction, quantum measurements may induce effective nonlinearity sufficient for realization of two-qubit gates. The original Knill-Laflamme-Milburn

scheme is, however, not economical in resources. Various groups have been working on reducing the complexity of the scheme while improving its theoretical efficiency (Koashi *et al.*, 2001; Pittman *et al.*, 2001; Ralph *et al.*, 2002a, 2002b). To be a supplement to the nice review on linear-optical quantum computing by Kok *et al.* (2007), we have to leave the detailed survey of many beautiful relevant developments, both on the theoretical and the experimental sides. For more details, we refer to that review.

So far, various quantum computation primitives have been demonstrated with photons alone—including conditional phase shift operations (Sanaka *et al.*, 2004), and destructive (Pittman *et al.*, 2002, 2003; O’Brien *et al.*, 2003) and even non-destructive CNOT gates (Gasparoni *et al.*, 2004; Zhao *et al.*, 2005b). All these schemes use unentangled states as inputs on which the quantum gates operate.

For scalable optical quantum computing, a crucial requirement is the *classical feed-forwardability* (Scheel *et al.*, 2006). Specifically, it must be in principle possible to detect when the gate has succeeded by measurement of ancilla photons in some appropriate states. This information can then be feed-forward in such a way as to condition future operations on the photon modes. For those destructive CNOT operations, they necessarily destroy the output states such that schemes based on them are not classically feed-forwardable. Fortunately, it has been suggested (Pittman *et al.*, 2001) that a destructive CNOT gate together with the quantum parity check can be combined with a pair of entangled photons to implement a nondestructive (conventional) CNOT gate that satisfies the feed-forwardability criterion. Moreover, when combined with single-qubit Hadamard rotations to perform a controlled-sign gate [so as to build the cluster states via Nielsen’s method (Nielsen, 2004)] this gate also satisfies the criterion that when it fails the qubits can be projected out in the computational basis. In this section, we present, for pedagogical purposes, the working principle and a proof-of-principle demonstration (Zhao *et al.*, 2005b) of a nondestructive CNOT gate for two independent photons.

To see the working principle of the scheme shown in Fig. 35(a), suppose that one aims to act a CNOT gate on an arbitrary two-qubit state $|\chi\rangle_{25}$ [see Eq. (98)] by using an ancilla entangled photon pair in the Bell state $|\psi^-\rangle_{34}$. Note that PBS₂ in Fig. 35(a) transmits $|H'\rangle$ while reflects $|V'\rangle$ polarization. The output state of the whole apparatus is (Pittman *et al.*, 2001)

$$\begin{aligned}
|\chi\rangle_{25} |\psi^-\rangle_{34} \rightarrow & \frac{1}{4} [|V'\rangle_{3'} |V\rangle_{4'} (\text{CNOT}_{2'5'} |\chi\rangle_{2'5'}) \\
& + |H'\rangle_{3'} |V\rangle_{4'} (\hat{z}_{5'} \text{CNOT}_{2'5'} |\chi\rangle_{2'5'}) \\
& + |H'\rangle_{3'} |H\rangle_{4'} (\hat{x}_{5'} \hat{z}_{5'} \text{CNOT}_{2'5'} |\chi\rangle_{2'5'}) \\
& + |V'\rangle_{3'} |H\rangle_{4'} (\hat{x}_{5'} \text{CNOT}_{2'5'} |\chi\rangle_{2'5'})] \\
& + \frac{\sqrt{3}}{2} |\dots\rangle_{\text{not four mode case}} \cdot \quad (109)
\end{aligned}$$

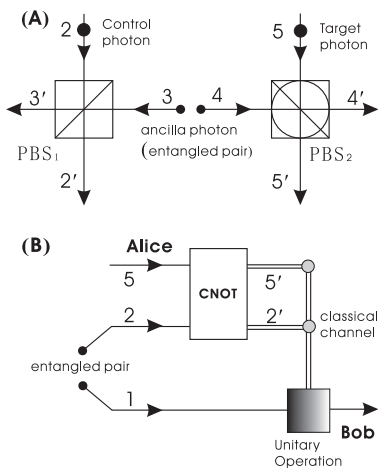


FIG. 35 (A) A nondestructive CNOT gate constructed by PBS, half-wave plates (HWP) and an ancilla entangled photon pair $|\psi^-\rangle_{34}$ (Pittman *et al.*, 2001). (B) Quantum circuit for quantum teleportation based on a CNOT gate. By using the CNOT operation, Alice can discriminate the four orthogonal Bell state simultaneously such that a complete teleportation can be achieved. (Zhao *et al.*, 2005b)

It is ready to see that, conditioned on the detections of one and only one photon (the four-mode case) in certain polarization at the output modes $3'$ and $4'$ (occurring with the probability of $1/4$), a (nondestructive) CNOT gate will be successfully acted on $|\chi\rangle_{2'5'}$, up to a local unitary transformation, without having to destroying the output photons $2'$ and $5'$.

One immediate application of the proposed CNOT gate is that it can be used to generate, though probabilistically, entanglement between the control qubit and target qubit (see section IV.B). Another important application is that the nondestructive CNOT gate can be used to simultaneously identify all the four Bell states (section V.F.1), which is essential for achieving a complete quantum teleportation. A quantum circuit for this purpose is shown in Fig. 35(b), where Alice wants to teleport to Bob an unknown polarization state $|\chi\rangle_5 = \alpha|H\rangle_5 + \beta|V\rangle_5$ of photon 5, with an entangled pair of the photons 1 and 2 shared by Alice and Bob in the Bell state $|\psi^-\rangle_{12}$. The crucial Bell-state measurement can be accomplished probabilistically by applying a nondestructive CNOT operation and performing a subsequent polarization analysis on photons 2 and 5.

As explained above, to demonstrate the proposed nondestructive CNOT gate one has to prepare one ancilla entangled pair and two independent single photons⁵⁷. The experimental setup on entanglement purification (Pan *et*

al., 2003b; section VII.D.3) could be, in principle, modified to implement this probabilistic CNOT gate, the creation of two entangled photon pairs into the same pair of modes would, however, contribute spurious four-fold events of the same order of magnitude, hence leading to a very low visibility. Experimentally, Zhao *et al.* (2005b) overcame this drawback and performed a five-photon experiment (Zhao *et al.*, 2004) to demonstrate both the nondestructive CNOT gate and quantum teleportation with complete Bell-state analysis (see also Walther and Zeilinger, 2005).

C. One-way quantum computing with photons

Another significant step is the discovery of “one-way quantum computing” (Raussendorf and Briegel, 2001; Raussendorf *et al.*, 2003), which is based on the preparation of highly entangled multi-qubit states, the so-called “cluster states” (Briegel and Raussendorf, 2001) and on simple adaptive one-qubit measurements. In the following, we will summarize the basic ideas underlying one-way quantum computing (for other development, see Aïferis and Leung, 2004; Childs *et al.*, 2005), its optical implementation and the experimental demonstration.

1. Cluster states and one-way quantum computing: general ideas

In the one-way quantum computing model, the so-called cluster state is the central physical resource. The entire quantum computation consists only of a sequence one-qubit projective measurements in a particular pattern of measurement eigenbases and in a particular order on this entangled state. We call this scheme the “one-way quantum computer” since the entanglement in the cluster state is destroyed by the one-qubit measurements and therefore it can only be used once. While it is possible to simulate any unitary evolution with the one-way quantum computer (i.e., the one-way quantum computer is universal), the computational model of the one-way quantum computer makes no reference to the concept of unitary evolution. A quantum computation corresponds, instead, to a sequence of simple projections in the Hilbert space of the cluster state; different algorithms require only a different pattern of adapted single-qubit operations on a sufficiently large cluster state. The information that is processed is extracted from the measurement outcomes and is thus a purely classical quantity.

As can be seen from the computational model underlying the one-way quantum computer (Raussendorf and Briegel, 2002; Raussendorf *et al.*, 2003) shown in Fig. 36, the one-way quantum computer is dramatically different from the standard one based on sequences of unitary quantum logic gates that process qubits. The very possibility of one-way quantum computing might well change our understanding of the requirements for quantum com-

⁵⁷ Recently, Bao *et al.* (2007) experimentally demonstrated a novel optical nondestructive CNOT gate without using entangled ancilla, but four single photons instead.

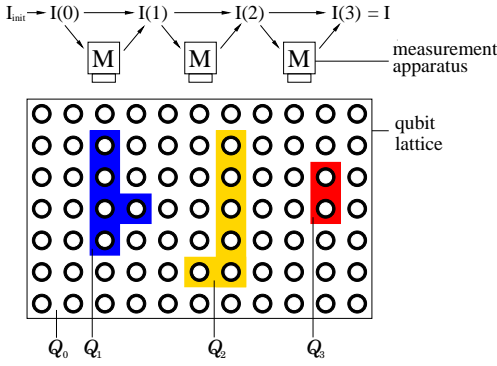


FIG. 36 General scheme of the one-way quantum computer (Raussendorf and Briegel, 2002; Raussendorf *et al.*, 2003). The sets Q_t of lattice qubits are measured one after the other. The results of earlier measurements determine the measurement bases of later ones. All classical information from the measurement results needed to steer the computer is contained in the information flow vector $\mathbf{I}(t)$. After the last measurement round t_{\max} , $\mathbf{I}(t_{\max})$ contains the result of the computation.

putation and more generally how we think about quantum physics.

As a universal quantum computing resource, cluster states are special multi-qubit entangled states located on a cluster \mathcal{C} . This cluster is a connected subset of a simple cubic lattice \mathbb{Z}^d in $d \geq 1$ dimensions. The cluster states $|\phi_{\{\kappa\}}\rangle_{\mathcal{C}}$ are characterized by the set of eigenequations

$$K^{(a)} |\phi_{\{\kappa\}}\rangle_{\mathcal{C}} = (-1)^{\kappa_a} |\phi_{\{\kappa\}}\rangle_{\mathcal{C}}, \quad (110)$$

with the correlation operators

$$K^{(a)} = \sigma_x^{(a)} \bigotimes_{b \in nb(a)} \sigma_z^{(b)}. \quad (111)$$

Therein, $\{\kappa_a \in \{0,1\} | a \in \mathcal{C}\}$ is a set of binary parameters which specify the cluster state and $nb(a)$ is the set of all neighboring lattice sites of a . All states $|\phi_{\{\kappa\}}\rangle_{\mathcal{C}}$ are equally good for computation. A cluster state is completely specified by the eigenvalue equations (110). From the set of states which obey (110) with the eigenvalues specified by $\{\kappa\}$ a representative $|\phi_{\{\kappa\}}\rangle_{\mathcal{C}}$ is taken. There are $2^{|\mathcal{C}|}$ such classes of states, and hence $2^{|\mathcal{C}|}$ mutually orthogonal representatives $|\phi_{\{\kappa\}}\rangle_{\mathcal{C}}$. Therefore, the representative cluster states form a basis $\{|\phi_{\{\kappa\}}\rangle_{\mathcal{C}} | \{\kappa\} \in \{0,1\}^{|\mathcal{C}|}\}$ of the $|\mathcal{C}|$ -qubit Hilbert space. Particularly, two states $|\phi_{\{\kappa\}_0}^{(a)}\rangle_{\mathcal{C}}$ and $|\phi_{\{\kappa\}_0}^{(b)}\rangle_{\mathcal{C}}$ obeying (110) with the same set $\{\kappa\}_0$ are the same modulo a possible global phase. Consequently, any method that creates a state obeying Eq. (110) with a specific set $\{\kappa_a | a \in \mathcal{C}\}$ creates the same state. The state $|\phi\rangle_{\mathcal{C}_2}$ is local unitary equivalent to a Bell state and $|\phi\rangle_{\mathcal{C}_3}$ to the GHZ state. $|\phi\rangle_{\mathcal{C}_4}$ is not equivalent to a 4-particle GHZ state. In particular, the entanglement in $|\phi\rangle_{\mathcal{C}_4}$ cannot be destroyed by a single local operation (Briegel and

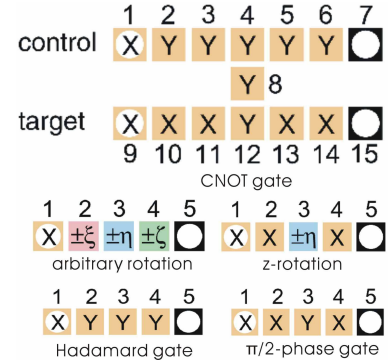


FIG. 37 Realization of elementary quantum gates (CNOT gate between neighbouring qubits, the arbitrary rotation specified by three Euler angles ξ , η , and ζ ; the \hat{z} -rotation; the Hadamard gate; and the $\pi/2$ -phase gate) on an one-way quantum computer (Raussendorf and Briegel, 2001; Raussendorf *et al.*, 2003). Each square represents a lattice qubit. The squares in the extreme left column marked with white circles denote the input qubits, those in the right-most column denote the output qubits.

Raussendorf, 2001). Note that cluster states are a subset of the so-called graph states (Hein *et al.*, 2004; for a comprehensive survey, see Hein *et al.*, 2006).

The eigenequations (110) and the quantum correlations they imply are central for the described scheme of computation. Briefly speaking, a cluster state on a two-dimensional cluster of rectangular shape, say, is a resource that allows for any computation that fits on the cluster. Actually, the CNOT gate and general one-qubit rotations, which form a set of universal quantum logic gates, can all be implemented via one-qubit measurements on a cluster state, see Fig. 37 [For details on how this follows, we refer to (Raussendorf and Briegel, 2001; Raussendorf *et al.*, 2003)].

Ways to create a cluster state in principle are to measure all the correlation operators $K^{(a)}$ ($a \in \mathcal{C}$) of (111) on an arbitrary $|\mathcal{C}|$ -qubit state or to cool into the ground state of a Hamiltonian $H_K = -\hbar g \sum_{a \in \mathcal{C}} \kappa_a K^{(a)}$. Another way that is more suitable for practical realization is as follows. First, a product state $|+\rangle_{\mathcal{C}} = \bigotimes_{a \in \mathcal{C}} |+\rangle_a$ is prepared and then subject to a unitary transformation

$$\hat{S}^{(\mathcal{C})} = \prod_{a,b \in \mathcal{C} | b-a \in \gamma_d} \hat{S}^{ab}. \quad (112)$$

In (112), for the cases of dimension $d = 1, 2, 3$, we have, respectively, $\gamma_1 = \{1\}$, $\gamma_2 = \{(1,0)^T, (0,1)^T\}$ and $\gamma_3 = \{(1,0,0)^T, (0,1,0)^T, (0,0,1)^T\}$, and the two-qubit transformation $\hat{S}^{ab} = \frac{1}{2}(\hat{\mathbf{1}} + \hat{z}^{(a)} + \hat{z}^{(b)} - \hat{z}^{(a)} \otimes \hat{z}^{(b)})$ is a CPhase gate [also known as the controlled- \hat{z} (CZ) gate or CSign]. As $[\hat{S}^{(\mathcal{C})}] \sigma_x^{(a)} [\hat{S}^{(\mathcal{C})}]^\dagger = \sigma_x^{(a)} \bigotimes_{b \in nb(a)} \sigma_z^{(b)}$, it is easy to verify that the state $|\phi\rangle_{\mathcal{C}} = \hat{S}^{(\mathcal{C})} |+\rangle_{\mathcal{C}}$ generated via S is a cluster state $|\phi_{\{\kappa\}}\rangle_{\mathcal{C}}$ with $\kappa_a = 0$ ($\forall a \in \mathcal{C}$). The specific preparation procedure allows a nice intuitive

graphical representation of cluster states (see Fig. 39 below). To prepare cluster states specified by different sets $\{\kappa_a\}$, one simply applies phase-flip operators $\hat{z}^{(a)}$. Note that all operations \hat{S}^{ab} in $\hat{S}^{(C)}$ mutually commute and can therefore be carried out simultaneously. Initial individual preparation of the cluster qubits in $|+\rangle_{a \in C}$ can also be done in parallel. Thus, the creation of the cluster state is a two step process. The temporal resources to create the cluster state are constant in the size of the cluster.

Cluster states can be created by controllable Ising-type interaction as described above (Briegel and Raussendorf, 2001; Raussendorf and Briegel, 2001; Raussendorf *et al.*, 2003); for an implementation with quantum dots, see (Weinstein *et al.*, 2005). It was recently shown that the efficient preparation of cluster states is possible with probabilistic two-qubit controlled phase flip gates (Duan and Raussendorf, 2005; Chen *et al.*, 2006a). Generation of atomic cluster states through the cavity input-output process was suggested by Cho and Lee (2005). Few-qubit cluster states of photons were created in several recent experiments (Zhang *et al.*, 2006a; Walther *et al.*, 2005b; Kiesel *et al.*, 2005; Schmid *et al.*, 2007; Lu *et al.*, 2007).

Open theoretical questions remain about the scalability under realistic noise conditions required for fault-tolerant one-way quantum computation. A threshold has been proved to exist (Nielsen and Dawson, 2005; Dawson *et al.*, 2006a, 2006b; Aliferis and Leung, 2006); particularly, in the context of scalable optical cluster-state quantum computing, Nielsen and coworkers have shown that, for photon loss noise and depolarizing noise, fault-tolerant threshold regions are $< 3 \times 10^{-3}$ for photon loss probabilities and $< 10^{-4}$ for depolarization probabilities. Yet, it is unknown whether cluster state quantum computation will be more or less sensitive to noise than the standard model. Loss tolerance for optical quantum computing has been considered by Ralph *et al.* (2005) and Varnava *et al.* (2006).

2. Linear-optical one-way quantum computing

There are several schemes for one-way quantum computing with linear optics (e.g., Nielsen, 2004; Browne and Rudolph, 2005; Bodiya and Duan, 2006; Chen *et al.*, 2008, to mention a few). In particular, Nielsen has shown that efficient linear-optical quantum computation based on cluster states is possible without the elaborate teleportation and \hat{z} -measurement error correction steps in the Knill-Laflamme-Milburn scheme. Nielsen's method works for any non-trivial linear optical gate which succeeds with finite probability, but which, when it fails, effects a measurement in the computational basis. By introducing two elementary linear-optical operations (the type-I/II "two-qubit fusion"), Browne and Rudolph (2005) suggested a robust scheme achieving a much greater degree of efficiency and a simpler implementation than previous proposals. Other physical imple-

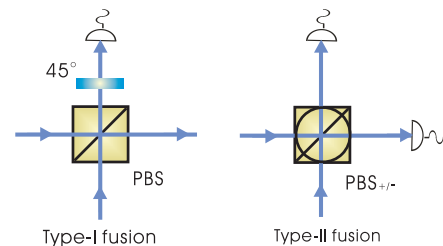


FIG. 38 The two-qubit fusion nondeterministic gates. In the type-I fusion only one of the two outputs is measured by a polarization-discriminating photon counter after a 45° polarization rotation. The type-II fusion uses a rotated PBS, and both outputs are measured. (Browne and Rudolph, 2005)

mentations include, e.g., the scheme with matter qubits and linear optics as proposed by Barrett and Kok (2006) using single-photon interference effects, and a method using only local unitaries and type-I fusion operations (Gilbert *et al.*, 2006). Here we focus on a linear-optical architecture for one-way quantum computing.

a. A linear-optical architecture Below we discuss the Browne-Rudolph scheme in more details. The scheme has a practically important advantage in that it requires stable interferometry over only the coherence length of the photons. Its two basic operations are the type-I and type-II "two-qubit fusion" operations (Fig. 38). The type-I fusion is also known as parity check (Pan and Zeilinger, 1998; Pan *et al.*, 2001b; Cerf *et al.*, 1998; Pittman *et al.*, 2001). Starting from a supply of polarization Bell states $\frac{1}{2}(|HH\rangle + |VH\rangle + |HV\rangle - |VV\rangle)$ (which are equivalent to a 2-qubit cluster state and can be created via the method described in section VIII.C.2.b), the type-I fusion operation allows us to efficiently generate arbitrarily long linear cluster states. If the Type-I fusion is applied to the end-qubits of linear (i.e., one-dimensional) clusters of lengths n and m , successful outcomes generate a linear cluster of length $(n + m - 1)$ (Fig. 39). The type-I fusion operation is considered to have failed when either zero or two photons of either polarization are detected. The failure outcomes have the effect of measuring both input qubits in the \hat{z} -eigenbasis (the effects of the \hat{x} -eigenbasis and the \hat{y} -eigenbasis are also shown in Fig. 39). Measuring a cluster state qubit in the computational basis leaves the remaining qubits in a cluster state of the same layout as before the measurement, but now with all the bonds connected to the measured qubit severed.

Linear clusters are not, however, sufficient for universal quantum computation, as their geometry does not permit the implementation of 2-qubit gates. We thus need to create two-dimensional clusters. Type-I fusion operation alone is not appropriate for carrying out these fusions, since its failure outcome would split the linear clusters in two (Fig. 39).

The strategy (Chen *et al.*, 2008) of preparing a two-

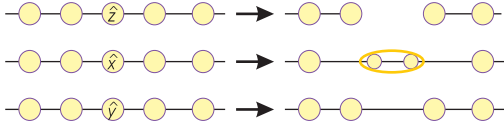


FIG. 39 Certain measurements on a cluster qubit will leave the remaining qubits in a new cluster state with a different layout: A \hat{z} -eigenbasis measurement removes the qubit from the cluster and breaks all bonds between that qubit and the rest of the cluster; an \hat{x} -measurement on a linear cluster removes the measured qubit and causes the neighboring qubits to be joined such that they now represent a single logical qubit with logical basis $|HH\rangle$ and $|VV\rangle$; a \hat{y} -measurement removes the qubit from the linear cluster but links the neighboring qubits. These gain an extra $\pi/2$ rotation around the z -axis which is accounted for when they are measured. Here each circle represents a qubit prepared in the state $|+\rangle$ and each line (“bond”) indicates that a CPhase gate having been applied between the two connected qubits. (Browne and Rudolph, 2005)

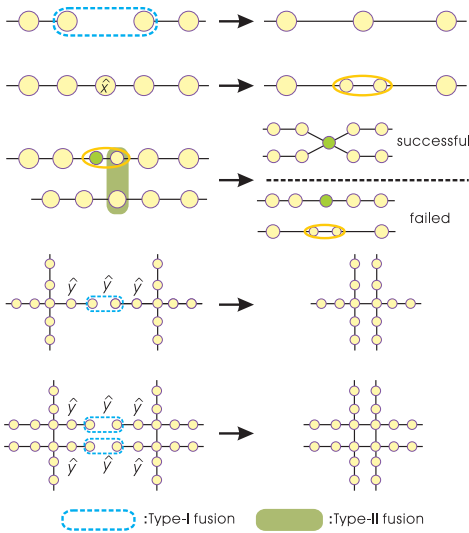


FIG. 40 Step-by-step picture of the procedure for creating a two-dimensional cluster state with type-I and type-II fusion operations and \hat{y} -measurements. (Chen *et al.*, 2007b)

dimensional cluster is depicted in Fig. 40 and consists of the following procedures:

- First prepare in parallel two linear clusters, one of length $2n_0 + 1$ and another of length $2n_0 + 3$; then perform an \hat{x} -measurement on the middle qubit in the longer cluster so that a new cluster of $2n_0 + 1$ is generated, but with its middle point redundantly encoded with 2 photons. This step can be accomplished very efficiently (i.e., the total time scales logarithmically with the cluster length, and the number of the total type-I fusions scales linearly).
- Create a “+”-shape cluster (Duan and Raussendorf, 2005), with four ancillary legs

each of length n_0 , by type-II fusing the two middle qubits of two linear clusters. The number of attempts to accomplish this depends on the successful probability of the type-II operation.

- For two such +”-shape clusters, their center qubits are connected by type-I fusing always the two end qubits each from one of the four legs. Due to the property of the type-I fusion, we can try the connection at most n_0 times before reaching the center qubits (n_0 is then chosen such that the connection can succeed at any wanted high probability). If any one of these n_0 connections succeeds and there are still redundant leg qubits between the two center qubits, we simply remove these redundant qubits by single-qubit \hat{y} -measurements. The new cluster created in this way have more ancillary legs. Each of these legs has a length of n_0 such that the procedure can be continued..

It is proved that the above strategy can finally prepare a square-lattice cluster of N qubits with a temporal overhead scaling logarithmically with N , and with an operational overhead (i.e., number of fusion operations) scaling as $\sim N \ln N$ (Chen *et al.*, 2008). The described protocol is a linear-optical realization of the Duan-Raussendorf proposal (2005), but combines the advantages of the Browne-Rudolph scheme, whose overall efficiency is thereby demonstrated. A crucial element for a realistic realization is quantum memory for polarization qubits, which is crucial for all large-scale optical quantum computing based on polarization encoding. Such memory was discussed in section VII.E.3. Following the above protocol, complex multi-party quantum network can in principle be created very efficiently. This provides an exciting perspective for manipulating a huge number of photons applicable to quantum computing.

b. Event-ready polarization entanglement with linear optics

So far, though up to six photonic qubits can be experimentally manipulated using SPDC, the number of entangled photonic qubits are rather hard to increase due to the intrinsic limitations of the SPDC entanglement sources. The reasons are the following. On the one hand, to get higher multi-fold coincidences, one has to increase the probability p of creating an entangled pair with a single pulse. However, this then also increases the probability of the events for creating more than one pair by the same pulse, which usually gives unwanted terms in the resulting entangled states. On the other hand, as the SPDC entanglement sources are probabilistic, the probability of entangling $2n$ photonic qubits, using a similar technique discussed in section V.E.2, scales as p^n , which will be exponentially small with increasing n .

In the above linear-optical architecture, two-photon entangled pairs are the basic resource. Now let us describe a scheme (Zhang *et al.*, 2006b; Bao *et al.*, 2007;

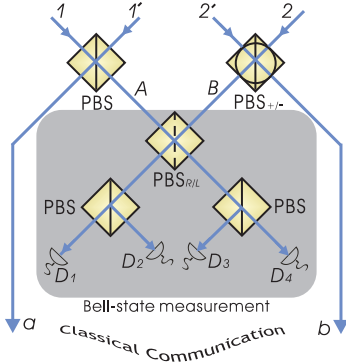


FIG. 41 Deterministic single-photon polarization entangler. PBS ($\text{PBS}_{+/-}$; $\text{PBS}_{R/L}$) reflects photons with vertical-polarization $|V\rangle$ ($|V'\rangle$ -polarization; $|L\rangle$ -polarization) and transmits photons with horizontal-polarization $|H\rangle$ ($|H'\rangle$ -polarization; $|R\rangle$ -polarization). In the present case, a coincidence count between single-photon detectors D_1 and D_4 (D_1 and D_3) or between D_2 and D_3 (D_2 and D_4) leaving photons along paths a and b deterministically entangled in $|\phi_{ab}^-\rangle$ ($|\phi_{ab}^+\rangle$). (Zhang *et al.*, 2006b; Bao *et al.*, 2007; Chen *et al.*, 2007a)

Chen *et al.*, 2007) that generates event-ready polarization entanglement by linear optics and projective measurement for the purpose of quantum computing. The basic elements of the scheme are four single photons, linear optics and even-ready detections. As one can easily check, the setup in Fig. 41 is a deterministic single-photon polarization-entangler: By selecting only the “four-mode” case where there is one and only one photon in each of the four output modes (a , b , A , B), one obtains, with the probability of $1/4$, the four-photon state expanded in the standard Bell basis of photons A and B :

$$\begin{aligned} |\psi\rangle &= |V'\rangle_1 |V\rangle_2 |H'\rangle_{1'} |H\rangle_{2'} \\ &\rightarrow \frac{1}{2} (|\psi^-\rangle_{ab} |\phi^+\rangle_{AB} + \hat{x}_b |\psi^-\rangle_{ab} |\psi^+\rangle_{AB} \\ &\quad + \hat{z}_a |\psi^-\rangle_{ab} |\phi^-\rangle_{AB} + \hat{z}_a \hat{x}_b |\psi^-\rangle_{ab} |\psi^-\rangle_{AB}). \end{aligned} \quad (113)$$

Then the Bell-state measurement on photons A and B will collapse photons a and b into a *definite* Bell state by classically communicating the result of the Bell-state measurement. As only two (e.g., $|\phi^+\rangle_{AB}$ and $|\psi^+\rangle_{AB}$) out of the four Bell states can be identified with linear optics (section V.F.1), the overall success probability of single-photon polarization-entangler is $\frac{1}{4} \times \frac{1}{2} = \frac{1}{8}$ for perfect detections. Yet, such a linear-optics setup can deterministically entangle two polarization qubits and is thus an “event-ready” entangler in the sense that one knows when entanglement is successfully created. Zhang *et al.* (2006b) experimentally realized the scheme using the triggered single photons from SPDC.

For the above scheme to work ideally, it requires on-demand single photons and ideal photon-number count-

ing, which can differentiate 0, 1 and more photons.⁵⁸ There indeed exist several atomic-ensemble-based techniques [high-efficiency photon counting and quantum memory (see section VII.E.3); single-photon creation (see section VII.E.2)] which allow a scalable and efficient multi-photon entanglement creation by following the linear-optical architecture in section VIII.C.2.a. Such an efficient generation of a large-scale photonic cluster-state entanglement opens up a realistic and fascinating possibility of manipulating a huge number photons, particularly for photonic one-way quantum computing with many photonic qubits and linear optics.

An important resource for quantum information science is a source of single photons, either on demand or heralded. For many applications in quantum information processing with photons, it is desirable to have a single-photon source with *controllable* emission time, direction, and pulse shape in order to have perfect spatial and temporal overlap at optical elements and larger collection efficiency. Early utility of single photons makes use of SPDC: a conditional detection of one photon from an entangled pair triggers the presence of the partner photon. However, such triggered single photons have large bandwidth (i.e., small coherent time) and can not be created at controllable time due to the randomness of SPDC. In the past few years, there are significant advance on the single-photon emitter and its controllability, using solid-state devices, atoms and ions. These demonstrated single-photon emitting mechanisms include quantum dots (Michler *et al.*, 2000b; Santori *et al.*, 2001, 2002; Pelton *et al.*, 2002), nitrogen-vacancy color centers (Brouri *et al.*, 2000; Kurtsiefer *et al.*, 2000), neutral atoms (Kuhn *et al.*, 2002; McKeever *et al.*, 2004; Darquie *et al.*, 2005), ions (Keller *et al.*, 2004), and molecules (Brunel *et al.*, 1999; Lounis and Moerner, 2000). Solid-state devices may allow high single-photon rates. But due to inhomogeneities in both the environment of the emitters and the emitters themselves, it is a major problem for preparing a few truly identical sources. A fully controllable single-photon source is achievable if one could trap single-atoms in high-finesse optical cavities for a sufficiently long time. Such a source is spectrally narrow, and the photons are emitted into a well-defined spatial mode. However, the operation of high-finesse cavities is a experimentally challenging work, and the single-photon rate is limited by the cavity. So far, the measured efficiency to detect a single photon per trial is typically less than 1%. In this respect, a fully controllable single-photon source based on atomic ensembles (see section VII.E.2) is more promising.

⁵⁸ The visible light photon counter can indeed do such a photon-number discrimination with 99% accuracy (Waks *et al.*, 2003, 2004). But for other frequency regime, there is no similar technique demonstrated. Khoury *et al.* (2006) used such a photon-number-resolving detector to do the Fock-state projection, effectively inducing high-order optical nonlinearities.

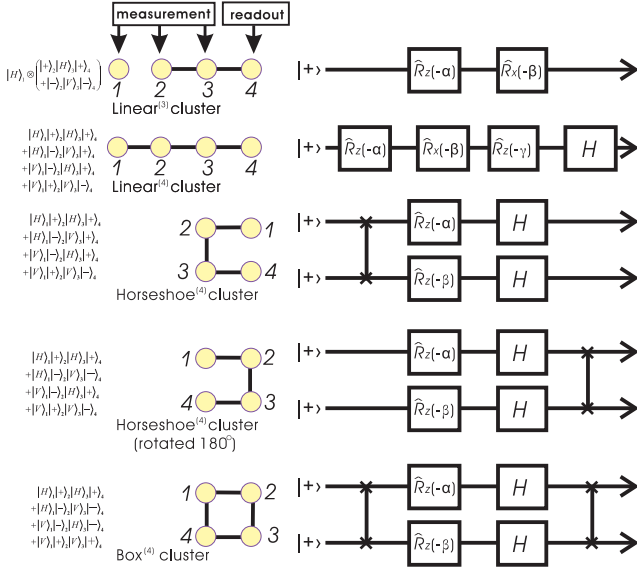


FIG. 42 Few-qubit cluster states and the quantum circuits they implement. For each three- and four-qubit cluster, its quantum state ($|\Phi_{\text{lin}3}\rangle$, $|\Phi_{\text{lin}4}\rangle$, $|\Phi_{\square 4}\rangle$, $|\Phi_{\square 4}\rangle$, or $|\Phi_{\square 4}\rangle$) and the computation carried out in the one-way quantum computer model is shown. (Walther *et al.*, 2005)

3. Experimental one-way quantum computing

So far, the largest optical one-way quantum computer, namely, six photons entangled in cluster states, was reported by Lu *et al.* (2007). The experiment by Walther *et al.* (2005b) demonstrated the basic idea of the one-way optical quantum computing. In this experiment, four-photon polarization-entangled cluster state close to

$$|\Phi_{\text{cluster}}\rangle = \frac{1}{2}(|H\rangle_1 |H\rangle_2 |H\rangle_3 |H\rangle_4 + |H\rangle_1 |H\rangle_2 |V\rangle_3 |V\rangle_4 + |V\rangle_1 |V\rangle_2 |H\rangle_3 |H\rangle_4 - |V\rangle_1 |V\rangle_2 |V\rangle_3 |V\rangle_4) \quad (114)$$

was created via SPDC. $|\Phi_{\text{cluster}}\rangle$ is equivalent to the four-qubit linear cluster $|\Phi_{\text{lin}4}\rangle$, and $|\Phi_{\square 4}\rangle$ and $|\Phi_{\square 4}\rangle$ (Fig. 42) under the local unitary operation $\hat{H}_1 \otimes \hat{I}_2 \otimes \hat{I}_3 \otimes \hat{H}_4$ on the physical qubits, where \hat{H} (\hat{I}) is a Hadamard (identity) operation. $|\Phi_{\text{cluster}}\rangle$ can easily be reduced to $|\Phi_{\text{lin}3}\rangle$ by measuring qubit 1 in the computational basis. It can also be converted to $|\Phi_{\square 4}\rangle$ by the local unitary operation $\hat{H}_1 \otimes \hat{H}_2 \otimes \hat{H}_3 \otimes \hat{H}_4$ and a swap (or relabelling) of qubits 2 and 3.

To completely characterize the state so generated, quantum-state tomography was performed to extract the density matrix from a discrete set of experimental measurements, which in this case consist of $16 \times 16 = 256$ linearly independent four-photon polarization projections. The measured fidelity $F_{\text{exp}} = \langle \Phi_{\text{cluster}} | \rho | \Phi_{\text{cluster}} \rangle = 0.63 \pm 0.02$. As we just mentioned, $|\Phi_{\text{cluster}}\rangle$ can be reduced to $|\Phi_{\text{lin}3}\rangle$ by measuring qubit 1 in the computational basis. Whereas the loss of one qubit in a GHZ state

is already sufficient to completely disentangle the state, $[N/2]$ particles have to be removed from an N -particle cluster state in order to leave a separable state. The cluster states share this persistency of entanglement (Briegleb and Raussendorf, 2001). Both of the two remarkable entanglement properties of the four-qubit cluster state were confirmed from the full tomographic measurements.

Using the cluster state $|\Phi_{\text{cluster}}\rangle$, the essentials of cluster-state quantum computation were demonstrated by realizing a universal set of quantum logic operations: single-qubit rotations and non-trivial two-qubit gates. The latter can be realized with two-dimensional cluster states— $|\Phi_{\square 4}\rangle$, $|\Phi_{\square 4}\rangle$, and $|\Phi_{\square 4}\rangle$. The quality of each quantum computation was experimentally characterized by comparing the measured output state to the ideal using the state fidelity. Interesting avenues for study include full quantum gate characterization using quantum process tomography (Chuang and Nielsen, 1997; Poyatos *et al.*, 1997).

Interestingly, Walther *et al.* also demonstrated a two-qubit implementation of Grover's fast quantum search (Grover, 1997) using the cluster state model. The goal of a search is to identify one out of N elements of a database. Formally, one could consider the database as a black box that labels one of N possible inputs leaving all others unchanged. The challenge, then, is to find that labelled state. The best classical strategy chooses the inputs randomly one by one and checks for the label; it takes, on average, about $N/2$ calculations to find the special input. Quantum parallelism in Grover's algorithm allows for all inputs to be processed simultaneously in superposition, while interference enhances the probability of finding the desired outcome in only $O(\sqrt{N})$ calculations of the function. In the case of a two-bit function ($N = 4$), the difference is even more dramatic, as Grover's algorithm needs only one calculation of the function, whereas classically three evaluations are needed in the worst case, and 2.25 evaluations are needed on average. In this experiment, the quantum circuit implemented by the box cluster $|\Phi_{\square 4}\rangle$ can be seen as precisely that one required for Grover's algorithm provided that the final readout measurements are made in the R/L basis. The measured probability of the quantum computer determining the correct outcome is about 90%, whereas the theoretical probability is unit in the ideal case.

As a proof of principle, the described experiment used no feedforward or subsequent corrections given a successful measurement. This reduces the success rate of the computation by a factor of two for every measurement as compared to ideal, deterministic gate operations. An important challenge is to implement fast feedforward where earlier measurement outcomes actually change the setting of a future measurement in real time. Recently Prevedel *et al.* (2007) reported a concatenated scheme of measurement and active, fast feed-forward in a one-way quantum computing experiment.

IX. CONCLUDING REMARKS

Harnessing the Hilbert-space structure of quantum physics to encode and process information may well be a crucial component for the future quantum engineering that could dramatically affect even our everyday life. The development of quantum information science has based on quantum mechanics and calls for an in-depth understanding of the very relation between physics and information in general. Quite probably, it would also refresh our today's view on quantum mechanics itself. Experiments with photons have had a pioneering role in this context. The topics we reviewed are featured by emerging technology and rapid development. This makes it impossible to cover in detail all the ongoing developments and many have to be left out with regret.

The photon idea has achieved fertile applications so far. As for the future, we would like to remark that, according to several recent proposals reviewed above, photons can be a strong candidate not only for long-distance quantum communication, but also for large-scale quantum computing. Given several atomic-ensemble-based technologies, linear-optical quantum information processing has a brilliant future. As we have emphasized throughout this review, linear-optical elements can manipulate photons with very high accuracy. The interface of photons and atomic ensembles offers the fascinating playground for integrating the linear-optical and atomic-ensemble-based techniques for long-distance quantum communication (sections VII.E.2) and scalable optical quantum computing (section VIII.C.2). This would open up an exciting perspective for manipulating quantum states of a huge number of photons.

Despite tremendous progress in the reviewed topics, many technological challenges remain. These include

- single photons on demand (for applications in quantum cryptography and these mentioned in sections VIII.C.2.b and VII.E.2);
- deterministic and narrow bandwidth entangled photon sources;
- quantum memory for photons with high efficiency and fidelity (for applications in optical quantum network, particularly these mentioned in sections VIII.C.2.b and VIII.C.2);
- highly-efficient photon counting (for applications in, e.g., the loophole-free test of local realism with photons, and these mentioned in sections VIII.C.2.b and VIII.C.2).

To end this review, let us say, “happy new centenary, photon”.

Acknowledgments

We would like to thank Xiao-Hui Bao and Chao-Yang Lu for valuable comments and help. This work

was supported by the National NSF of China, the Chinese Academy of Sciences, the National Fundamental Research Program (under grant No. 2006CB921900) and the Fok Ying Tung Education Foundation. This work was also supported by the Alexander von Humboldt Foundation and the Marie Curie Excellence Grant of the EU. M.Ž. was supported by Professorial Subsidy of FNP and the MNiI Grant No 1 P03B 04927. H.W. acknowledges the supports from DFG and the EU 6FP program QAP. A.Z. acknowledges the supports from EPSRC, QIPIRC, FWF and EC under the Integrated Project Qubit Application.

References

- [1] Akopian, N., N.H. Lindner, E. Poem, Y. Berlatzky, J. Avron, and D. Gershoni, B. D. Gerardot, and P. M. Petroff, 2006, *Phys. Rev. Lett.* **96**, 130501.
- [2] Alber, G., T. Beth, M. Horodecki, P. Horodecki, R. Horodecki, M. Rotteler, H. Weinfurter, R. Werner, and A. Zeilinger, 2001, *Quantum Information: An Introduction to Basic Theoretical Concepts and Experiments* (Springer-Verlag, Berlin/Heidelberg).
- [3] Aliferis, P. and D.W. Leung, 2004, *Phys. Rev. A* **70**, 062314.
- [4] Aliferis, P. and D.W. Leung, 2006, *Phys. Rev. A* **73**, 032308.
- [5] Allen, L., S.M. Barnett, and M.J. Padgett (eds.), 2003, *Optical Angular Momentum* (IOP Publishing, Bristol).
- [6] Alley C.O., and Y.H. Shih, 1987, *Proc. of 2nd Int. Symp. Foundations of Quantum Mechanics*, ed. M. Namiki (Physical Society of Japan, Tokyo).
- [7] Altepeter, J.B., P.G. Hadley, S.M. Wendelken, A.J. Berglund, and P.G. Kwiat, 2004, *Phys. Rev. Lett.* **92**, 147901.
- [8] Ardehali, M., 1992, *Phys. Rev. A* **46**, 5375.
- [9] Aspect, A., P. Grangier, and G. Roger, 1981, *Phys. Rev. Lett.* **47**, 460.
- [10] Aspect, A., P. Grangier, and G. Roger, 1982a, *Phys. Rev. Lett.* **49**, 91.
- [11] Aspect, A., J. Dalibard, and G. Roger, 1982b, *Phys. Rev. Lett.* **49**, 1804.
- [12] Aspect, A., 1999, *Nature (London)* **390**, 189.
- [13] Aspelmeyer, M., H. R. Böhm, T. Gyatso, T. Jennewein, R. Kaltenbaek, M. Lindenthal, G. Molina-Terriza, A. Poppe, K. Resch, M. Taraba, R. Ursin, P. Walther, and A. Zeilinger, 2003a, *Science* **301**, 621.
- [14] Aspelmeyer, M., T. Jennewein, M. Pfenningbauer, W.R. Leeb, and A. Zeilinger, 2003b, *IEEE J. Sel. Top. Quantum Electron.* **9**, 1541.
- [15] Bacon, D. and B.F. Toner, 2003, *Phys. Rev. Lett.* **90**, 157904.
- [16] Bacon, D., D.A. Lidar, and K.B. Whaley, 1999, *Phys. Rev. A* **60**, 1944.
- [17] Bajcsy, M., A.S. Zibrov, and M.D. Lukin, 2003, *Nature (London)* **426**, 638.
- [18] Bao, X.-H., T.-Y. Chen, Q. Zhang, J. Yang, H. Zhang, T. Yang, and J.-W. Pan, 2007, *Phys. Rev. Lett.* **98**, 170502.
- [19] Barbieri, M., C. Cinelli, P. Mataloni, and F. De Martini, 2005, *Phys. Rev. A* **72**, 052110.

- [20] Barenco, A., C.H. Bennett, R. Cleve, D.P. DiVincenzo, N. Margolus, P. Shor, T. Sleator, J.A. Smolin, and H. Weinfurter, 1995a, *Phys. Rev. A* **52**, 3457.
- [21] Barenco, A., D. Deutsch, A. Ekert, and R. Jozsa, 1995b, *Phys. Rev. Lett.* **74**, 4083.
- [22] Barnett, S.M., J. Jeffers, A. Gatti, and R. Loudon, 1989, *Phys. Rev. A*, **57** 2134.
- [23] Barreiro, J.T., N.K. Langford, N.A. Peters, and P.G. Kwiat, 2005, *Phys. Rev. Lett.* **95**, 260501.
- [24] Barrett, M.D., J. Chiaverini, T. Schaetz, J. Britton, W.M. Itano, J.D. Jost, E. Knill, C. Langer, D. Leibfried, R. Ozeri, D.J. Wineland, 2004, *Nature (London)* **429**, 737.
- [25] Barrett, S.D. and P. Kok, 2005, *Phys. Rev. A* **71**, 060310(R).
- [26] Bechmann-Pasquinucci, H., and A. Peres, 2000, *Phys. Rev. Lett.* **85**, 3313.
- [27] Belinskii, A.V. and D.N. Klyshko, 1993, *Phys. Usp.* **36**, 653.
- [28] Bell, J.S., 1964, *Physics (Long Island City, N.Y.)* **1**, 195.
- [29] Bell, J.S., 1966, *Rev. Mod. Phys.* **38**, 447.
- [30] Bell, J.S., 1987, *Speakable and Unsayable in Quantum Mechanics* (Cambridge University Press, New York).
- [31] Bennett, C.H., H.J. Bernstein, S. Popescu, and B. Schumacher, 1996a, *Phys. Rev. A* **53**, 2046.
- [32] Bennett, C.H. and G. Brassard, 1984, in *Proceedings of the IEEE International Conference on Computers, Systems and Singal Proceeding, Bangalore, India* (IEEE, New York), 175.
- [33] Bennett, C.H., G. Brassard, C. Crépeau, R. Jozsa, A. Peres, and W.K. Wootters, 1993, *Phys. Rev. Lett.* **70**, 1895.
- [34] Bennett, C.H., G. Brassard, S. Popescu, B. Schumacher, J.A. Smolin, and W.K. Wootters, 1996b, *Phys. Rev. Lett.* **76**, 722 - Erratum: 1997, *Phys. Rev. Lett.* **78**, 2031.
- [35] Bennett, C.H. and D.P. DiVincenzo, 2000, *Nature (London)* **404**, 247.
- [36] Bennett, C.H., D.P. DiVincenzo, J.A. Smolin, and W.K. Wootters, 1996c, *Phys. Rev. A* **54**, 3824.
- [37] Bennett, C.H. and S.J. Wiesner, 1992, *Phys. Rev. Lett.* **69**, 2881.
- [38] Bialynicki-Birula, I. and Z Bialynicka-Birula, 1975, *Quantum Electrodynamics* (Pergamon, Oxford).
- [39] Blinov, B.B., D.L. Moehring, L.-M. Duan, C. Monroe, 2004, *Nature (London)* **428**, 153.
- [40] Bodiya, T.P. and L.-M. Duan, 2006, *Phys. Rev. Lett.* **97**, 143601.
- [41] Bohm, D., 1951, *Quantum Theory* (Prentice Hall, Englewood Cliffs, NJ).
- [42] Boschi, D., S. Branca, F. De Martini, and L. Hardy, 1997, *Phys. Rev. Lett.* **79**, 2755.
- [43] Boschi, D., S. Branca, F. De Martini, L. Hardy, and S. Popescu, 1998, *Phys. Rev. Lett.* **80**, 1121.
- [44] Bose, S., P.L. Knight, M.B. Plenio, and V. Vedral, 1999, *Phys. Rev. Lett.* **83**, 5158.
- [45] Bose, S., V. Vedral, and P.L. Knight, 1998, *Phys. Rev. A* **57**, 822.
- [46] Boto, A.N., P. Kok, D.S. Abrams, S.L. Braunstein, C.P. Williams, and J.P. Dowling, 2000, *Phys. Rev. Lett.* **85**, 2733.
- [47] Bourennane, M., M. Eibl, S. Gaertner, C. Kurtsiefer, A. Cabello, and H. Weinfurter, 2004, *Phys. Rev. Lett.* **92**, 107901.
- [48] Bouwmeester, D., 2001, *Phys. Rev. A* **63**, 040301(R).
- [49] Bouwmeester, D., 2004, *Nature (London)* **429**, 139.
- [50] Bouwmeester, D., A. Ekert, and A. Zeilinger (eds.), 2001, *The Physics of Quantum Information* (Springer-Verlag, Berlin/Heidelberg).
- [51] Bouwmeester, D., J.-W. Pan, M. Daniell, H. Weinfurter, and A. Zeilinger, 1999a, *Phys. Rev. Lett.* **82**, 1345.
- [52] Bouwmeester, D., J.-W. Pan, M. Daniell, H. Weinfurter, M. Żukowski, and A. Zeilinger, 1998, *Nature (London)* **394**, 841.
- [53] Bouwmeester, D., J.-W. Pan, K. Mattle, M. Eibl, H. Weinfurter, and A. Zeilinger, 1997, *Nature (London)* **390**, 575.
- [54] Bouwmeester, D., J.-W. Pan, H. Weinfurter, and A. Zeilinger, 1999b, *J. Mod. Opt.* **47**, 279.
- [55] Branciard, C., N. Brunner, N. Gisin, C. Kurtsiefer, A. Lamas-Linares, A. Ling, and V. Scarani, 2008, *quant-ph/0801.2241*.
- [56] Branciard, C., A. Ling, N. Gisin, C. Kurtsiefer, A. Lamas-Linares, and V. Scarani, 2007, *Phys. Rev. Lett.* **99**, 210407.
- [57] Branning, D., W.P. Grice, R. Erdmann, and I.A. Walmisley, 1999, *Phys. Rev. Lett.* **83**, 955.
- [58] Branning, D., W.P. Grice, R. Erdmann, and I.A. Walmisley, 2000, *Phys. Rev. A* **62**, 013814.
- [59] Braunstein, S.L. and H.J. Kimble, 1998, *Nature (London)* **394**, 840.
- [60] Braunstein, S.L. and A. Mann, 1995, *Phys. Rev. A* **51**, R1727.
- [61] Braunstein, S.L. and P. van Loock, 2005, *Rev. Mod. Phys.* **77**, 513.
- [62] Brendel, J., N. Gisin, W. Tittel, and H. Zbinden, 1999, *Phys. Rev. Lett.* **82**, 2594.
- [63] Brendel, J., E. Mohler, and W. Martienssen, 1992, *Europhys. Lett.* **20**, 575.
- [64] Briegel, H.J. and R. Raussendorf, 2001, *Phys. Rev. Lett.* **86**, 910 .
- [65] Briegel, H.-J., W. Dür, J.I. Cirac, and P. Zoller, 1998, *Phys. Rev. Lett.* **81**, 5932.
- [66] Brouri, R., A. Beveratos, J.-Ph. Poizat, and P. Grangier, 2000, *Opt. Lett.* **25**, 1294.
- [67] Browne, D.E., M.B. Plenio, and S.F. Huelga, 2003, *Phys. Rev. Lett.* **91**, 067901.
- [68] Browne, D.E. and T. Rudolph, 2005, *Phys. Rev. Lett.* **95**, 010501.
- [69] Brukner, Č., M. Żukowski, J.-W. Pan, and A. Zeilinger, 2004, *Phys. Rev. Lett.* **92**, 127901.
- [70] Brunel, C., B. Lounis, P. Tamarat, and M. Orrit, 1999, *Phys. Rev. Lett.* **83**, 2722.
- [71] Bruß, D., J.I. Cirac, P. Horodecki, F. Hulpke, B. Kraus, M. Lewenstein, and A. Sanpera, 2002, *J. Mod. Opt.* **49**, 1399.
- [72] Bruß, D., A. Ekert, S.F. Huelga, J.-W. Pan, and A. Zeilinger, 1997, *Phil. Trans. R. Soc. Lond. A* **355**, 2259.
- [73] Burnham, D.C. and D.L. Weinberg, 1970, *Phys. Rev. Lett.* **25**, 84.
- [74] Cabello, A., 2001a, *Phys. Rev. Lett.* **86**, 1911.
- [75] Cabello, A., 2001b, *Phys. Rev. Lett.* **87**, 010403.
- [76] Cabello, A., 2003, *Phys. Rev. Lett.* **90**, 258902.
- [77] Cabrillo, C., J.I. Cirac, P. García-Fernández, and P. Zoller, 1999, *Phys. Rev. A* **59**, 1025.
- [78] Calderbank, A.R. and P.W. Shor, 1996, *Phys. Rev. A* **54**, 1098.

- [79] Carmichael, H.J. and D.F. Walls, 1976, *J. Phys. B* **9**, L43; *J. Phys. B* **9**, 1199.
- [80] Carteret, H.A., A. Higuchi, and A. Sudbery, 2000, *J. Math. Phys.* **41**, 7932
- [81] Cerf, N.J., C. Adami, and P.G. Kwiat, 1998, *Phys. Rev. A*, **57** R1477.
- [82] Cerf, N.J., M. Bourennane, A. Karlsson, and N. Gisin 2002, *Phys. Rev. Lett.* **88**, 127902.
- [83] Chanelière, T., D.N. Matsukevich, S.D. Jenkins, S.-Y. Lan, T.A.B. Kennedy, and A. Kuzmich, 2005, *Nature (London)* **438**, 833.
- [84] Chen, Q., J. Cheng, K.-L. Wang, and J.F. Du, 2006a, *Phys. Rev. A* **73**, 012303.
- [85] Chen, S., Y.-A. Chen, T. Strassel, Z.-S. Yuan, B. Zhao, J. Schmiedmayer, and J.-W. Pan, 2006b, *Phys. Rev. Lett.* **97**, 173004.
- [86] Chen, Y.-A., A.-N. Zhang, Z. Zhao, X.-Q. Zhou, C.-Y. Lu, C.-Z. Peng, T. Yang, J.-W. Pan, 2005, *Phys. Rev. Lett.* **95**, 200502.
- [87] Chen, Y.-A., A.-N. Zhang, Z. Zhao, X.-Q. Zhou, and J.-W. Pan, 2006c, *Phys. Rev. Lett.* **96**, 220504.
- [88] Chen, Z.-B., J.-W. Pan, Y.-D. Zhang, Č. Brukner, and A. Zeilinger, 2003, *Phys. Rev. Lett.* **90**, 160408.
- [89] Chen, Z.-B., Q. Zhang, X.-H. Bao, J. Schmiedmayer, and J.-W. Pan, 2006d, *Phys. Rev. A* **73**, 050302(R).
- [90] Chen, Z.-B., B. Zhao, Y.-A. Chen, J. Schmiedmayer, and J.-W. Pan, 2007, *Phys. Rev. A* **76**, 022329.
- [91] Chen, Z.-B., Y.-K. Zhao, B. Zhao, and J.-W. Pan, 2008, to be published.
- [92] Chiaverini, J., D. Leibfried, T. Schaetz, M.D. Barrett, R.B. Blakestad, J. Britton, W.M. Itano, J. D. Jost, E. Knill, C. Langer, R. Ozeri, and D.J. Wineland, 2004, *Nature (London)* **432**, 602.
- [93] Childress, L., J.M. Taylor, A.S. Sørensen, and M.D. Lukin, 2005, *Phys. Rev. A* **72**, 052330.
- [94] Childress, L., J.M. Taylor, A.S. Sørensen, and M.D. Lukin, 2006, *Phys. Rev. Lett.* **96**, 070504.
- [95] Childs, A.M., D.W. Leung, and M.A. Nielsen, 2005, *Phys. Rev. A* **71**, 032318.
- [96] Cho, J. and H.W. Lee, 2005, *Phys. Rev. Lett.* **95**, 160501.
- [97] Chou, C.W., S.V. Polyakov, A. Kuzmich, and H.J. Kimble, 2004, *Phys. Rev. Lett.* **92**, 213601.
- [98] Chuang, I.L. and M.A. Nielsen, 1997, *J. Mod. Opt.* **44**, 2455.
- [99] Cinelli, C., M. Barbieri, R. Perris, P. Mataloni, and F. De Martini, 2005, *Phys. Rev. Lett.* **95**, 240405.
- [100] Cinelli, C., G. Di Nepi, F. De Martini, M. Barbieri, and P. Mataloni, 2004, *Phys. Rev. A* **70**, 022321.
- [101] Cirac, J.I. and P. Zoller, 1994, *Phys. Rev. A* **50**, R2799.
- [102] Cirac, J.I., P. Zoller, H.J. Kimble, and H. Mabuchi, 1997, *Phys. Rev. Lett.* **78**, 3221.
- [103] Cirel'son, B.S., 1980, *Lett. Math. Phys.* **4**, 93.
- [104] Clauser, J.F., M.A. Horne, A. Shimony, and R.A. Holt, 1969, *Phys. Rev. Lett.* **23**, 880.
- [105] Clauser, J.F. and A. Shimony, 1978, *Rep. Prog. Phys.* **41**, 1881.
- [106] Cleve, R., D. Gottesman, and H.-K. Lo, 1999, *Phys. Rev. Lett.* **83**, 648.
- [107] Cory, D.G., M.D. Price, W. Maas, E. Knill, R. Laflamme, W.H. Zurek, T.F. Havel, and S.S. Somaroo, 1998, *Phys. Rev. Lett.* **81**, 2152.
- [108] Darquié, B., M.P.A. Jones, J. Dingjan, J. Beugnon, S. Bergamini, Y. Sortais, G. Messin, A. Browaeys, and P. Grangier, 2005, *Science* **309**, 454.
- [109] Dawson, C.M., H.L. Haselgrove, and M.A. Nielsen, 2006a, *Phys. Rev. Lett.* **96**, 020501.
- [110] Dawson, C.M., H.L. Haselgrove, and M.A. Nielsen, 2006b, *Phys. Rev. A* **73**, 052306.
- [111] De Barros M.R.X. and P.C. Becker, 1993, *Opt. Lett.* **18**, 631.
- [112] De Caro, L. and A. Garuccio, 1994, *Phys. Rev. A* **50**, R2803.
- [113] DelRe, E., B. Crosignani, and P. Di Porto, 2000, *Phys. Rev. Lett.* **84**, 2989.
- [114] de Riedmatten, H., I. Marcikic, W. Tittel, H. Zbinden, and N. Gisin, 2003, *Phys. Rev. A* **67**, 022301.
- [115] Deutsch, D., A. Ekert, R. Jozsa, C. Macchiavello, S. Popescu, and A. Sanpera, 1996, *Phys. Rev. Lett.* **77**, 2818 [Erratum: 1998, *Phys. Rev. Lett.* **80**, 2022].
- [116] Dewdney, C., P.R. Holland, and A. Kyprianidis, 1987, *J. Phys. A: Math. Gen.* **20**, 4717.
- [117] Diedrich, F. and H. Walther, 1987, *Phys. Rev. Lett.* **58**, 203.
- [118] Dieks, D., 1982, *Phys. Lett. A* **92**, 271.
- [119] Di Giuseppe, G., L. Haiberger, F. De Martini, A.V. Sergienko, 1997, *Phys. Rev. A* **56**, R21.
- [120] Dirac, P.A.M., 1927, *Proc. R. Soc. London A* **114**, 243.
- [121] DiVincenzo, D.P., 2000, *Fortschr. Phys.* **48**, 771.
- [122] Dowling, J.P., 1998, *Phys. Rev. A* **57**, 4736.
- [123] Duan, L.-M. and G.C. Guo, 1997, *Phys. Rev. Lett.* **79**, 1953.
- [124] Duan, L.-M., M.D. Lukin, J.I. Cirac, and P. Zoller, 2001, *Nature (London)* **414**, 413.
- [125] Duan, L.-M., J.I. Cirac, and P. Zoller, 2002, *Phys. Rev. A* **66**, 023818.
- [126] Duan, L.-M. and R. Raussendorf, 2005, *Phys. Rev. Lett.* **95**, 080503.
- [127] Dür, W. and H.-J. Briegel, 2003, *Phys. Rev. Lett.* **90**, 067901.
- [128] Dür, W., H.-J. Briegel, J.I. Cirac, and P. Zoller, 1999, *Phys. Rev. A* **59**, 169 [Erratum: 1999, *Phys. Rev. A* **60**, 725].
- [129] Eberhard, P.H., 1993, *Phys. Rev. A* **47**, R747.
- [130] Eibl, M., S. Gaertner, M. Bourennane, C. Kurtsiefer, M. Żukowski, and H. Weinfurter, 2003, *Phys. Rev. Lett.* **90**, 200403.
- [131] Einstein, A., 1905, *Ann. Phys.* **17**, 132.
- [132] Einstein, A., B. Podolsky, and N. Rosen, 1935, *Phys. Rev.* **47**, 777.
- [133] Eisaman, M.D., A. André, F. Massou, M. Fleischhauer, A.S. Zibrov, and M.D. Lukin, 2005, *Nature (London)* **438**, 837.
- [134] Eisaman, M.D., L. Childress, A. André, F. Massou, A.S. Zibrov, and M.D. Lukin, 2004, *Phys. Rev. Lett.* **93**, 233602.
- [135] Eisenberg, H.S., G. Khoury, G.A. Durkin, C. Simon, and D. Bouwmeester, 2004, *Phys. Rev. Lett.* **93**, 193901.
- [136] Ekert, A.K., 1991, *Phys. Rev. Lett.* **67**, 661.
- [137] Fattal, D., K. Inoue, J. Vučković, C. Santori, G.S. Solomon, and Y. Yamamoto, 2004, *Phys. Rev. Lett.* **92**, 037903.
- [138] Fearn H. and R. Loudon, 1987, *Opt. Commun.*, **64** 485.
- [139] Feng, X.-L., Z.-M. Zhang, X.-D. Li, S.-Q. Gong, and Z.-Z. Xu, 2003, *Phys. Rev. Lett.* **90**, 217902.
- [140] Feynman, R.P., R.B. Leighton, and M. Sands, 1963, *The Feynman Lectures on Physics III* (Addison-Wesley,

- Reading, Mass.).
- [141] Fiorentino, M., T. Kim, and F.N.C. Wong, 2005, Phys. Rev. A **72**, 012318.
- [142] Fiorentino, M. and F.N.C. Wong, 2004, Phys. Rev. Lett. **93**, 070502.
- [143] Fleischhauer, M., A. Imamoglu, and J.P. Marangos, 2005, Rev. Mod. Phys. **77**, 633.
- [144] Fleischhauer, M. and M.D. Lukin, 2000, Phys. Rev. Lett. **84**, 5094.
- [145] Fleischhauer, M. and M.D. Lukin, 2002, Phys. Rev. A **65**, 022314.
- [146] Franson, J.D., 1989, Phys. Rev. Lett. **62**, 2205.
- [147] Freedman, S.J. and J.F. Clauser, 1972, Phys. Rev. Lett. **28**, 938.
- [148] Furusawa, A., J.L. Sørensen, S.L. Braunstein, C.A. Fuchs, H.J. Kimble, and E.S. Polzik, 1998, Science **282**, 706.
- [149] Garg A. and N.D. Mermin, 1987, Phys. Rev. A **35**, 3831.
- [150] Gasparoni, S., J.-W. Pan, P. Walther, T. Rudolph, and A. Zeilinger, 2004, Phys. Rev. Lett. **93**, 020504.
- [151] Genovese, M., 2005, Phys. Rep. **413**, 319.
- [152] Genovese, M. and C. Novero, 2002, Eur. Phys. J. D **21**, 109.
- [153] Gilbert, G., M. Hamrick, and Y.S. Weinstein, 2006, Phys. Rev. A **73**, 064303.
- [154] Gill, R.D., G. Weihs, A. Zeilinger, and M. Żukowski, 2002, Proc. Nat. Acad. Sci. **99**, 14632.
- [155] Gisin, N., 1996, Phys. Lett. A **210**, 151.
- [156] Gisin, N. and H. Bechmann-Pasquinucci, 1998, Phys. Lett. A **246**, 1.
- [157] Gisin N. and A. Peres, 1992, Phys. Lett. A **162**, 15.
- [158] Gisin, N., G. Ribordy, W. Tittel, and H. Zbinden, 2002, Rev. Mod. Phys. **74**, 145.
- [159] Glauber, R.J., 1963, Phys. Rev. **130**, 2529.
- [160] Gottesman, D., 1997, Ph.D. thesis (California Institute of Technology, Pasadena, CA).
- [161] Gottesman, D., and I.L. Chuang, 1999, Nature (London) **402**, 390.
- [162] Grangier, P., G. Roger, and A. Aspect, 1986, Europhys. Lett. **1**, 173.
- [163] Greenberger, D.M., M.A. Horne, and A. Zeilinger, 1989, in *Bell's Theorem, Quantum Theory, and Conceptions of the Universe*, edited by M. Kafatos (Kluwer Academic, Dordrecht).
- [164] Greenberger, D.M., M.A. Horne, A. Shimony, and A. Zeilinger, 1990, Am. J. Phys. **58**, 1131.
- [165] Greenberger, D.M., M.A. Horne, and A. Zeilinger, 1993, Phys. Today **46** (8), 22.
- [166] Grice, W.P., R. Erdmann, I.A. Walmsley, and D. Branning, 1998, Phys. Rev. A **57**, R2289.
- [167] Grice, W.P. and I.A. Walmsley, 1997, Phys. Rev. A **56**, 1627.
- [168] Gröblacher, S., T. Jennewein, A. Vaziri, G. Weihs, and A. Zeilinger, 2006, New J. Phys. **8**, 75.
- [169] Gröblacher, S., T. Paterek, R. Kaltenbaek, Č. Brukner, M. Żukowski, M. Aspelmeyer, and A. Zeilinger, 2007, Nature (London) **446**, 871.
- [170] Grover, L.K., 1997, Phys. Rev. Lett. **79**, 325.
- [171] Halder, M., A. Beveratos, N. Gisin, V. Scarani, C. Simon, and H. Zbinden, 2007, Nature Phys. **3**, 692.
- [172] Hanbury Brown R. and R.Q. Twiss, 1956, Nature (London) **177**, 27.
- [173] Hardy, L., 1993, Phys. Rev. Lett. **71**, 1665.
- [174] Haroche, S., 1995, Ann. N.Y. Acad. Sci. **755**, 73.
- [175] Hayashi, A., T. Hashimoto, and M. Horibe, 2005, Phys. Rev. A **72**, 032325.
- [176] Hein, M., W. Dür, J. Eisert, R. Raussendorf, M. Van den Nest, H.-J. Briegel, 2006, quant-ph/0602096.
- [177] Hein, M., J. Eisert, and H.J. Briegel, 2004, Phys. Rev. A **69**, 062311.
- [178] Holevo, A.S., 1973, Probl. Inf. Transm. **9**, 177.
- [179] Holland, M.J. and K. Burnett, 1993, Phys. Rev. Lett. **71**, 1355.
- [180] Holman, K.W., D. D. Hudson, J. Ye, and D.J. Jones, 2005, Opt. Lett. **30**, 1225.
- [181] Hong, C.K. and L. Mandel, 1985, Phys. Rev. A **31**, 2409.
- [182] Hong, C.K., Z.Y. Ou, and L. Mandel, 1987, Phys. Rev. Lett. **59**, 2044.
- [183] Horne, M., A. Shimony, and A. Zeilinger, 1989, Phys. Rev. Lett. **62**, 2209.
- [184] Horne, M., A. Shimony, and A. Zeilinger, 1990, Nature (London) **347**, 429.
- [185] Horne, M. and A. Zeilinger, 1986, Ann. N.Y. Acad. Sci. **480**, 469.
- [186] Horodecki, M., P. Horodecki, and R. Horodecki, 1996, Phys. Lett. A **223**, 1.
- [187] Horodecki, M., P. Horodecki, and R. Horodecki, 1997, Phys. Rev. Lett. **78**, 547.
- [188] Horodecki, R., P. Horodecki, M. Horodecki, and K. Horodecki, 2007, quant-ph/0702225.
- [189] Horodecki, R., P. Horodecki, and M. Horodecki, 1995, Phys. Lett. A **200**, 340.
- [190] Howell, J.C., A. Lamas-Linares, and D. Bouwmeester, 2002, Phys. Rev. Lett. **88**, 030401.
- [191] Huang, Y.-F., C.-F. Li, Y.-S. Zhang, J.-W. Pan, and G.-C. Guo, 2003, Phys. Rev. Lett. **90**, 250401.
- [192] Imamoglu, A., 2002, Phys. Rev. Lett. **89**, 163602.
- [193] Jacobson, J., G. Björk, I. Chuang, and Y. Yamamoto, 1995, Phys. Rev. Lett. **74**, 4835.
- [194] James, D.F.V. and P.G. Kwiat, 2002, Phys. Rev. Lett. **89**, 183601.
- [195] Javan, A., E.A. Ballik, and W.L. Bond, 1962, J. Opt. Soc. Am. **52**, 96.
- [196] Jennewein, T., G. Weihs, J.-W. Pan, and A. Zeilinger, 2002, Phys. Rev. Lett. **88**, 017903.
- [197] Jiang, L., J.M. Taylor, and M.D. Lukin, 2007, Phys. Rev. A **76**, 012301.
- [198] Julsgaard, B., J. Sherson, J.I. Cirac, J. Fiurášek, and E.S. Polzik, 2004, Nature (London) **432**, 482.
- [199] Kaltenbaek, R., B. Blauensteiner, M. Żukowski, M. Aspelmeyer, and A. Zeilinger, 2006, Phys. Rev. Lett. **96**, 240502.
- [200] Karlsson, A. and M. Bourennane, 1998, Phys. Rev. A **58**, 4394.
- [201] Kash, M.M., V.A. Sautenkov, A.S. Zibrov, L. Hollberg, G.R. Welch, M.D. Lukin, Yu. Rostovtsev, E.S. Fry, and M.O. Scully, 1999, Phys. Rev. Lett. **82**, 5229.
- [202] Kaszlikowski, D., P. Gnaniński, M. Żukowski, W. Miklaszewski, and A. Zeilinger, 2000, Phys. Rev. Lett. **85**, 4418.
- [203] Keller, M., B. Lange, K. Hayasaka, W. Lange, and H. Walther, 2004, Nature (London) **431**, 1075.
- [204] Keller, T.E., and M.H. Rubin, 1997, Phys. Rev. A **56**, 1534.
- [205] Keller, T.E., and M.H. Rubin, and Y. Shih, 1998, Phys.

- Let. A **244**, 507.
- [206] Kempe, J., D. Bacon, D.A. Lidar, and K.B. Whaley, 2001, Phys. Rev. A **63**, 042307.
- [207] Khoury, G., H.S. Eisenberg, E.J.S. Fonseca, and D. Bouwmeester, 2006, Phys. Rev. Lett. **96**, 203601.
- [208] Kiesel, N., C. Schmid, U. Weber, G. Tóth, O. Gühne, R. Ursin, and H. Weinfurter, 2005, Phys. Rev. Lett. **95**, 210502.
- [209] Kim, Y.-H., M.V. Chekhova, S.P. Kulik, M.H. Rubin, and Y.H. Shih, 2001, Phys. Rev. A **63**, 062301.
- [210] Kim, Y.-H., S.P. Kulik, and Y.H. Shih, 2001, Phys. Rev. Lett. **86**, 1370.
- [211] Kimble, H.J., M. Dagenais, and L. Mandel, 1977, Phys. Rev. Lett. **39**, 691.
- [212] Kimble, H.J., M. Dagenais, and L. Mandel, 1978, Phys. Rev. A **18**, 201.
- [213] Klyshko, D.N., 1967, Soviet Phys-JETP Lett. **6**, 23.
- [214] Klyshko, D.N., 1993, Phys. Lett. A **172**, 399.
- [215] Klyshko, D.N., 1988, *Photons and Nonlinear Optics* (Gordon and Breach, New York).
- [216] Knill, E., R. Laflamme, R. Martinez, and C. Negrevergne, 2001, Phys. Rev. Lett. **86**, 5811.
- [217] Knill, E., R. Laflamme, and G. Milburn, 2001, Nature (London) **409**, 46.
- [218] Koashi, M., T. Yamamoto, and N. Imoto, 2001, Phys. Rev. A, **63** 030301.
- [219] Kochen, S. and E.P. Specker, 1967, J. Math. Mech. **17**, 59.
- [220] Kok, P. and S.L. Braunstein, 2000, Phys. Rev. A **61**, 042304.
- [221] Kok, P., H. Lee, and J.P. Dowling, 2002, Phys. Rev. A **65**, 052104.
- [222] Kok, P., A.N. Boto, D.S. Abrams, C.P. Williams, S.L. Braunstein, and J.P. Dowling, 2001, Phys. Rev. A **63**, 063407.
- [223] Kok, P., W.J. Munro, K. Nemoto, T.C. Ralph, J.P. Dowling, and G.J. Milburn, 2007, Rev. Mod. Phys. **79**, 135.
- [224] Kozhokin, A.E., K. Mølmer, and E. Polzik, 2000, Phys. Rev. A **62**, 033809.
- [225] Krenn, G. and A. Zeilinger, 1996, Phys. Rev. A **54**, 1793.
- [226] Kuhn, A., M. Hennrich, and G. Rempe, 2002, Phys. Rev. Lett. **89**, 067901.
- [227] Kurtsiefer, C., S. Mayer, P. Zarda, and H. Weinfurter, 2000, Phys. Rev. Lett. **85**, 290.
- [228] Kurtsiefer, C., M. Oberparleiter, and H. Weinfuter, 2001, Phys. Rev. A, **64**, 023802.
- [229] Kurtsiefer, C., P. Zarda, M. Halder, H. Weinfurter, P.M. Gorman, P.R. Tapster, and J.G. Rarity, 2002, Nature (London) **419**, 450.
- [230] Kuzmich, A., I.A. Walmsley, and L. Mandel, 2000, Phys. Rev. Lett. **85**, 1349.
- [231] Kwiat, P.G., 1997, J. Mod. Opt. **44**, 2173.
- [232] Kwiat, P.G., S. Barraza-Lopez, A. Stefanov, and N. Gisin, 2001, Nature (London) **409**, 1014.
- [233] Kwiat, P.G., A.J. Berglund, J.B. Altepeter, and A.G. White, 2000, Science **290**, 498.
- [234] Kwiat, P.G., P.H. Eberhard, A.M. Steinberg, and R.Y. Chiao, 1994, Phys. Rev. A **49**, 3209.
- [235] Kwiat, P.G., K. Mattle, H. Weinfurter, A. Zeilinger, A.V. Sergienko, and Y. Shih, 1995, Phys. Rev. Lett. **75**, 4337.
- [236] Kwiat, P.G., A.M. Steinberg, and R.Y. Chiao, 1993, Phys. Rev. A **47**, R2472.
- [237] Kwiat, P.G. and H. Weinfurter, 1998, Phys. Rev. A **58**, R2623.
- [238] Laflamme, R., E. Knill, W.H. Zurek, P. Catasti, and S.V.S. Mariappen. 1998, Phil. Trans. R. Soc. Lond. A **356**, 1941.
- [239] Laflamme, R., C. Miquel, J.P. Paz and W.H. Zurek, 1996, Phys. Rev. Lett. **77**, 198.
- [240] Laloë, F., 2001, Am. J. Phys. **69**, 655.
- [241] Lamas-Linares, A., J.C. Howell, and D. Bouwmeester, 2001, Nature (London) **412**, 887.
- [242] Landau, L.J., 1987, Phys. Lett. A **120**, 54.
- [243] Laurat, J., H. de Riedmatten, D. Felinto, C.-W. Chou, E. Schomburg, and H.J. Kimble, 2006, Opt. Express **14**, 6912.
- [244] Legero, T., T. Wilk, M. Hennrich, G. Rempe, and A. Kuhn, 2004, Phys. Rev. Lett. **93**, 070503.
- [245] Leggett, A.J., 2003, Found. Phys. **33**, 1469.
- [246] Leibfried, D., R. Blatt, C. Monroe, and D. Wineland, 2003, Rev. Mod. Phys. **75**, 281.
- [247] Leonhardt, U., 2003, Rep. Prog. Phys. **66**, 1207.
- [248] Lewenstein, M., B. Kraus, J.I. Cirac, and P. Horodecki, 2000, Phys. Rev. A **62**, 052310.
- [249] Lewis, G.N., 1926, Nature (London) **118**, 874.
- [250] Lidar, D.A., I.L. Chuang, and K.B. Whaley, 1998, Phys. Rev. Lett. **81**, 2594.
- [251] Liu, C., Z. Dutton, C.H. Behroozi, and L.V. Hau, 2001, Nature (London) **409**, 490.
- [252] Lloyd, S., 1995, Phys. Rev. Lett. **75**, 346.
- [253] Lloyd, S., 1998, Phys. Rev. A **57**, R1473.
- [254] Lloyd, S., M.S. Shahriar, and J.H. Shapiro, and P. R. Hemmer, 2001, Phys. Rev. Lett. **87**, 167903.
- [255] Loss, D. and D.P. DiVincenzo, 1998, Phys. Rev. A **57**, 120.
- [256] Lounis, B. and W. E. Moerner, 2000, Nature (London) **407**, 491.
- [257] Lounis B. and M. Orrit, 2005, Rep. Prog. Phys **68**, 1129.
- [258] Lu, C.-Y., X.-Q. Zhou, O. Gühne, W.-B. Gao, J. Zhang, Z.-S. Yuan, A. Goebel, T. Yang, and J.-W. Pan, 2007, Nature Phys. **3**, 91.
- [259] Lukin, M.D., 2003, Rev. Mod. Phys. **75**, 457.
- [260] Lukin, M.D. and A. Imamoglu, 2001, Nature (London) **413**, 273.
- [261] Lukin, M.D., S.F. Yelin, and M. Fleischhauer, 2000, Phys. Rev. Lett. **84**, 4232.
- [262] Lütkenhaus, N., J. Calsamiglia, and K.-A. Suominen, 1999, Phys. Rev. A **59**, 3295.
- [263] Lvovsky, A.I., 2002, Phys. Rev. Lett. **88**, 098901.
- [264] Ma, L.-S., R. K. Shelton, H. C. Kapteyn, M. M. Murnane, and J. Ye, 2001, Phys. Rev. A **64**, 021802.
- [265] Madsen, M.J., D.L. Moehring, P. Maunz, R.N. Kohn, Jr., L.-M. Duan, and C. Monroe, 2006, Phys. Rev. Lett. **97**, 040505.
- [266] Magyar, G. and L. Mandel, 1963, Nature (London) **198**, 255.
- [267] Mair, A., A. Vaziri, G. Weihs, and A. Zeilinger, 2001, Nature (London) **412**, 313.
- [268] Makhlin, Y., G. Schön, and A. Shnirman, 2001, Rev. Mod. Phys. **73**, 357.
- [269] Mandel, L., 1983, Phys. Rev. A **28**, 929.
- [270] Mandel, L. and E. Wolf, 1995, *Optical Coherence and Quantum Optics* (Cambridge University Press, Cambridge).
- [271] Marcikic, I., H. de Riedmatten, W. Tittel, V. Scarani,

- H. Zbinden, and N. Gisin, 2002, Phys. Rev. A **66**, 062308.
- [272] Marcikic, I., H. de Riedmatten, W. Tittel, H. Zbinden, N. Gisin, 2003, Nature (London) **421**, 509.
- [273] Marcikic, I., H. de Riedmatten, W. Tittel, H. Zbinden, M. Legré and N. Gisin, 2004, Phys. Rev. Lett. **93**, 180502.
- [274] Marinatto, L., 2003, Phys. Rev. Lett. **90**, 258901.
- [275] Massar, S. and S. Popescu, 1995, Phys. Rev. Lett. **74**, 1259.
- [276] Matsukevich, D.N., T. Chanelière, S.D. Jenkins, S.-Y. Lan, T.A.B. Kennedy, and A. Kuzmich, 2006a, Phys. Rev. Lett. **96**, 030405.
- [277] Matsukevich, D.N., T. Chanelière, S.D. Jenkins, S.-Y. Lan, T.A.B. Kennedy, and A. Kuzmich, 2006b, Phys. Rev. Lett. **97**, 013601.
- [278] Matsukevich, D.N., and A. Kuzmich, 2004, Science **306**, 663.
- [279] Mattle, K., H. Weinfurter, P.G. Kwiat, and A. Zeilinger, 1996, Phys. Rev. Lett. **76**, 4656.
- [280] McKeever, J., A. Boca, A.D. Boozer, R. Miller, J.R. Buck, A. Kuzmich, and H.J. Kimble, 2004, Science **303**, 1992.
- [281] Mermin, N.D., 1990a, Phys. Today **43** (6), 9.
- [282] Mermin, N.D., 1990b, Phys. Rev. Lett. **65**, 1838.
- [283] Mermin, N.D., 1990c, Phys. Rev. Lett. **65**, 3373.
- [284] Mermin, N.D., 1993, Rev. Mod. Phys. **65**, 803.
- [285] Michler, M., K. Mattle, H. Weinfurter, and A. Zeilinger, 1996, Phys. Rev. A **53**, R1209.
- [286] Michler, M., H. Weinfurter, and M. Żukowski, 2000a, Phys. Rev. Lett. **84**, 5457.
- [287] Michler, P., A. Kiraz, C. Becher, W.V. Schoenfeld, P.M. Petroff, L. Zhang, E. Hu, and A. Imamoglu, 2000b, Science **290**, 2282.
- [288] Mintert, F., A.R.R. Carvalho, M. Kuś, and A. Buchleitner, 2005, Phys. Rep. **415**, 207.
- [289] Mitchell, M.W., J.S. Lundeen, and A.M. Steinberg, 2004, Nature (London) **429**, 161.
- [290] Mohseni, M., J.S. Lundeen, K.J. Resch, and A.M. Steinberg, 2003, Phys. Rev. Lett. **91**, 187903.
- [291] Molina-Terriza, G., A. Vaziri, J. Řeháček, Z. Hradil, and A. Zeilinger, 2004, Phys. Rev. Lett. **92**, 167903.
- [292] Mollow, B.R., 1973, Phys. Rev. A **8**, 2684.
- [293] Ne'eman, Y., 1986, Found. Phys. **16**, 361.
- [294] Nielsen, M.A., 2004, Phys. Rev. Lett. **93**, 040503.
- [295] Nielsen, M. and I.L. Chuang, 2000, *Quantum Computation and Quantum Information* (Cambridge University Press, Cambridge).
- [296] Nielsen, M.A. and C.M. Dawson, 2005, Phys. Rev. A **71**, 042323.
- [297] Nielsen, M.A., E. Knill, and R. Laflamme, 1998, Nature (London) **396**, 52.
- [298] O'Brien, J.L., G.J. Pryde, A.G. White, T.C. Ralph, and D. Branning, 2003, Nature (London) **426**, 264.
- [299] O'Sullivan-Hale, M.N., I.A. Khan, R.W. Boyd, and J.C. Howell, 2005, Phys. Rev. Lett. **94**, 220501.
- [300] Ou, Z.Y. and L. Mandel, 1988a, Phys. Rev. Lett. **61**, 50.
- [301] Ou, Z.Y. and L. Mandel, 1988b, Phys. Rev. Lett. **61**, 54.
- [302] Palma, G.M., K.-A. Suominen, and A.K. Ekert, 1996, Proc. R. Soc. London A **452**, 567.
- [303] Pan, J.-W., D. Bouwmeester, M. Daniell, H. Weinfurter, and A. Zeilinger, 2000, Nature (London) **403**, 515.
- [304] Pan, J.-W., D. Bouwmeester, H. Weinfurter, and A. Zeilinger, 1998, Phys. Rev. Lett. **80**, 3891.
- [305] Pan, J.-W., M. Daniell, S. Gasparoni, G. Weihs, and A. Zeilinger, 2001a, Phys. Rev. Lett. **86**, 004435.
- [306] Pan, J.-W., S. Gasparoni, M. Aspelmeyer, T. Jennewein, and A. Zeilinger, 2003a, Nature (London) **421**, 721.
- [307] Pan, J.-W., S. Gasparoni, R. Ursin, G. Weihs, and A. Zeilinger, 2003b, Nature (London) **423**, 417.
- [308] Pan, J.-W., C. Simon, C. Brukner, and A. Zeilinger, 2001b, Nature (London) **410**, 1067.
- [309] Pan, J.-W. and A. Zeilinger, 1998, Phys. Rev. A **57**, 2208.
- [310] Paterek, T., A. Fedrizzi, S. Gröblacher, T. Jennewein, M. Żukowski, M. Aspelmeyer, and A. Zeilinger, 2007, Phys. Rev. Lett. **99**, 210406.
- [311] Paul, H., 1986, Rev. Mod. Phys. **58**, 209.
- [312] Pelton, M., C. Santori, J. Vučković, B.Y. Zhang, G.S. Solomon, J. Plant, and Y. Yamamoto, 2002, Phys. Rev. Lett. **89**, 233602.
- [313] Peng, C.-Z., T. Yang, X.-H. Bao, J. Zhang, X.-M. Jin, F.-Y. Feng, B. Yang, J. Yang, J. Yin, Q. Zhang, N. Li, B.-L. Tian, and J.-W. Pan, 2005, Phys. Rev. Lett. **94**, 150501.
- [314] Peng, C.-Z., J. Zhang, D. Yang, W.-B. Gao, H.-X. Ma, H. Yin, H.-P. Zeng, T. Yang, X.-B. Wang, and J.-W. Pan, 2007, Phys. Rev. Lett. **98**, 010505.
- [315] Peres, A., 1996, Phys. Rev. Lett. **77**, 1413.
- [316] Peres, A., 2000, J. Mod. Opt. **47**, 531.
- [317] Peres, A., 2002, *Quantum Theory: Concepts and Methods* (Kluwer Academic Publishers, New York).
- [318] Peters, N.A., J.B. Altepeter, D. Branning, E.R. Jeffrey, T.-C. Wei, and P.G. Kwiat, 2004, Phys. Rev. Lett. **92**, 133601.
- [319] Pfleeger, R.L. and L. Mandel, 1967, Phys. Rev. **159**, 1084.
- [320] Phillips, D.F., A. Fleischhauer, A. Mair, R.L. Walsworth, and M.D. Lukin, 2001, Phys. Rev. Lett. **86**, 783.
- [321] Pittman, T.B., M.J. Fitch, B.C. Jacobs, and J.D. Franson, 2003, Phys. Rev. A **68**, 032316.
- [322] Pittman, T.B., B.C. Jacobs, and J.D. Franson, 2001, Phys. Rev. A **64** 062311.
- [323] Pittman, T.B., B.C. Jacobs, and J.D. Franson, 2002, Phys. Rev. Lett. **88**, 257902.
- [324] Pittman T.B. and J.D. Franson, 2003, Phys. Rev. Lett. **90**, 240401.
- [325] Popescu, S., 1995, quant-ph/9501020.
- [326] Popescu, S., L. Hardy, and M. Żukowski, 1997, Phys. Rev. A **56**, R4353.
- [327] Poyatos, J.F., J.I. Cirac, and P. Zoller, 1997, Phys. Rev. Lett. **78**, 390.
- [328] Preskill, J., 1998, *Lecture Notes on Quantum Computation* (CIT Physics 219/Computer Science 219) at <http://www.theory.caltech.edu/people/preskill/ph229/>.
- [329] Prevedel, R., P. Walther, F. Tiefenbacher, P. Böhi, R. Kaltenbaeck, T. Jennewein, and A. Zeilinger, 2007, Nature (London) **445**, 65.
- [330] Radloff, W., 1971, Ann. Phys. (Leipzig) **26**, 178.
- [331] Raimond, J.M., M. Brune, and S. Haroche, 2001, Rev. Mod. Phys. **73**, 565.
- [332] Ralph, T.C., A.J.F. Hayes, and A. Gilchrist, 2005, Phys. Rev. Lett. **95** 100501.

- [333] Ralph, T.C., N.K. Langford, T.B. Bell, and A.G. White, 2002a, Phys. Rev. A **65**, 062324.
- [334] Ralph, T.C., A.G. White, W.J. Munro, and G.J. Milburn, 2002b, Phys. Rev. A **65**, 012314.
- [335] Rarity, J.G., 1995, Ann. N.Y. Acad. Sci. **755**, 624.
- [336] Rarity, J.G. and P.R. Tapster, 1990, Phys. Rev. Lett. **64**, 2495.
- [337] Rarity, J.G., P.R. Tapster, and R. Loudon, 1996, in *Quantum Interferometry*, edited by F. De Martini, G. Denardo, and Y. Shih (VCH, Weinheim).
- [338] Raussendorf, R., D.E. Browne, and H.J. Briegel, 2003, Phys. Rev. A **68**, 022312.
- [339] Raussendorf, R. and H.J. Briegel, 2001, Phys. Rev. Lett. **86**, 5188.
- [340] Raussendorf, R. and H.J. Briegel, 2002, Quant. Inf. Comp. **6**, 433.
- [341] Reck, M., A. Zeilinger, H. J. Bernstein, and P. Bertani, 1994, Phys. Rev. Lett., **73** 58.
- [342] Resch, K.J., M. Lindenthal, B. Blauensteiner, H.R. Böhm, A. Fedrizzi, C. Kurtsiefer, A. Poppe, T. Schmitt-Manderbach, M. Taraba, R. Ursin, P. Walther, H. Weier, H. Weinfurter, and A. Zeilinger, 2005, Opt. Express **13**, 202.
- [343] Riebe, M., H. Häffner, C.F. Roos, W. Hänsel, J. Benhelm, G.P.T. Lancaster, T.W. Körber, C. Becher, F. Schmidt-Kaler, D.F.V. James, and R. Blatt, 2004, Nature (London) **432**, 602.
- [344] Roy, S.M. and V. Singh, 1991, Phys. Rev. Lett. **67**, 2761.
- [345] Rosenberg, D., J.W. Harrington, P.R. Rice, P.A. Hiskett, C.G. Peterson, R.J. Hughes, A.E. Lita, S.W. Nam, and J.E. Nordholt, 2007, Phys. Rev. Lett. **98**, 010503.
- [346] Rowe, M.A., D. Kielpinski, V. Meyer, C.A. Sackett, W.M. Itano, C. Monroe, and D. J. Wineland, 2001, Nature (London) **409**, 791.
- [347] Rubin, M.H., D.N. Klyshko, Y.H. Shih, and A.V. Sergienko, 1994, Phys. Rev. A **50**, 5122.
- [348] Ryff, L.C., 1997, Am. J. Phys. **65**, 1197.
- [349] Sanaka, K., T. Jennewein, J.-W. Pan, K. Resch, and A. Zeilinger, 2004, Phys. Rev. Lett. **92**, 017902.
- [350] Santori, C., D. Fattal, J. Vučković, G.S. Solomon, and Y. Yamamoto, 2002, Nature (London) **419**, 594.
- [351] Santori, C., M. Pelton, G. Solomon, Y. Dale, and Y. Yamamoto, 2001, Phys. Rev. Lett. **86**, 1502.
- [352] Scarani, V. and N. Gisin, 2001, Phys. Rev. Lett. **87**, 117901.
- [353] Scheel, S., W.J. Munro, J. Eisert, K. Nemoto, and P. Kok, 2006, Phys. Rev. A **73**, 034301.
- [354] Schlosshauer, M., 2004, Rev. Mod. Phys. **76**, 1267.
- [355] Schmid, C., N Kiesel, W Wiczorek, and H Weinfurter, 2007, New J. Phys. **9**, 236.
- [356] Schmidt-Kaler, F., H. Häffner, M. Riebe, S. Gulde, G.P.T. Lancaster, T. Deuschle, C. Becher, C.F. Roos, J. Eschner, and R. Blatt, 2003, Nature (London) **422**, 408.
- [357] Schmitt-Manderbach, T., H. Weier, M. Fürst, R. Ursin, F. Tiefenbacher, T. Scheidl, J. Perdignes, Z. Sodnik, C. Kurtsiefer, J.G. Rarity, A. Zeilinger, and H. Weinfurter, 2007, Phys. Rev. Lett. **98**, 010504.
- [358] Schori, C., B. Julsgaard, J.L. Sørensen, and E.S. Polzik, 2002, Phys. Rev. Lett. **89**, 057903.
- [359] Schrödinger, E., 1935, Naturwissenschaften **23**, 807; **23**, 823; **23**, 844; the English translation appears in Wheeler J.A. and W.H. Zurek, 1983, *Quantum Theory and Measurement* (Princeton University Press, New York).
- [360] Schuck, C., G. Huber, C. Kurtsiefer, and H. Weinfurter, 2006, Phys. Rev. Lett. **96**, 190501.
- [361] Scully, M.O., B.-G. Englert, and C.J. Bednar, 1999, Phys. Rev. Lett. **83**, 4433.
- [362] Scully, M.O., B.-G. Englert, and H. Walther, 1991, Nature (London) **351**, 111.
- [363] Scully, M.O. and M.S. Zubairy, 1997, *Quantum Optics* (Cambridge University Press, Cambridge).
- [364] Seevinck, M. and G. Svetlichny, 2002, Phys. Rev. Lett. **89**, 060401.
- [365] Sergienko, A.V., M. Atatüre, Z. Walton, G. Jaeger, B.E.A. Saleh, and M.C. Teich, 1999, Phys. Rev. A **60**, R2622.
- [366] Shelby, R.M., M.D. Levenson, S.H. Perlmuter, R.G. DeVoe, and D.F. Walls, 1986, Phys. Rev. Lett. **57**, 691.
- [367] Shih, Y.H., 2003, Rep. Prog. Phys. **66**, 1009.
- [368] Shih, Y.H. and C.O. Alley, 1988, Phys. Rev. Lett. **61**, 2921.
- [369] Shor, P.W., 1995, Phys. Rev. A **52**, R2493.
- [370] Simon, C. and D. Bouwmeester, 2003, Phys. Rev. Lett. **91**, 053601.
- [371] Simon, C. and Irvine, W.T.M. 2003, Phys. Rev. Lett. **91**, 110405.
- [372] Simon, C. and J.-W. Pan, 2002, Phys. Rev. Lett. **89**, 257901.
- [373] Simon, C., M. Żukowski, H. Weinfurter, and A. Zeilinger, 2000, Phys. Rev. Lett. **85**, 1783.
- [374] Slusher, R.E., L.W. Hollberg, B. Yurke, J.C. Mertz, and J.F. Valley, 1985, Phys. Rev. Lett. **55**, 2409.
- [375] Smithey, D.T., M. Beck, M. Belsley, and M.G. Raymer, 1992, Phys. Rev. Lett. **69**, 2650.
- [376] Spedalieri, F.M., H. Lee, and J.P. Dowling, 2006, Phys. Rev. A **73**, 012334.
- [377] Steane, A.M., 1996, Phys. Rev. Lett. **77**, 793.
- [378] Steane, A., 1998, Rep. Prog. Phys. **61** 117.
- [379] Stevenson, R.M., R.J. Young, P. Atkinson, K. Cooper, D.A. Ritchie, and A.J. Shields, 2006, Nature (London) **439**, 179.
- [380] Sun, C.P., Y. Li, and X.F. Liu, 2003, Phys Rev Lett **91**, 147903.
- [381] Taylor, G.I., 1909, Proc. Camb. Phil. Soc. Math. Phys. Sci. **15**, 114.
- [382] Terhal, B., 2000, Phys. Lett. A **271**, 319.
- [383] Tittel, W. and G. Weihs, 2001, Quant. Inf. Comp. **1**(2), 3.
- [384] Torres, J.P., A. Alexandrescu, and L. Torner, 2003, Phys. Rev. A **68**, 050301.
- [385] Uffink, J., 2002, Phys. Rev. Lett. **88**, 230406.
- [386] Ursin, R., T. Jennewein, M. Aspelmeyer, R. Kaltenbaeck, M. Lindenthal, P. Walther, and A. Zeilinger, 2004, Nature (London) **430**, 849.
- [387] Vaidman, L. and N. Yoran, 1999, Phys. Rev. A **59**, 116.
- [388] van der Wal, C.H., M.D. Eisaman, A. Andre, R.L. Walsworth, D.F. Phillips, A.S. Zibrov, M.D. Lukin, 2003, Science **301**, 196.
- [389] van Enk, S.J., J.I. Cirac, and P. Zoller, 1997, Phys. Rev. Lett. **78**, 4293.
- [390] van Houwelingen, J.A.W., N. Brunner, A. Beveratos, H. Zbinden, and N. Gisin, 2006, Phys. Rev. Lett. **96**, 130502.
- [391] van Loock, P., T.D. Ladd, K. Sanaka, F. Yamaguchi, K. Nemoto, W.J. Munro, and Y. Yamamoto, 2006, Phys.

- Rev. Lett. **96**, 240501.
- [392] Varnava, M., D.E. Browne, and T. Rudolph, 2006, Phys. Rev. Lett. **97**, 120501.
- [393] Vaziri, A., J.-W. Pan, T. Jennewein, G. Weihs, and A. Zeilinger, 2003, Phys. Rev. Lett. **91**, 227902.
- [394] Vaziri, A., G. Weihs, and A. Zeilinger, 2002, Phys. Rev. Lett. **89**, 240401.
- [395] Vitali, D., M. Fortunato, and P. Tombesi, 2000, Phys. Rev. Lett. **85**, 445.
- [396] Waks, E., K. Inoue, E. Diamanti, and Y. Yamamoto, 2003, quant-ph/0308054.
- [397] Waks, E., E. Diamanti, B.C. Sanders, S.D. Bartlett, and Y. Yamamoto, 2004, Phys. Rev. Lett. **92**, 113602.
- [398] Waks, E., A. Zeevi, Y. Yamamoto, 2002, Phys. Rev. A **65**, 052310.
- [399] Walborn, S.P., A.N. de Oliveira, S. Pádua, and C.H. Monken, 2003a, Phys. Rev. Lett. **90**, 143601.
- [400] Walborn, S.P., S. Pádua, and C.H. Monken, 2003b, Phys. Rev. A **68**, 042313.
- [401] Walls, D.F. and G.J. Milburn, 1994, *Quantum Optics* (Springer-Verlag, Berlin).
- [402] Walther, P., J.-W. Pan, M. Aspelmeyer, R. Ursin, S. Gasparoni, and A. Zeilinger, 2004, Nature (London) **429**, 158.
- [403] Walther, P., K.J. Resch, C. Brukner, A.M. Steinberg, J.-W. Pan, and A. Zeilinger, 2005a, Phys. Rev. Lett. **94**, 040504.
- [404] Walther, P., K.J. Resch, T. Rudolph, E. Schenck, H. Weinfurter, V. Vedral, M. Aspelmeyer, and A. Zeilinger, 2005b, Nature (London) **434**, 169.
- [405] Walther, P. and A. Zeilinger, 2005, Phys. Rev. A **72**, 010302.
- [406] Wang, X.-B., 2004, Phys. Rev. A **69**, 022320.
- [407] Weihs, G., T. Jennewein, C. Simon, H. Weinfurter, and A. Zeilinger, 1998, Phys. Rev. Lett. **81**, 5039.
- [408] Weihs, G., M. Reck, H. Weinfurter, and A. Zeilinger, 1996, Opt. Lett., **21** 302.
- [409] Weinfurter, H., 1994, Europhys. Lett. **25**, 559.
- [410] Weinfurter, H. and M. Żukowski, 2001, Phys. Rev. A **64**, 010102.
- [411] Weinstein, Y.S., C.S. Hellberg, and J. Levy, 2005, Phys. Rev. A **72**, 020304(R).
- [412] Werner, R.F., 1989, Phys. Rev. A **40**, 4277.
- [413] Werner R.F. and M.M. Wolf, 2001, Quantum Inf. Comput. **1** (3), 1.
- [414] White, A.G., D.F.V. James, P.H. Eberhard, and P.G. Kwiat, 1999, Phys. Rev. Lett. **83**, 3103.
- [415] Wiesner, S., 1983, SIGACT News **15**, 78.
- [416] Wootters, W.K. and W.H. Zurek, 1982, Nature (London) **299**, 802.
- [417] Wu, L.-A., H.J. Kimble, J.L. Hall, and H. Wu, 1986, Phys. Rev. Lett. **57**, 2520.
- [418] Yamamoto, T., M. Koashi, and N. Imoto, 2001, Phys. Rev. A **64**, 012304.
- [419] Yamamoto, T., M. Koashi, Ş.K. Özdemir, and N. Imoto, 2003, Nature (London) **421**, 343.
- [420] Yang, T., Q. Zhang, J. Zhang, J. Yin, Z. Zhao, M. Żukowski, Z.-B. Chen, and J.-W. Pan, 2005, Phys. Rev. Lett. **95**, 240406.
- [421] Yang, T., Q. Zhang, T.-Y. Chen, S. Lu, J. Yin, J.-W. Pan, Z.-Y. Wei, J.-R. Tian, and J. Zhang, 2006, Phys. Rev. Lett. **96**, 110501.
- [422] Young, R.J, R.M. Stevenson, P. Atkinson, K. Cooper, D.A. Ritchie, and A.J Shields, 2006, New J. Phys. **8**, 29.
- [423] Yu, S., Z.-B. Chen, J.-W. Pan, and Y.-D. Zhang, 2003, Phys. Rev. Lett. **90**, 080401.
- [424] Yurke B. and D. Stoler, 1992a, Phys. Rev. Lett. **68**, 1251.
- [425] Yurke B. and D. Stoler, 1992b, Phys. Rev. A **46**, 2229.
- [426] Zanardi, P., 1999, Phys. Rev. A **60**, R729.
- [427] Zanardi, P. and M. Rasetti, 1997, Phys. Rev. Lett. **79**, 3306.
- [428] Zeilinger, A., 1981, Am. J. Phys. **49**, 882.
- [429] Zeilinger, A., H. J. Bernstein, D. M. Greenberger, M. A. Horne, and M. Żukowski, 1993, in *Quantum Control and Measurement*, edited by H. Ezawa and Y. Murayama (North Holland, Amsterdam), p. 9.
- [430] Zeilinger, A., M.A. Horne, H. Weinfurter, and M. Żukowski, 1997, Phys. Rev. Lett. **78**, 3031.
- [431] Zeilinger, A., G. Weihs, T. Jennewein, and M. Aspelmeyer, 2005, Nature (London) **433**, 230.
- [432] Zel'dovich, Ya.B. and D.N. Klyshko, 1969, JETP Lett. **9**, 40.
- [433] Zhang, A.-N., C.-Y. Lu, X.-Q. Zhou, Y.-A. Chen, Z. Zhao, T. Yang, and J.-W. Pan, 2006a, Phys. Rev. A **73**, 022330.
- [434] Zhang, Q., X.-H. Bao, C.-Y. Lu, X.-Q. Zhou, T. Yang, T. Rudolph, and J.-W. Pan, 2006b, quant-ph/0610145.
- [435] Zhang, Q., A. Goebel, C. Wagenknecht, Y.-A. Chen, B. Zhao, T. Yang, A. Mair, J. Schmiedmayer, and J.-W. Pan, 2006c, Nature Phys. **2**, 678.
- [436] Zhang, Q., J. Yin, T.-Y. Chen, S. Lu, J. Zhang, X.-Q. Li, T. Yang, X.-B. Wang, and J.-W. Pan, 2006d, Phys. Rev. A **73**, 020301(R).
- [437] Zhao, B., Z.-B. Chen, Y.-A. Chen, J. Schmiedmayer, and J.-W. Pan, 2007, Phys. Rev. Lett. **98**, 240502.
- [438] Zhao, Z., J.-W. Pan, and M.S. Zhan, 2001, Phys. Rev. A **64**, 014301.
- [439] Zhao, Z., T. Yang, Y.-A. Chen, A.-N. Zhang, M. Żukowski, and J.-W. Pan, 2003a, Phys. Rev. Lett. **91**, 180401.
- [440] Zhao, Z., T. Yang, Y.-A. Chen, A.-N. Zhang, and J.-W. Pan, 2003b, Phys. Rev. Lett. **90**, 207901.
- [441] Zhao, Z., Y.-A. Chen, A.-N. Zhang, T. Yang, H.J. Briegel, and J.-W. Pan, 2004, Nature (London) **430**, 54.
- [442] Zhao, Z., A.-N. Zhang, Y.-A. Chen, H. Zhang J.-F. Du, T. Yang, and J.-W. Pan, 2005b, Phys. Rev. Lett. **94**, 030501.
- [443] Żukowski, M., 1993, Phys. Lett. A **177** 290.
- [444] Żukowski, M. and Č. Brukner, 2002, Phys. Rev. Lett. **88**, 210401.
- [445] Żukowski, M. and D. Kaszlikowski, 1997, Phys. Rev. A **56**, R1682.
- [446] Żukowski, M. and J. Pykacz, 1988, Phys. Lett. A **127**, 1.
- [447] Żukowski, M., A. Zeilinger, and M.A. Horne, 1997, Phys. Rev. A **55**, 2464.
- [448] Żukowski, M., A. Zeilinger, M.A. Horne, and A.K. Ekert, 1993, Phys. Rev. Lett. **71**, 4287.
- [449] Żukowski, M., A. Zeilinger, M.A. Horne, and H. Weinfurter, 1998, Acta Phys. Pol. **93**, 187.
- [450] Żukowski, M., A. Zeilinger, M.A. Horne, and H. Weinfurter, 1999, Int. J. Theor. Phys. **38**, 501.
- [451] Żukowski, M., A. Zeilinger, and H. Weinfurter, 1995,

Ann. N.Y. Acad. Sci. **755**, 91.

[452] Zurek, W.H., 2003, Rev. Mod. Phys. **75**, 715.